BIO-BASED PLASTICS REINFORCED WITH NATURAL FIBERS/HYBRID COMPOSITES THROUGH REACTIVE PROCESSING

By

MISS Phornwalan NANTHANANON

A Thesis Submitted in Partial Fulfillment of the Requirements

for Doctor of Philosophy (POLYMER SCIENCE AND ENGINEERING)

Department of MATERIALS SCIENCE AND ENGINEERING

Graduate School, Silpakorn University

Academic Year 2018

มหาวิทยาลัยศิลปากร

มหาวิทยาลัยศิลปากร

-

โดย
นางสาวภรวลัญช์ นันท์ธนานนท์

วิทยานิพนธ์นี้เป็นส่วนหนึ่งของการศึกษาตามหลักสูตรปรัชญาดุษฎีบัณฑิต
สาขาวิชาวิทยาการและวิศวกรรมพอลิเมอร์ แบบ 1.1 ปรัชญาดุษฎีบัณฑิต
ภาควิชาวิทยาการและวิศวกรรมวัสดุ
บัณฑิตวิทยาลัย มหาวิทยาลัยศิลปากร
ปีการศึกษา 2561

BIO-BASED PLASTICS REINFORCED WITH NATURAL FIBERS/HYBRID COMPOSITES THROUGH REACTIVE PROCESSING

By

MISS Phornwalan NANTHANANON

A Thesis Submitted in Partial Fulfillment of the Requirements

for Doctor of Philosophy (POLYMER SCIENCE AND ENGINEERING)

Department of MATERIALS SCIENCE AND ENGINEERING

Graduate School, Silpakorn University

Academic Year 2018

Title	Bio-based plastics reinforced with natural fibers/hybrid composites through reactive processing
By	Phornwalan NANTHANANON
Field of Study	(POLYMER SCIENCE AND ENGINEERING)
Advisor	Supakij Suttiruengwong

Graduate School Silpakorn University in Partial Fulfillment of the Requirements for the Doctor of Philosophy

---------- Dean of graduate school
(Associate Professor Jurairat Nunthanid, Ph.D.)

Approved by

---------- Chair person
(Associate Professor Nattakarn Hongsriphan , D.Eng.)
---------- Advisor
(Assistant Professor Supakij Suttiruengwong , Dr.Ing.)
---------- Co Advisor
(Assistant Professor Sommai Pivsa-Art , Ph.D.)
---------- Co Advisor
(Professor Hiroyuki Hamada)
---------- External Examiner
(Assistant Professor Tatiya Trongsatitkul , Ph.D.)

57402802 : Major (POLYMER SCIENCE AND ENGINEERING)
Keyword : in situ compatibilization, reactive hybrid composite, poly(lactic acid) (PLA), one-step twin-screw extrusion, natural fibers, direct feeding fiber injection molding

MISS PHORNWALAN NANTHANANON : BIO-BASED PLASTICS REINFORCED WITH NATURAL FIBERS/HYBRID COMPOSITES THROUGH REACTIVE PROCESSING THESIS ADVISOR : ASSISTANT PROFESSOR SUPAKIJ SUTTIRUENGWONG, Dr.Ing.

The reinforced PLA composite and hybrid composites with natural fibers, inorganic filler and/or synthetic fiber were fabricated by *in situ* reactive melt-blending in one-step process and their properties were investigated. The PLA/natural fiber interfacial adhesion was improved due to the presented multifunctional epoxide-based reactive agent (CEGMA) as proved by SEM images and Molau test. The highest tensile strength was obtained from PLA biocomposites incorporated with 1.0 phr CEGMA, which was improved by 13.9% compared to non-reactive biocomposite. The reactive PLA hybrid composite with 1:1 fiber:talc ratio fabricated using twin-screw extruder showed the highest improvement on storage modulus in the rubbery region. In order to provide more reactive site on filler surface, fiber and talc were successfully treated with MAH during the drying process, which was revealed by FT-IR spectra. Tensile strength and impact strength of the PLA hybrid composites were slightly improved by 6% when only CEGMA was added. However, MAH-treated fillers reinforced PLA with CEGMA and peroxide loading not only showed the most improvement on tensile and impact strength by 11 and 36% but also their interfacial adhesion compared to non-reactive hybrid composite. The reactive PLA/MAH-treated Jute/Carbon fiber hybrid composite was prepared using direct fiber feeding injection molding in term of practical use. Tensile strength of the reactive composite and hybrid composite was higher than non-reactive hybrid composite by 14.9 and 6.8% due to strong interfacial adhesion. It was confirmed that the *in situ* compatibilization between MAH-treated fiber and PLA chain could occur in short reaction time.

ACKNOWLEDGEMENTS

My dissertation would not have been possible without the support of several kind and generous individuals. First of all, I would like to express my thankfulness to my advisor, Asst. Prof. Dr. Supakij Suttiruengwong that believes in me and gives me the motivation, opportunity, encouragement and great advice throughout my study. I also considerably thankful to my co-advisors Asst. Prof. Dr. Sommai Pivsa-Art and Prof. Hiroyuki Hamada for giving me the help, consulting and facilities. I also sincerely thank Assoc. Prof. Manus Seadan who gave me the guidance, encouragement, research discussion, and many supports. I am grateful to the examination committee, Assoc. Prof. Dr. Nattakarn Hongsriphan and Asst. Prof. Dr. Tatiya Trongsatitkul for their invaluable time and comments on my research.

I would like to gratefully thank the Department of Materials Science and Engineering, Faculty of Engineering and Industrial Technology, Silpakorn University for research funding and facilities. I also would like to gratefully thank Department of Physics, Faculty of Science, Silpakorn University for the facility. National Research Council of Thailand was gratefully acknowledged for financial support. I also appreciate SCG Packaging PLC., Thailand for Bleach Eucalyptus Kraft Paper Pulps supply and Mr. Kosin Hachawee for his help. I gratefully appreciate Asst. Prof. Dr. Putinun Uawongsuwan for consulting and opportunity for using the direct fiber feeding injection molding machine and Mr. Prattakorn Sarasook for his help. I would like to thank all lab staffs; Mr. Pinit Jaenraluek, Mr. Phairote Tangsupphathawat and Miss Lookkwang Ounsiri for their support, guidance and helps. A special acknowledgment is extended to all my research group members for their encouragement and supports. Most importantly, none of this would have been possible without the love of my family that helps me get through the difficult times.

Phornwalan NANTHANANON

TABLE OF CONTENTS

LIST OF TABLES

Page

LIST OF FIGURES

Page

Charpter 1 Introduction

1.1. Background

An accumulative non-biodegradable plastic waste is becoming a severe threat for generations to come. The aim at reducing the waste disposal of non-biodegradable plastic and the consumption of non-renewable fossil feedstock are needed to be firmly addressed to attack the sustainability issues. In terms of plastics, using bioplastics; biodegradable plastics and/or renewable plastics derived from bio-resource can best tackle this problem. The bioplastics, such as biodegradable polyesters and cellulose-based plastics and other polysaccharides have been readily applied in many fields; from biomedical products, utensils, and food packaging to automotive and electronic parts. However, the practical utilization of biodegradable polyesters such as Poly(lactic acid) (PLA), poly(butylene succinate) (PBS), poly(caprolactone) (PCL), and poly(3-hydroxybutyrate-co-3- hydroxyvalerate) (PHBV) has been limited by their either poor mechanical or thermal properties compared to conventional thermoplastics such as poly(propylene) and poly(ethylene terephthalate). The reinforcement of bioplastics with micro- or nanomaterial could cope with the poor mechanical and even thermal drawbacks.

Poly(lactic acid) (PLA) has been widely used for several applications due to its renewability, biodegradability, and the large-scale commercial availability. PLA is well known for its short period of biodegradable time within 2 years (faster than 6 months under composting conditions) in contrast with need 500–1000 years for conventional plastics. Furthermore, PLA is polyester thermoplastic, which has good mechanical properties. PLA has high strength and modulus with capable using in either medical applications or the industrial packaging field. However, the heat distortion temperature (HDT) of PLA currently limits its applications (low stiffness at elevated temperature) [1]. To extend its use with desirable product properties, PLA has been blended with other polymers or compounded with several fillers such as fibers, and micro- and nanoparticles [2-8]. Huda et al., 2008 reported that PLA composites reinforced with kenaf showed a significant increase in HDT, compared to that of neat

PLA resin [9]. PLA was used as matrix with several lignocelluloses reinforcing fibers such as kenaf [10-13], flax [14-16], abaca [17], jute [18, 19], coir [20], miscanthus [21], ramie [22, 23], bamboo [24, 25], coconut [24], and vetiver [24].

Hybrid composite materials are one of the most currently efficient solutions and suitable as a reinforcement for improving properties of biodegradable polyesters. Hybrid composite is defined as two types; firstly, two or more different types of reinforcing materials presented in a single polymer matrix, for instance, synthetic fibers/natural fiber, natural fiber/natural fiber, fibers/particles and particles/particles reinforcement [3, 8, 26-33], secondly, one type of reinforcing material presented in a blend of different polymer matrices [29, 33, 34]. The main advantage of using hybrid composite is an increment with the lack of the other fillers leading to a balance in terms of performance and cost of composite materials [35].

The short-fibers and particles can be loaded into thermoplastics by conventional processes, such as extrusion processing and injection molding [26]. However, there are only few reports using particles and natural fibers reinforced PLA, for example, PLA/newspaper fiber/talc [30], PLA/montmorillonite/cellulose fiber [8], PLA/nano calcium carbonate/cellulose fiber [8], PLA/hemp fiber/nanosilica [27], PLA/cellulose fiber/clay [32]. In literatures, the addition of inorganic particle to polymer efficiently improved the mechanical properties of polymer matrix [26]. The addition of filler particle, such as talcum (talc) in thermoplastics is generally seen in many reported [30, 36-38] because talc can improve mechanical and thermal properties with cost-effectiveness [26, 38]. Furthermore, there is the novel processing technique, called “direct fiber feeding injection molding (DFFIM)”, for fabricating short fiber reinforced composite and/or hybrid composite without compounding process [39-42]. DFFIM is a technique that long fiber can be directly fed into small vented of injection barrel during polymer pellets are normally fed through a hopper under rotation motion of injection screw. Many composites and hybrid composites were done with this DFFIM process, for example, POM/GF [41], PLA/Sisal Fiber [42] composites, ABS/GF/CF [39] and PP/GF/CF [40] hybrid composites.

1.2. Statement of the Problem

The important drawback of composite or hybrid composite systems is the poor interfacial adhesion between the fiber or particle filler and polymer matrix due to the difference between their hydrophobic and hydrophilic nature [43]. The weak interfacial adhesion between filler and polymer matrix regularly diminishes the capability of filler reinforcement. Thus it limits their practical application [30, 43]. Coupling reactions are frequently used for improving interfacial adhesion between the polymer and filler. Organo-functional silane is the most common one for tuning the fibers and fillers surface in composites [30, 43]. For example, Barletta and co-workers used organosilanes (glycidyl, amino, and isocyanate groups) to functionalize talc surface in order to capably react with the hydroxyl or carboxyl groups at the end of PLA chain [36]. On the other hand, the highly reactive functions such as maleic anhydride (MAH) has been used for modifying the polymeric surface though grafting reactions onto the backbone of polymer using different methods [6, 44-48]. Nevertheless, such methods consume a lot of energy and time due to many step of procedure and difficult to scale up for mass production of composite/hybrid composite. In this respect, *in situ* reactive processing has been introduced and applied for manufacturing polymer blends and composites, with it offers an increase of interfacial adhesion as well as shortened time and cost-effectiveness. The highly reactive groups such as isocyanate, amine, anhydride, carboxylic acid and epoxide have been frequently used to produce functionalized polymer during reactive processing [49]. Combination of amine/anhydride, amine/epoxide, anhydride/epoxide and amine/lactam for reactive processing are also reported [50, 51]. In case of *in situ* reactive processing for composite, Hao and co-workers used an epoxy-functionalized terpolymer elastomer (EGMA) as an *in situ* compatibilizer for PLA and sisal fiber (SF), which resulted in the improvement of interfacial adhesion, toughness and tensile strength of PLA/SF composite [52].

To the best of our knowledge, an *in situ* reactive compatibilization of PLA reinforced with natural fiber and particle hybrid composites in the one-step process have not yet been researched. Furthermore, most of the researchers have focused

on the grafting of MAH onto the polymeric backbone in order to allow polymer to bond the hydrophilic cellulose fiber. Nevertheless, none has worked on grafting MAH onto the cellulose fiber before loading into polymer to fabricate composites and hybrid composites. The fabrication of the hybrid composite with a high content of fillers by using conventional twin-screw extruder without side-feeding or masterbatch preparation is challenging since its composed the different density of materials.

1.3. Objectives of research

The aim of this work is to simply prepare of PLA hybrid composites by reactive melt-blending in the one-step process including twin-screw extrusion and direct fiber feeding injection molding. The initial studies focused on the addition of different bleach eucalyptus kraft pulp (BEKP) fiber content to PLA, followed by addition of reactive agent as *in situ* compatibilizer in order to improve interfacial adhesion. The effect of three reactive agent types, such as multifunctional epoxide-based and anhydride-based terpolymers on rheology, morphology, and mechanical properties of PLA biocomposites were studied. In the second section, BEKP fiber was hybridized with talcum and then incorporated into PLA with and without reactive agents to produce a hybrid composite by the one-step melt-mixing process in twin screws extruder. The effect of the filler ratios (fiber and talc) and the *in situ* reactive compatibilizer on properties of PLA hybrid composite were also studied. In the last section, long fibers were directly fed with and without reactive agents into PLA for developing PLA composites and hybrid composites as a one-step process in term of practical usage using DFFIM.

Charpter 2 Literature review

2.1 Bio-base polyester

2.1.1. Poly(lactic acid)

Poly(lactic acid) (PLA) is a semi-crystalline thermoplastic polyester, biodegradable and bio-based renewable polymer. PLA is a desirable alternative to fossil-based polymers due to less environmental impact in term of global material sustainability. PLA production relatively decreases in CO_2 emission compared to other polymers [53]. PLA is an aliphatic polyester produced by industrial ring-opening polymerization of lactide and/or polycondensation of lactic acid monomer. PLA is classified as a hydrophobic polymer, although its chemical structure has oxygen single and double bonds [54].

Figure 2.1 Schematic of Poly Lactic Acid (PLA) lifecycle [55].

PLA has glass transition and melting temperatures of 55 – 60 °C and 155 – 170 °C, respectively [56]. PLA has a UV stability, gloss, low toxicity and good mechanical properties, such as high strength and modulus with capable using in medical applications, textile and the industrial packaging field [55]. Furthermore, PLA

has good processability in conventional industrial processing techniques such as extrusion, injection molding, film blowing and blow molding [42, 43, 57]. However, slow crystallization and low heat distortion temperature (HDT) are major drawbacks of PLA, which currently limits its applications (low stiffness at elevated temperatures) [1, 9]. To extend product uses with desirable product properties, PLA has been blended with other polymers or compounded with several fillers such as fibers, and micro- and nanoparticles [2-8].

2.2. Reinforcements

2.2.1. Natural fiber

Plant-based natural fibers consist of cellulose, hemicelluloses, lignin, pectin, and waxy substances. The chemical structure of components in fiber is displayed in Figure 2.2. Cellulose is considered as the major component of the fiber structure due to providing strength, stiffness and structural stability of the fiber [58]. Cellulose molecule contains three hydroxyl groups (- OH); two of them form hydrogen bonds within the cellulose macromolecules (intramolecular) while another group forms a hydrogen bond with other cellulose molecules (intermolecular) [59]. Hemicellulose is a branched polymer consisting of five and six carbon sugars of varied chemical structures and takes place mainly in the primary cell wall [59]. Lignin is amorphous and has an aromatic structure [59]. Mechanical properties of natural fiber over synthetic fiber are presented in Table 2.1. Although natural fibers have relatively lower strength properties compared to the synthetic fibers, the specific modulus and elongation at break signify the potentiality of these fibers to replace synthetic fibers in engineering polymer composites [58].

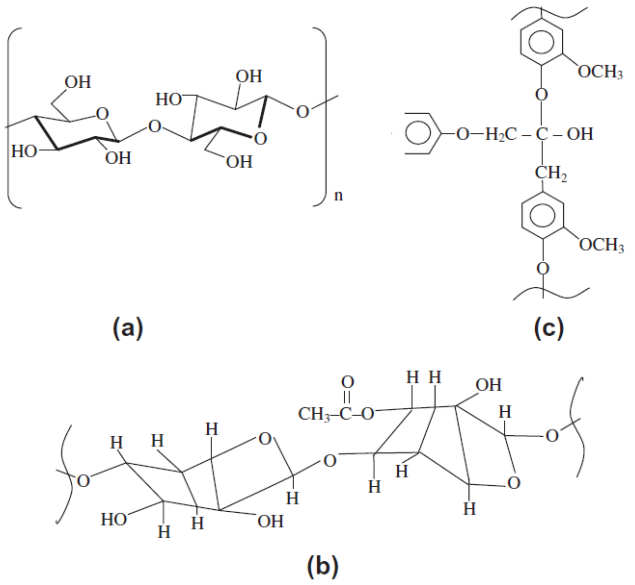

Figure 2.2 Chemical structures of cellulose (a), hemicelluloses (b) and lignin (c) [59].

Table 2.1 Comparative properties of natural fibers with synthetic fibers [58-61].

Fiber Types	Density (g/cm^3)	Tensile strength (MPa)	Young's modulus (GPa)	Specific strength (GPa/g/cm^3)	Specific modulus (GPa/g/cm^3)	Elongation at break (%)
Jute	1.3–1.4	393–773	13–26.5	0.3–0.5	10–18.3	1.16–1.5
Flax	1.50	345–1100	27.6	0.2–0.7	18.4	2.7–3.2
Hemp	1.14	690	30–60	0.6	26.3–52.6	1.6
Ramie	1.50	400–938	61.4–128	0.3–0.6	40.9–85.3	1.2–3.8
Sisal	1.45	468–640	9.4–22.0	0.3–0.4	6.4–15.2	3–7
PALF	1.52	170–1627	34.5–82.51	0.3–1.1	22.7–54.3	1.6-3
Cotton	1.5–1.6	287–800	5.5–12.6	0.2–0.5	3.7–7.8	7.0–8.0
Vetiver	1.5	247–723	12.0–49.8	0.2–0.5	8–33.2	1.6–2.4
E-glass	2.5	2000–3500	70	0.8–1.4	28	2.5
S-glass	2.5	4570	86	1.8	34.4	2.8
Aramid	1.4	3000–3150	63–67	2.1–2.2	45–47.8	3.3–3.7
Carbon	1.7	4000	230-240	1.71	130	1.4-1.8

Bleached Eucalyptus Kraft Pulp (BEKP)

Eucalyptus is a hardwood specie, which is a fast growing plant in the tropical region. Eucalyptus is a good fiber quality and relatively cheap in market price. In hardwood species, they are different in chemical composition and structure. Eucalyptus stands out for its high cellulose content and low lignin content [62] and has the potential for the production of micro/nano short-fiber [63]. Bleached Eucalyptus Kraft Pulp (BEKP) is the most plentiful and more available than other pulps in several countries [63]. BEKP has a white color, odorless, lightweight, high aspect ratio with a length within 1 mm and uniform diameter about 20 μm of individual cellulose fiber, and high cellulose content (>80%), thus, it is used as an alternative source of cellulose fiber in term of cost-effectiveness [62, 64]. The high amount of pure cellulose is because of the removal of other wood components during the pulping and bleaching processes leading to relatively constant fiber aspect ratios (fiber length/fiber width) [62, 65]. Bleached Kraft Pulp has been commonly used in the papermaking industry, but now it is attractively used as natural based reinforcement by many researchers [64, 66-68].

2.2.2. Talcum (Talc)

Talc is a hydrated magnesium silicate with $Mg_3SiO_{10}(OH)_2$ formula. Its chemical structure is shown in Figure 2.3. Talc has a plate-like structure held together by weak Van der Waal's forces so that the talc platelets can be easily dispersed at low shear stress [68]. Talc can play in two roles; acting as nucleating agent at low loading content (< 3 wt.%) and reinforcing filler at high loading content (10 – 40 wt.%).

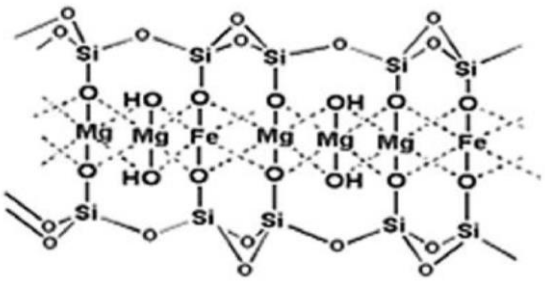

Figure 2.3 Chemical structure of talc [69].

2.3. Reactive agents

2.3.1. Epoxide-based compounds

The epoxide-based reactive agent is one of a highly reactive functional group. In this decade, Epoxide-based reactive agent has been extensively used as a compatibilizer for polymer/polymer blends and also filler/polymer composites. The examples for incorporating epoxide-based reactive agent as a compatibilizer in melt-blending are PLA/PBT blending [70], and also PLA/sisal fiber composite [71] as displayed in Figure 2.4 and Figure 2.5, respectively. The possible chemical reactions during melt blending can occur between the hydroxyl and carboxyl groups the chain ends of polymer or hydroxyl groups of fibers and epoxide groups through ring opening reactions to form covalent bonds [70, 71]. It has been reported that the epoxide groups react more readily with carboxyl groups than with hydroxyl groups [70].

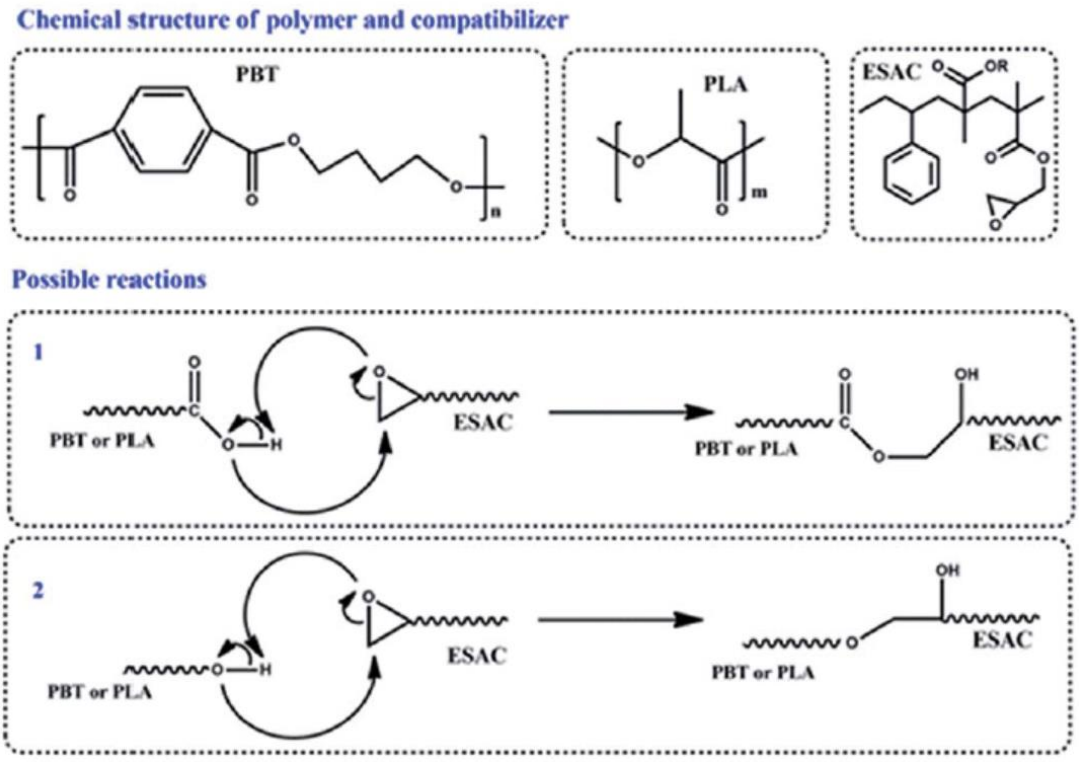

Figure 2.4 Possible reactions between PLA, PBT, and ESAC during melt-blending [70].

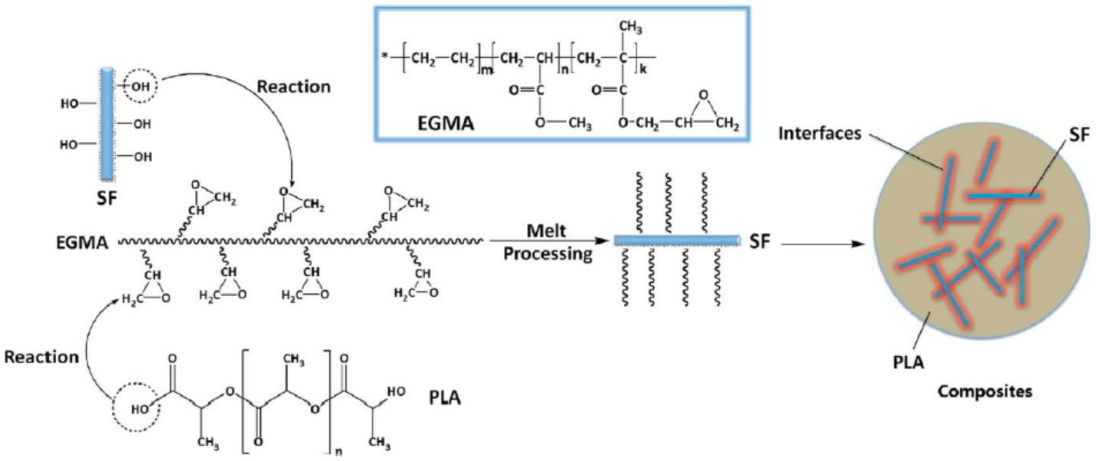

Figure 2.5 Interfacial compatibilization between PLA and SF via *in situ* reaction with EGMA during the melt-blending processing [71].

2.3.2. Anhydride-based reactive agent

In order to improve the adhesion of PLA and cellulose fiber, PLA surface can be chemically modified by grafting with MAH as a coupling agent through free radical reaction as illustrated in Figure 2.6. Firstly, free radical on PLA chains at tertiary carbon was induced by the initiator (peroxide). After that, MA-g-PLA is obtained by the reaction between PLA free radical and the double bond of MAH. Finally, anhydride groups in MA-g-PLA might react with hydroxide groups on fibers to form ester bonds or interact via hydrogen bonding, acting as a coupling agent between matrix and fibers. Therefore interfacial adhesion between fiber and the polymer chain is improved due to bonding between them [47].

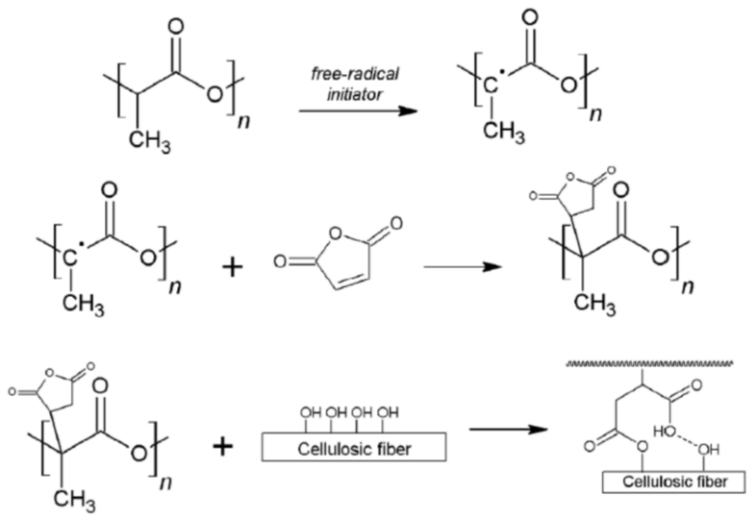

Figure 2.6 Proposed reaction mechanism between MA-g-PLA and cellulose fiber [47].

In another case, the functionalized PLA with MAH is also added to PLA/talc composite for improving their interfacial adhesion. It was expected that PLA-g-MA would react with talc via an esterification reaction as shown in Figure 2.7. The proposed reaction occurs between the anhydride group on PLA-g-MA and the hydroxyl groups on the edge of talc surface, suggesting in the formation of an ester linkage on the talc surface.

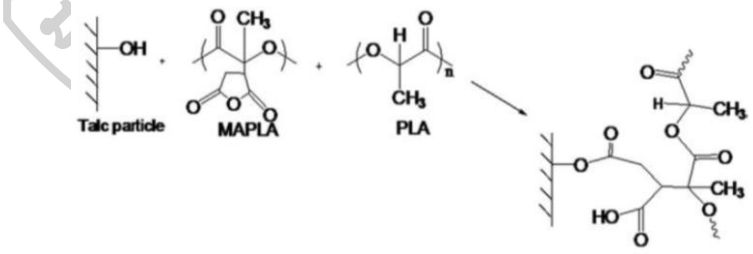

Figure 2.7 Proposed reaction between PLA, talc, and MA-g-PLA [72].

2.4. Fiber reinforced PLA composites

Goriparthi, B.K., and co-workers studied the effect of fiber surface treatments on mechanical properties of PLA/jute composites. PLA/jute composites were fabricated by using a solvent casting method. The tensile strength and modulus of the composites were significantly affected by fiber treatments in order of trimethoxy

methyl silane > 3-amino propyl trimethoxy silane > peroxide > permanganate > alkalization > untreated. Tensile strength and modulus of the composite fiber-treated with trimethoxy methyl silane showed the maximum improvement by 35 and 38%, respectively due to the improvement of fiber/PLA interfacial adhesion. Surface treatments of jute fiber not only resulted in improvement of tensile but also flexural properties, however, it was found the reduction in impact strength [18].

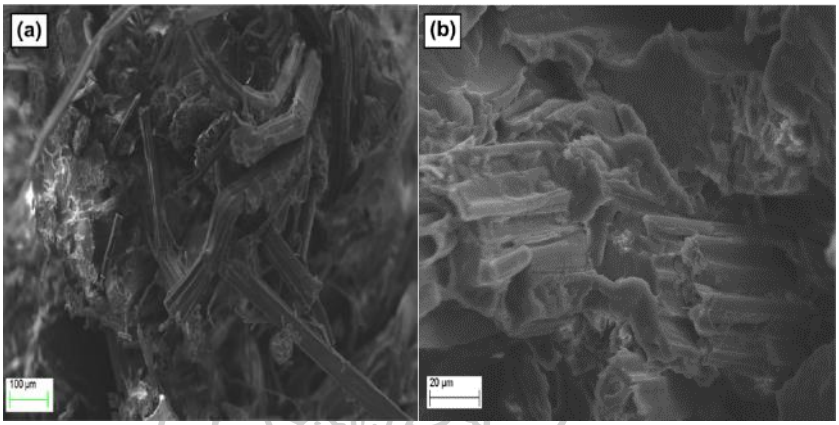

Figure 2.8 SEM micrographs of tensile fracture surfaces of (a) untreated composite (b) trimethoxy methyl silane-treated composite [18].

Gunti, R., and co-workers studied the effect of fiber loading and chemical treatment content of jute fiber on tensile properties of PLA/jute composites. PLA/jute composites were fabricated by melt-mixing using vertical injection molding machine. It was found that the mechanical properties of PLA/jute composites increased with the addition of fiber and then decreased when the fiber content was over 20 wt.%. The highest tensile strength was obtained for 10% NaOH content and H_2O_2 bleaching treated fiber reinforced PLA composite at 25 wt.% fiber loading, which was 7.7% higher than that of neat PLA and untreated fiber. From SEM images, it was revealed that the successive alkali surface treatment improved the compatibility of fiber and PLA matrix [19].

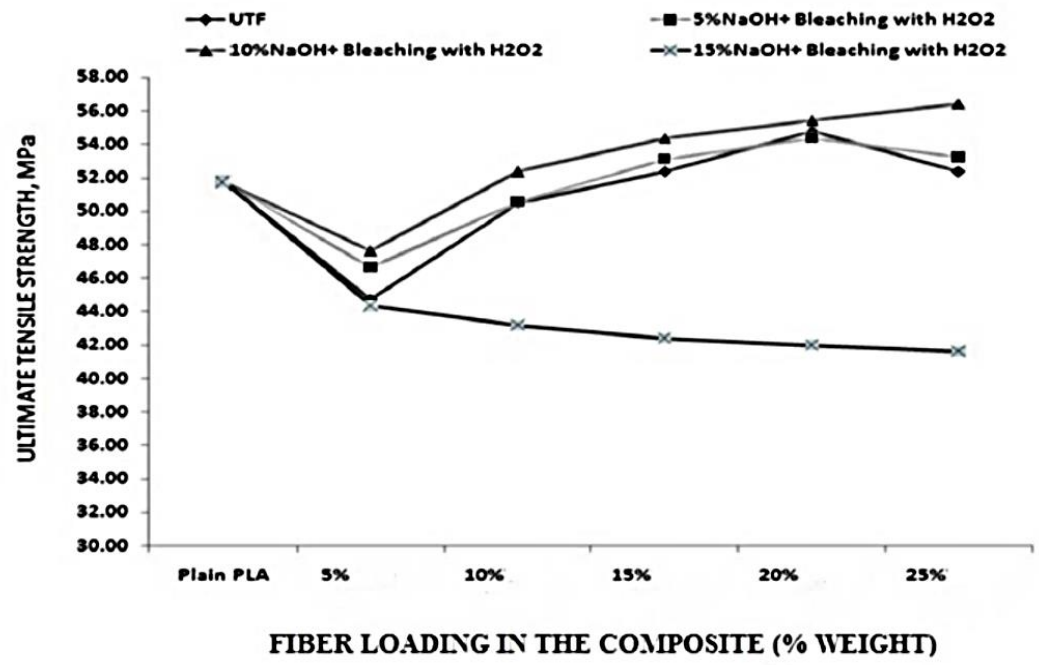

Figure 2.9 Effect of fiber loading and chemical treatment content of jute fiber on the tensile strength of PLA/jute composites [19].

Ren, H., and co-workers studied the mechanical properties of PLA reinforced with Eucalyptus short- and Botnia long- bleached pulp fibers without coupling agent fabricated by a torque rheometer. It was found that the addition of 40 wt.% pulp fiber in PLA composite showed a significantly higher mechanical strength as shown in Figure 2.10. It was suggested that the tensile strength was improved due to the stress transfer from PLA matrix to the added fiber. The impact strength was improved by the pull-out and movement of fiber within PLA matrix, which propagated energy and increased ductility and flexibility, thus, absorbed more impact energy. However, the tensile strength PLA reinforced with short and long fiber was an insignificant difference because both fiber types have pure cellulose with relatively constant aspect ratios. Therefore both fiber types could disperse into the matrix in similar patterns as seen in Figure 2.11, leading to similar stress transfer characteristics [65].

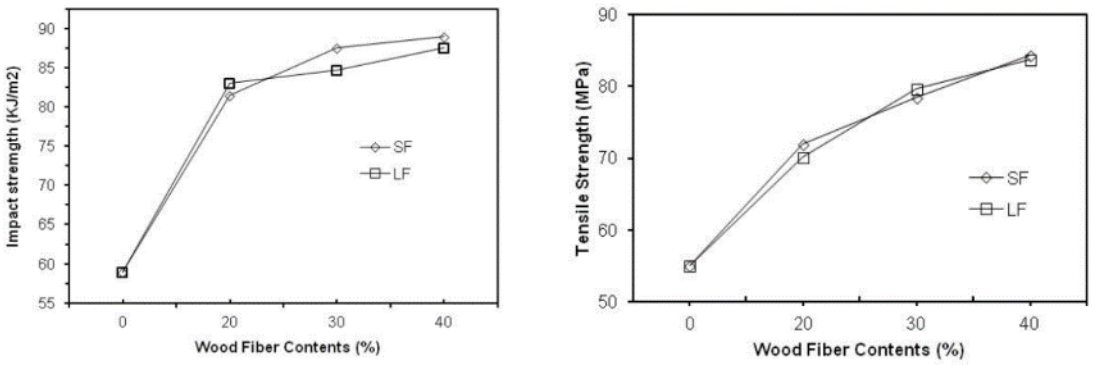

Figure 2.10 Mechanical properties of different pulp fiber contents reinforced PLA composites; light diamonds: short fiber (SF); light squares: long fiber (LF) [65].

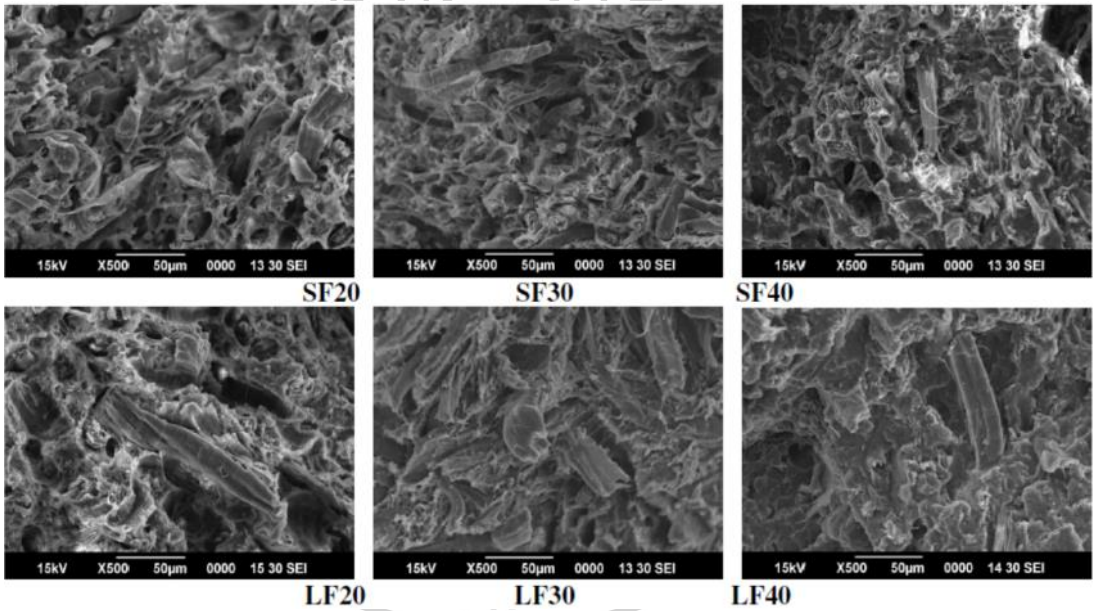

Figure 2.11 SEM micrographs of the fracture surface of PLA composites with short (SF) and long fiber (LF) of various pulp fiber content; 20, 30, and 40% [65].

Pan, Y.J., and co-worker studied the effects of PLA-g-MA on mechanical properties and surface compatibility of PLA/CF composites using DCP as an initiator for the grafting of MA onto PLA. It was found that MA was successfully grafted onto PLA chain as proved by FT-IR analyses so that the mechanical properties of PLA/CF composites were improved. The incorporation of 6 wt.% PLA-g-MA showed the most satisfying results; the tensile strength, tensile modulus, flexural strength flexural

modulus, and impact strength were improved by 7, 150, 18, 20, and 28%, respectively. These were due to the incorporation of PLA-g-MA could improve the interfacial compatibility that was clearly observed in SEM micrographs [73].

Table 2.2 Mechanical properties of PLA/CF composites [73].

Materials	Tensile strength (MPa)	Tensile modulus (MPa)	Elongation at break (%)	Flexural strength (MPa)	Flexural modulus (MPa)	Impact strength (MPa)
PLA/12CF	110.4 ± 3.2	2835.8 ± 28.1	10.6 ± 0.4	133.8 ± 1.0	8422.8 ± 0.0	74.3 ± 2.3
2 wt% (D0.1/M1)	99.6 ± 3.3	6256 ± 102.9	10.9 ± 0.3	155.2 ± 1.4	9822.1 ± 0.0	72.8 ± 4.5
2 wt% (D0.2/M2)	114.9 ± 2.3	6836.7 ± 44.7	11.5 ± 0.2	139.1 ± 3.9	7906.2 ± 0.2	80.9 ± 5.8
2 wt% (D0.3/M3)	100.3 ± 6.2	6437 ± 238.9	10.9 ± 0.7	141.4 ± 1.5	8283.9 ± 0.1	79.4 ± 5.0
4 wt% (D0.1/M1)	107.5 ± 2.9	6889.3 ± 93.4	10.6 ± 0.3	142.3 ± 1.0	9254.3 ± 0.0	78.1 ± 3.4
4 wt% (D0.2/M2)	107.4 ± 2.7	6770.7 ± 61.0	10.9 ± 0.3	140.4 ± 3.2	8384.0 ± 0.1	86.4 ± 4.2
4 wt% (D0.3/M3)	84.0 ± 1.1	5761.7 ± 124.4	10.8 ± 0.2	140.8 ± 2.0	8787.1 ± 0.1	80.9 ± 5.8
6 wt% (D0.1/M1)	113.2 ± 2.2	6752.5 ± 78.3	11.6 ± 0.1	158.3 ± 1.7	10102.6 ± 0.0	95.0 ± 10.5
6 wt% (D0.2/M2)	118.2 ± 2.4	7061.0 ± 51.8	11.4 ± 0.2	149.8 ± 1.7	9901.8 ± 0.0	78.0 ± 2.7
6 wt% (D0.3/M3)	113.0 ± 1.6	7087.0 ± 103.5	11.1 ± 0.1	144.5 ± 0.8	9502.6 ± 0.0	75.4 ± 3.7
8 wt% (D0.1/M1)	114.3 ± 4.1	6990.8 ± 92.4	11.2 ± 0.3	145.2 ± 1.2	9537.1 ± 0.1	79.4 ± 4.0
8 wt% (D0.2/M2)	118.1 ± 1.4	7106.8 ± 22.6	11.6 ± 0.0	146.7 ± 1.9	9012.7 ± 0.1	76.7 ± 1.4
8 wt% (D0.3/M3)	103.6 ± 1.0	6895.0 ± 55.9	10.7 ± 0.0	137.5 ± 0.8	8024.4 ± 0.1	68.8 ± 3.0

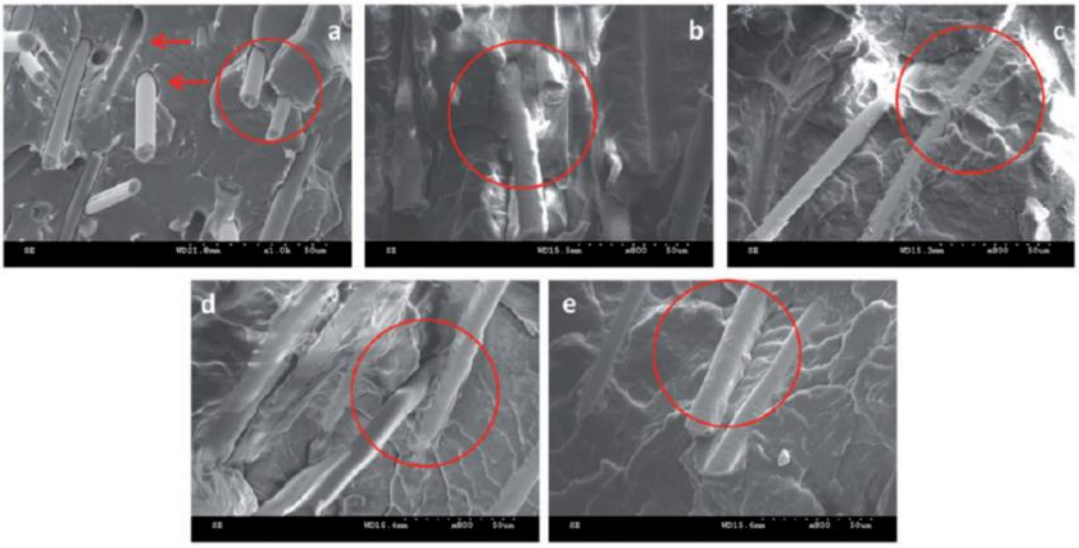

Figure 2.12 SEM micrographs (1000×) the fracture surface of PLA/CF composites containing PLA-g-MA; 0 (a), 2 (b), 4 (c), 6 (d), and 8 wt.% (e) [73].

2.5. Particles reinforced PLA composites

Fowlks, A.C. and co-workers studied the effect of maleated-PLA as an interfacial modifier on mechanical properties of PLA/talc composites. From Figure 2.13, the morphology of the composite without MAPLA (above left) displayed a lot of voids due to talc platelet debonding and no polymer adhered to the edge of talc surface indicating no adhesion at the interface. In PLA/talc composite containing 3% MAPLA (above right), it could be seen that many of the talc particles are placed in the polymer matrix, which the talc platelets were coated with PLA, resulting in fewer cavities and edges around the talc particles and matrix due to moderate adhesion. In addition, the talc platelets were smaller than that of non-compatibilized composite due to more embedded within the polymer. On the other hand, the composite with 5% MAPLA (below left) showed a more ductile failure of fracture surface and a localized deformation of PLA matrix in the form of fibrils. It was also obviously seen that the talc particles were more deeply impeded and failed within the matrix rather than debonded at the interface, indicated strong interfacial adhesion and better wetting of the talc by PLA in this system. These resulted in higher mechanical properties as seen in Table 2.3 due to stronger adhesion allowing effectively transferred from the matrix to filler under the applied load. However, the further MAPLA loading up to 10% (below right), it showed a flat fracture surface indicating brittle behavior characteristic due to rapid crack propagation. This was caused by the high MAPLA content exceeding its solubility limit in PLA, resulting in the lowest tensile strength and elongation at break. The brittle behavior of this composite with excess MAPLA was considered to have two effects; excessing interfacial adhesion between talc and PLA leading to preventing safe debonding of the component phases and/or increasing degradation of the composite leading to lower polymer molecular weight [72].

Table 2.3 Tensile properties of PLA/talc composites [72].

Sample	Tensile strength (MPa)	Young's modulus (GPa)	Elongation at break (%)
PLA	58.7 ± 2.2[a]	3.6 ± 0.2[a]	4.3 ± 1.0[a]
MAPLA	60.2 ± 2.1[a]	4.0 ± 0.2[a]	3.9 ± 0.8[a]
PLA/Talc (60:40)	59.6 ± 2.2[a]	7.0 ± 0.4[b]	1.1 ± 0.2[b]
PLA/MAPLA/Talc (57:3:40)	66.0 ± 3.1[b]	10.1 ± 0.1[c]	0.9 ± 0.1[b]
PLA/MAPLA/Talc (55:5:40)	72.4 ± 1.8[c]	11.1 ± 1.9[c]	1.5 ± 0.1[b]
PLA/MAPLA/Talc (55:10:40)	24.1 ± 2.3[d]	11.4 ± 1.7[c]	0.3 ± 0.1[c]

[a–d]Letters within the same column represent statistical significant differences at the 95% confidence level.

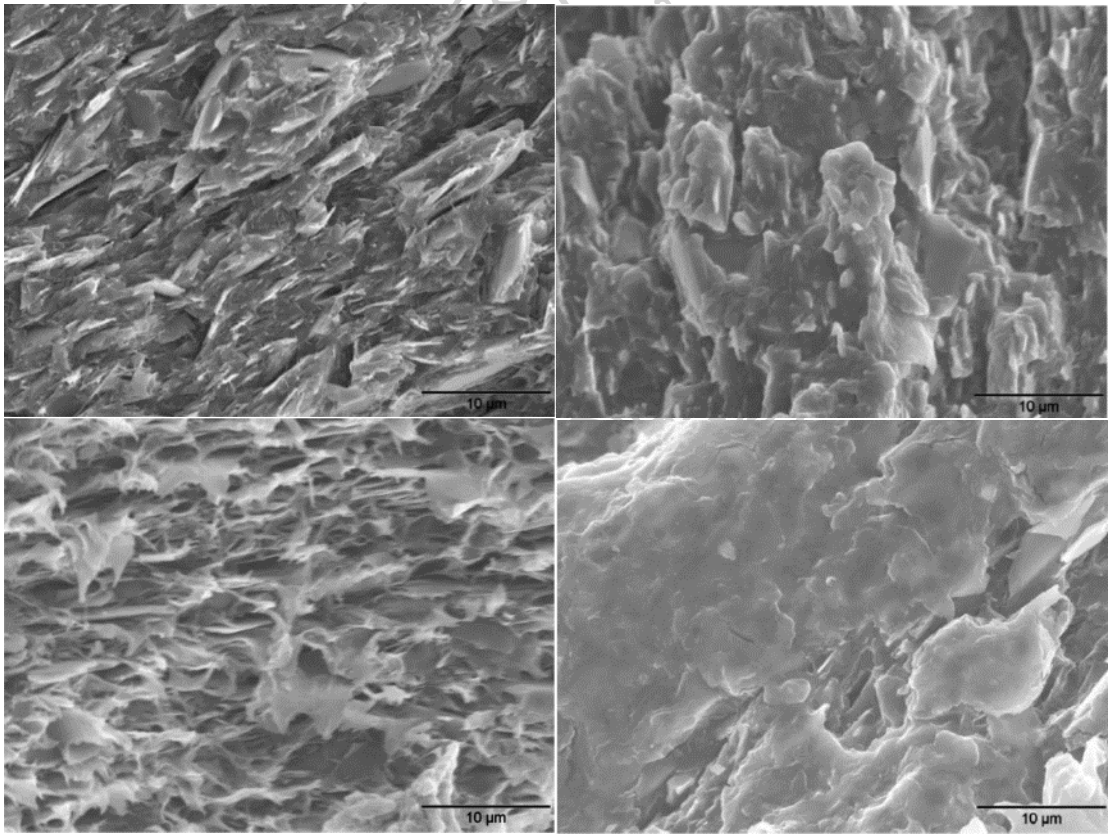

Figure 2.13 SEM micrographs of PLA/talc composites containing various content of MAPLA; 0% (above left), 3% (above right), 5% (below left), and 10% (below right) [72].

2.6. Fiber/particle reinforced PLA hybrid composites

Huda, M.S., and co-workers studied the effect of silane treated- and untreated-talc on the mechanical properties of PLA/newspaper fiber/talc hybrid composites. The hybrid composites were fabricated by melt-mixing using micro-extruder (screw length 150 mm). It was found that the storage modulus of PLA incorporated with the fiber and/or talc was increased for both treated and untreated talc, which acted as a stiff agent for PLA matrix and the effect of the silane-treated talc was more powerful. PLA crystallinity in PLA/newspaper fiber sample was decreased when talc was loaded, indicated that the fibers and talc impeded the diffusion and migration of PLA molecular chains to the surface of the nucleus in the hybrid composites. It was also suggested that the decrease in crystallinity helped to improve the impact strength of 1.6% of the hybrid composite due to the flexibility of molecular chains. In the case of PLA/newspaper fiber with silane-treated talc, the Izod impact strength was increased by 2.3 % due to better filler/matrix interfacial adhesion as seen in SEM micrographs [30].

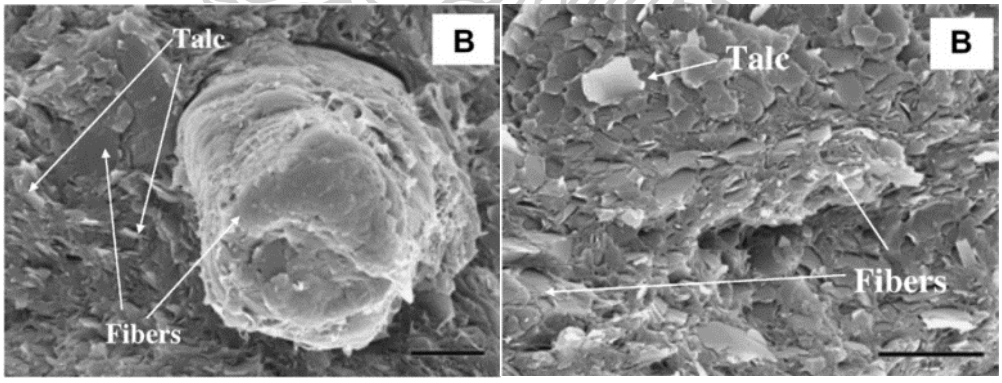

Figure 2.14 SEM micrographs of impact fracture surface of PLA/newspaper/talc (60/30/10 wt.%) hybrid composite (— 5 μm); untreated talc (left) and treated talc (right) [30].

Charpter 3 Research methodology

The experimental was divided into three sections and could be summarized as a flowchart shown in Figure 3.1 - Figure 3.3.

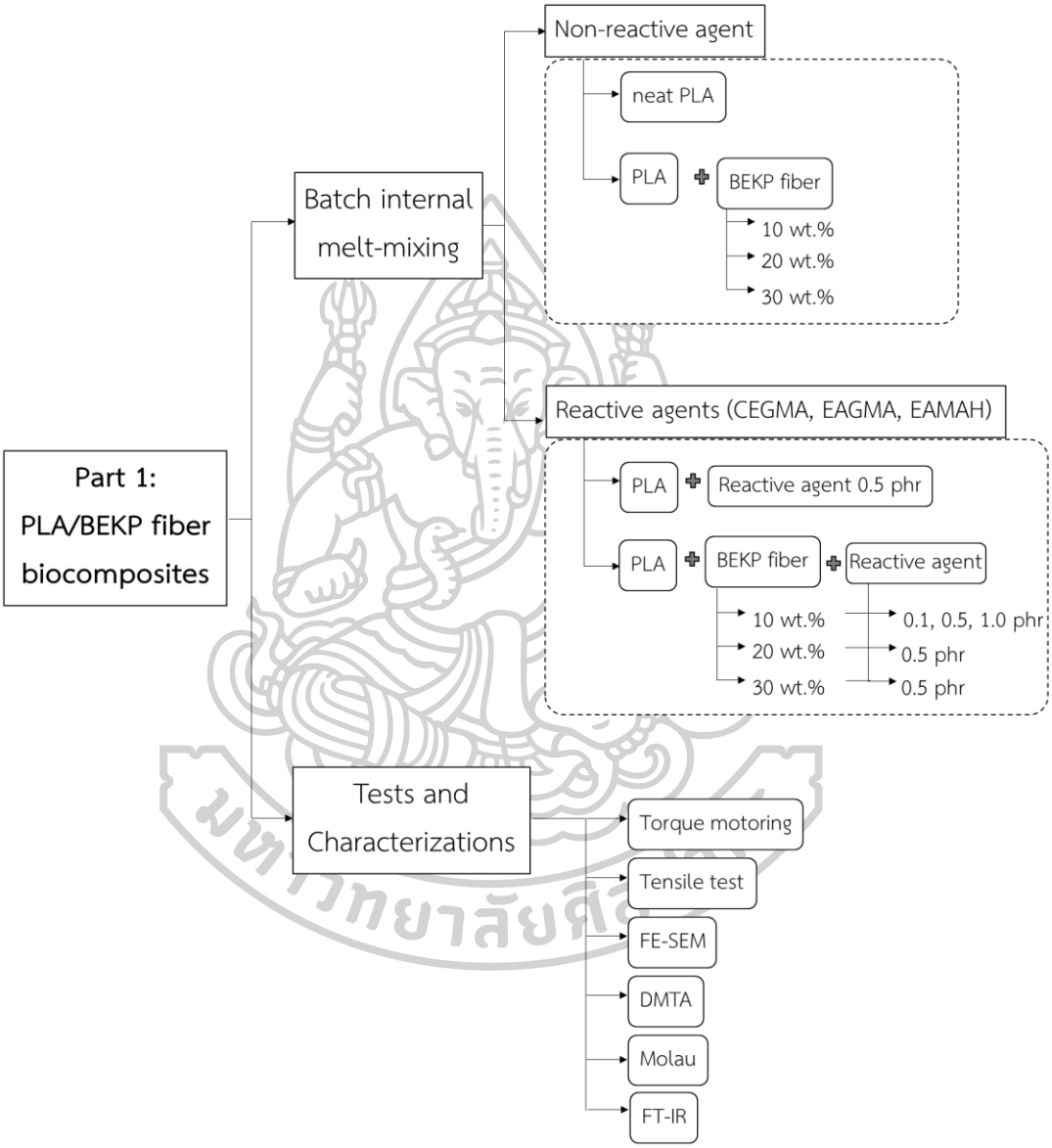

Figure 3.1 Schematic experimental setup of section 1.

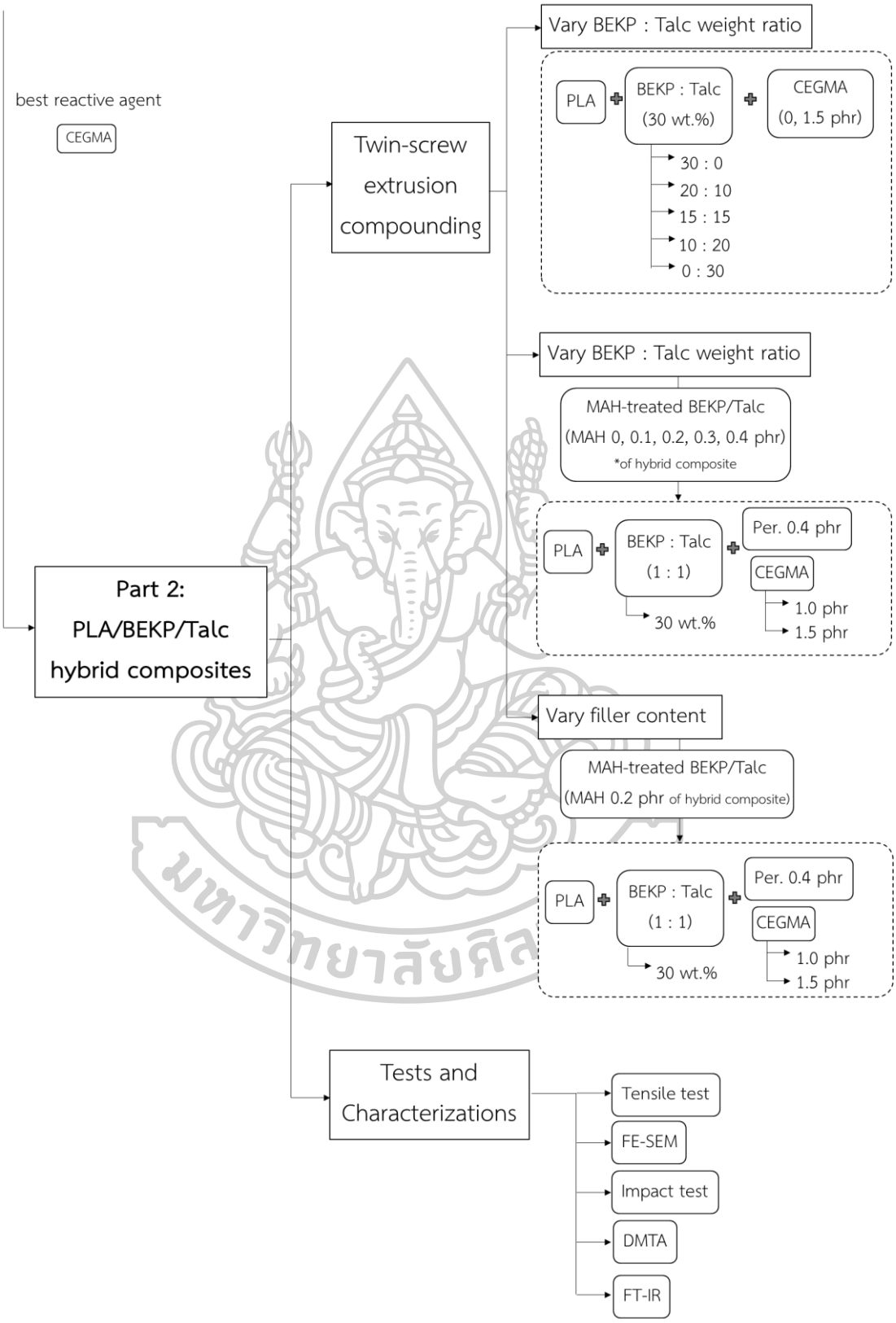

Figure 3.2 Schematic experimental setup of section 2.

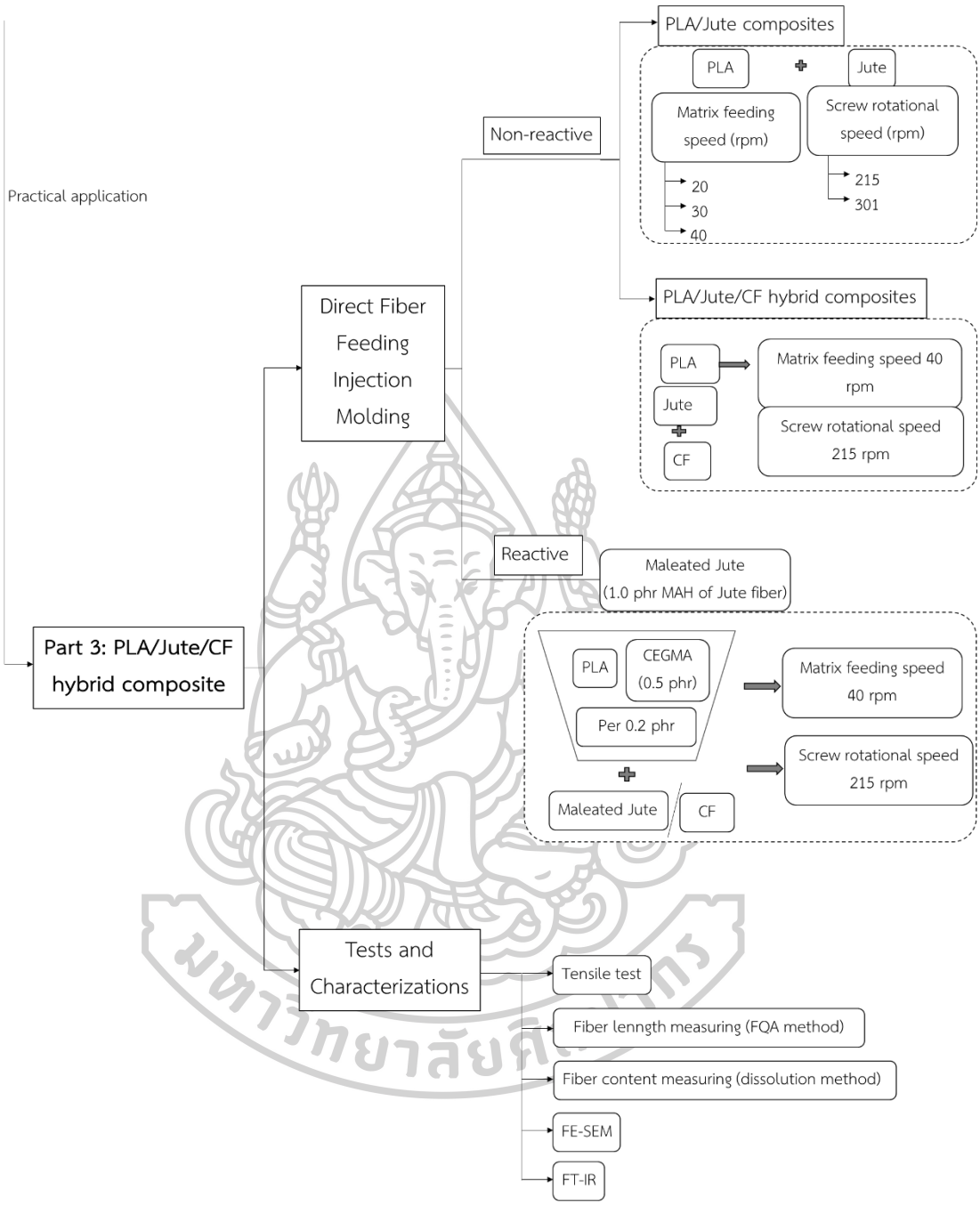

Figure 3.3 Schematic experimental setup of section 3.

3.1. Preparation of PLA/BEKP fiber biocomposites with and without three different reactive agent types

3.1.1. Materials

Poly(lactic acid) (PLA) (injection grade, 3052D) used as a polymer matrix, was purchased from NatureWorks® LLC (USA). Reinforcement fiber, Bleach Eucalyptus Kraft Pulp (BEKP) was kindly supplied by SCG Packaging PLC., shown in Figure 3.5. BEKP fiber was analyzed by Fiber Quality Analyzer (FQA) assisted by SCG packaging PLC that the average length and diameter were 0.538 mm and 13.90 μm, respectively. Chemical compositions of the BEKP fibers were 83 - 86% α-cellulose, 12 - 15% hemicellulose, 1.5% lignin and less 0.5% extractives, which were analyzed according to Technical Association of the Pulp and Paper Industry (TAPPI) standard T 223 cm-01, T 236 om-99, T 203 cm-99 and T 222 om-02. Multi-epoxide group chain extender, Joncryl® ADR-4368 (designated as CEGMA) was obtained from BASF Chemical Co., Ltd Thailand. Reactive agents, terpolymer (ethylene, acrylic ester, and glycidyl methacrylate) Lotader® AX8900 (designated as EAGMA) and a random terpolymer (ethylene, acrylic ester and maleic anhydride) Lotader® 4210 (designated as EAMAH) were kindly provided by 2 A.M. Connection Co. Ltd., Thailand. The chemical structures of three reactive agents were presented in Figure 3.4

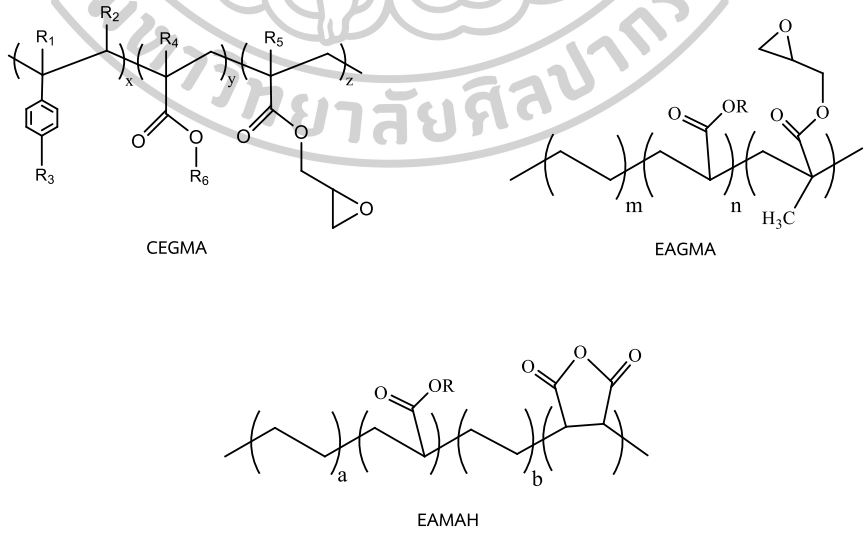

Figure 3.4 Chemical structures of three reactive agent types.

Figure 3.5 Bleached Eucalyptus Kraft Pulp fiber.

3.1.2. Preparation of PLA/BEKP biocomposites with and without a reactive agent

BEKP was dried at 80 ℃ and then ground to obtain short fibers using a high-speed grinder, with 28,000 rpm rotation speed. Prior to melt mixing, BEKP fiber was dried at 80 ℃ for 24 hrs but PLA was dried at 60 ℃ for 6 hrs in a hot air oven. Three types of multifunctional group compounds including CEGMA, EAGMA, and EAMAH used as reactive agents in PLA biocomposites. The composites were prepared in an internal mixer (Chareon tut CO. LTD., model MX 105-D40L50) with 60 rpm rotational speed and 190 ℃ of the temperature. The effect of BEKP fiber content 10, 20 and 30 wt. % of PLA, with and without reactive agent 0.5 phr, on properties of composites, were studied. To study effect content, reactive agent were varied 0.0, 0.1, 0.5 and 1.0 phr in 10 wt% BEKP fiber content PLA composites. The evolution torque of internal mixer for PLA biocomposites was monitored during melt-blending for a reaction time of 10 to 15 minutes.

3.1.3. Testing and characterizations

3.1.3.1. Tensile testing

Tensile specimens of neat PLA and PLA biocomposites with and without reactive agent were molded at 190 ℃ and 1,000 psi pressure for 4 minutes pre-heating and 1 minutes compressing using compression molding machine (Chareon tut CO. LTD.). Tensile properties were investigated using a universal testing machine (Instron 5969) in accordance with ASTM D638, specimen type V using 5 kN load cell.

Tensile testing was carried out in ambient conditions using a cross-head speed of 1 mm/min. All the reported values were obtained by averaging over five specimens.

3.1.3.2. Field Emission Scanning Electron Microscopy (FE-SEM)

For SEM analysis technique, PLA biocomposite samples were sputter-coated with a thin layer of gold/palladium to avoid charging. The tensile fracture surface morphology of PLA biocomposite specimens was observed by Field Emission Scanning Electron Microscope (FE-SEM) using TESCAN MIRA3 LMH Schottky machine at an accelerating voltage of 5 kV.

3.1.3.3. Dynamic mechanical thermal analysis (DMTA)

Neat PLA and PLA biocomposites were molded to the rectangular dimension of 10 × 1.16 × 40 mm3 for DMTA specimen by compression molded at 190 °C and 1,000 psi at the condition of pressing for 1 minute after pre-heating for 4 minutes. Dynamic mechanical thermal properties of PLA biocomposites were investigated by using an ANTON PAAR, Modular Compact Rheometer (MCR302) equipped with rectangular fixtures (SRF) holder under the DMTA torsion mode at a frequency of 1 Hz. A temperature sweep was carried out from 30 to 110 °C at a heating rate of 3 °C/min.

3.1.3.4. Molau test

Molau test was performed by dissolving 0.5 g of PLA biocomposite samples in 10 mL chloroform and thoroughly shaking. The solutions were left to stand for 48 hrs at room temperature before the visual observation recorded by a digital camera.

3.1.3.5. Fourier transformation infrared spectroscopy (FT-IR)

The BEKP fiber in Molau test solution was filtered and PLA solution was removed. Each filter fiber sample was rinsed and stirred in 50 mL chloroform and washed for three times to ensure that PLA was completely removed. The fiber was collected via filtration by vacuum suction. Afterward, the extracted fibers were dried in an oven at 80 °C for 24 hrs to complete solvent removal. Finally, the filtered fiber samples were analyzed by using FT-IR spectrometer (VERTEX70) at a 32 scans

resolution of 4 cm^{-1} in the spectral range of 4000-400 cm^{-1} in comparison with virgin BEKP.

3.2. Preparation of PLA/BEKP fiber/talc hybrid biocomposites with and without the selected reactive agent

3.2.1. Materials

PLA (injection grade, 3052D) was purchased from NatureWorks® LLC (Minnetonka, MN, USA). Bleach Eucalyptus Kraft Pulp (0.538 mm in average length and 13.90 μm in diameter) was kindly supplied by SCG Packaging PLC., Ratchaburi, Thailand. Talcum, 1250 grade was purchased from Thai Poly Chemicals Co., Ltd., Samut Sakhon, Thailand. An epoxy-based chain extender Joncryl® ADR-4368 (designated as CEGMA) was obtained from BASF Chemical Co., Ltd., Bangkok, Thailand. Maleic anhydride, 99.0% purity, (designated as MAH) was purchased from Sigma-Aldrich, Bangkok, Thailand. Peroxide (Perkadox® 14-40B-pd) was purchased from AkzoNobel (Bangkok, Thailand). Ethanol and chloroform were purchased from Better Syndicate Co., Ltd., Bangkok, Thailand.

3.2.2. Preparation of PLA/BEKP and PLA/Talc composites

Since the fiber could not be directly loaded along with PLA into twin-screw extruder, PLA/BEKP master blend was prepared. PLA 40 g was dissolved in 1000 ml of chloroform using a mechanic stirrer at 60 °C for 30 min and then 60 g of BEKP fiber was added. The suspension of mixed PLA/BEKP was evaporated to remove chloroform solvent at room temperature for 1 hr and then dried at 80 °C in a hot air oven for 6 hrs. Finally, the dried mixed PLA/BEKP was crushed into particles used as PLA/BEKP master blend, which was shown in Figure 3.6 (a). Talc was dried at 80 °C in a hot air oven for 24 hrs. Preparation of PLA/BEKP or PLA/Talc composites with 30 wt.% loading were done in twin-screw extruder (SHJ-36, L/D = 40, ENMACH Co., Ltd., Nonthaburi, Thailand), which temperature profile from the feed zone to die as 130, 140, 150, 170, 180, 190, 190, 180, 170, and 170 °C under a screw speed of 150 rpm. PLA composite extrudates were cut to pellets and then dried for 24 hrs at 60 °C in a hot air oven.

Figure 3.6 PLA/BEKP blend particles (a) and mixed BEKP fiber/talc particles (b).

3.2.3. Preparation of PLA/BEKP/Talc Hybrid Composites with CEGMA

Since the fiber and talc could not be directly loaded along with PLA into twin-screw extruder, BEKP/talc was firstly prepared into the particle form. 100 g of BEKP fiber/talc in various ratio; 2:1, 1:1 and 1:2 were added into 300 ml of ethanol by first dispersing talc in ethanol followed by adding BEKP fiber. The mixed suspension of BEKP fiber/talc was continuously stirred for 2 min using an electric mixer at room temperature to obtain the particles of mixed of BEKP fiber/talc as shown in Figure 3.6 (b). After that, mixed particles of BEKP/talc were dried at 80 ℃ in a hot air oven for 24 hrs. Finally, mixed particles of BEKP fiber/talc were obtained as particles ranging between 2–7 mm in diameter. For studying the effect of BEKP/talc ratios with and without CEGMA, PLA with and without 1.5 phr CEGMA was loaded along with 30 wt.% in various ratios of mixed particles into a hopper and then mixed in a twin-screw extruder as the same conditions as previous. After that, PLA hybrid composite extrudates were cut to pellets and then dried for 24 hrs at 60 ℃ in a hot air oven.

3.2.4. Preparation of PLA/maleated-BEKP/Talc Hybrid Composites with CEGMA and peroxide

In order to provide more reactive site on filler surface, BEKP fiber and talc were treated with MAH. MAH in various content of PLA hybrid composite related to

maleated BEKP/Talc preparation per batch was shown in Table 3.1. MAH was firstly dissolved in 300 ml ethanol and then 100 g of BEKP fiber/talc in 1:1 ratio was added into ethanol in the following order; talc then BEKP fiber under stirring for 2 min at room temperature. After that, mixed particles of BEKP fiber/talc were dried at 80 ℃ in a hot air oven for 24 hrs. Finally, mixed particles of BEKP fiber/talc were obtained as particles ranging between 2–7 mm in diameter. PLA hybrid composite with 20, 30 and 40 wt.% of maleated BKEP/talc and 1.0 or 1.5 phr of CEGMA were blended in a twin-screw extruder as the same conditions as previous. After that, PLA hybrid composite extrudates were cut to pellets and dried for 24 hrs at 60 ℃ in a hot air oven. Schematic representation of the facile preparation of reactive PLA/maleated BEKP/Talc hybrid composites was shown in Figure 3.7.

Table 3.1 MAH contents in PLA hybrid composite.

Compositions in PLA hybrid composite			**Maleated BEKP/Talc preparation per batch**	
PLA (wt.%)	Filler (wt.%) (BEKP:Talc = 1:1)	MAH (phr)	Filler (g) (BEKP:Talc = 1:1)	MAH (g)
80	20	0.2	100	1.00
70	30	0.1	100	0.33
70	30	0.2	100	0.67
70	30	0.3	100	1.00
70	30	0.4	100	1.33
60	40	0.2	100	0.50

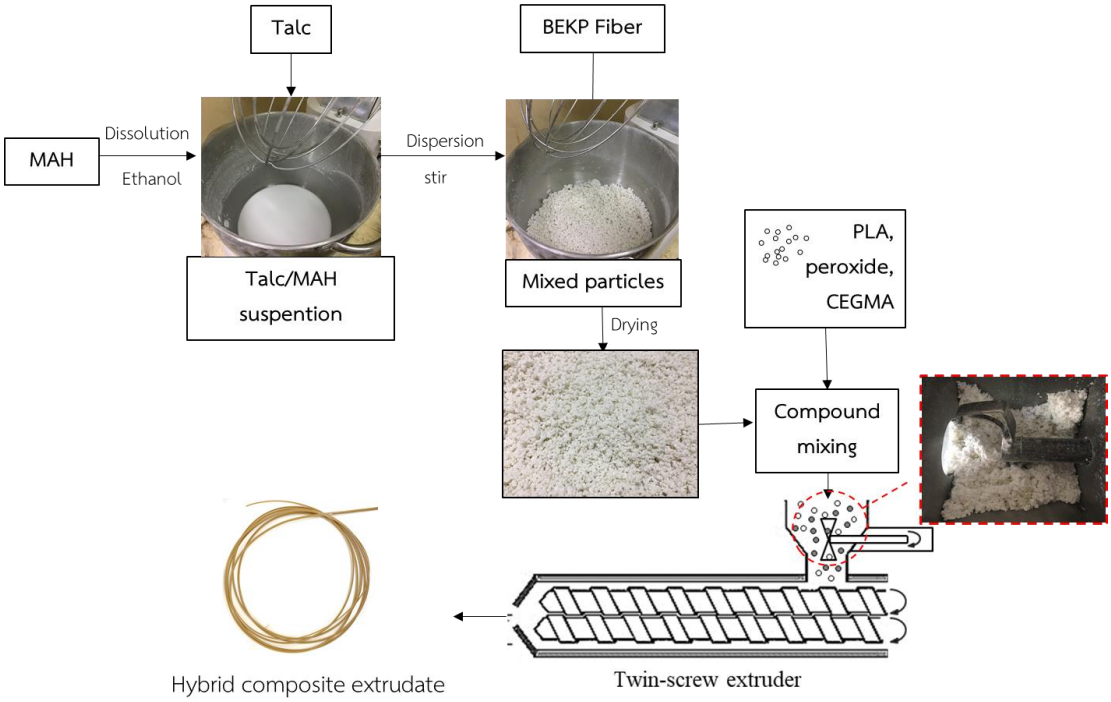

Figure 3.7 Schematic representation of the facile preparation of reactive PLA/maleated BEKP/Talc hybrid Composites

3.2.5. Tensile and impact specimens preparation

After drying, neat PLA and PLA hybrid composite pellets were injected to tensile and impact specimens using the injection molding machine (SM-22, BatteBEKPeld, Kottingbrunn, Austria). The processing conditions for the injection molding are summarized as follows: Nozzle temperature and mold temperature were 190°C and 25°C and cooling time was 42 s, respectively.

3.2.6. Testing and Characterization

3.2.6.1. Mechanical Properties

Mechanical properties were carried out by using a universal testing machine (Instron 5969, Norwood, MA, USA) according to ASTM D638, specimen type I using 5 kN load cell. The testing was conducted under ambient conditions using a cross-head speed of 5 mm/min. All reported values were obtained as averages of five specimens at least.

The Universal Pendulum Impact Tester (Instron, CEAST 9050) was used to determine the impact resistance of the hybrid composites. V-notched Hybrid composite specimens were tested according to ASTM D 256 (Izod standard) at impact energy of 2.75 Joules and the default release angle of 150. For each test, at least five specimens were tested and the average values were reported.

3.2.6.2. Morphological Observation

The tensile fracture surface morphology of PLA composite and hybrid composite specimens were observed using a Field Emission Scanning Electron Microscope (FE-SEM) (TESCAN MIRA3 LMH Schottky, Brno, Czech Republic) at an accelerating voltage of 5 kV. Prior to observations, the samples were sputter coated with a thin layer of gold/palladium to avoid charging.

3.2.6.3. Dynamic-Mechanical Thermal Analysis (DMTA)

DMTA specimens of PLA composite and hybrid composite were compression molded at a temperature of 190°C with pre-heated for 4 min and then compressed at 1000 psi pressure for 1 min to obtain DMA specimens of dimensions of 10 × 1.16 × 40 mm^3. Dynamic-mechanical thermal properties of PLA composites and the hybrid composite were tested on torsion mode using an ANTON PAAR, modular compact rheometer (MCR302, Graz, Austria) equipped with rectangular fixture (SRF) holders. A temperature was heated sweep from 30 to 110 °C at a heating rate of 3 °C/min under the DMTA torsion mode at a frequency of 1 Hz.

3.2.6.4. Fourier transformation infrared spectroscopy (FT-IR)

In order to investigate the reaction between MAH and BEKP or talc during the drying process at 80 °C, BEKP or talc was dispersed in MAH solution and then dried at 80 °C for 24 hours. After that BEKP or talc with MAH was washed with acetone to remove of unreacted MAH and then dried again at 80 °C for 24 hrs. The BEKP or talc with and without MAH was analyzed by using FT-IR spectrometer (VERTEX70) in 32 scans at a resolution of 4 cm^{-1} for background and sample in the spectral range of 4000-400 cm^{-1}. The extracted BEKP fiber from the non-reactive and reactive hybrid composites was also characterized to reveal the reaction.

3.3. Preparation of PLA/Jute/Carbon fiber hybrid composites with and without reactive agents

3.3.1. Materials

PLA (injection grade, 3052D) was purchased from NatureWorks® LLC (Minnetonka, MN, USA). Jute and/or Carbon fiber were used as reinforcement for PLA as shown in Figure 3.8. Rope of Jute fiber with 1 mm diameter for each (Taisonghua company, Thailand) was kindly supplied from Dr. Putinun Uawongsuwan, lecture at King Mongkut's University of Technology North Bangkok. Carbon fiber (CF), (type T300B, filaments 12000-50B) was purchased from Toraca Company, Japan. An epoxy-based chain extender Joncryl® ADR-4368 (designated as CEGMA) was obtained from BASF Chemical Co., Ltd., Bangkok, Thailand. Maleic anhydride, 99.0% purity, (designated as MAH) was purchased from Sigma-Aldrich, Bangkok, Thailand. Peroxide (Perkadox® 14-40B-pd) was purchased from AkzoNobel (Bangkok, Thailand). Acetone and chloroform were purchased from Better Syndicate Co., Ltd., Bangkok, Thailand.

Figure 3.8 Jute (left) and CF (right) fiber.

3.3.2. Preparation of tensile specimen of non-reactive PLA/Jute and PLA/CF composites and non-reactive PLA/Jute/CF fiber Hybrid composite

The dumbbell-tensile specimens were carried out through the direct fiber feeding injection molding (DFFIM) technique using 18-ton injection molding machine (model iM18, Sumitomo Heavy Industries, Ltd). The schematic drawing of short-fiber of Jute and/or CF reinforced PLA were fabricated using DFFIM technique was displayed in Figure 3.9. Long Jute and/or CF fiber were directly guided into the devolatilizing vent unit of injection barrel and fed into the melt by the shearing

rotation of the injection screw during plasticization process [41]. Meanwhile, PLA pellets were normally fed through a hopper of the injection molding machine, which was replaced with the controllable feeding hopper in order to control the fed amount of PLA resin [41]. The temperature profile in the screw barrel was 190/200/200/195 °C from feed to die zone and the mold temperature was 40 °C. The processing conditions as matrix feeding rate (30, 40 and 50 rpm), screw speed (215 and 301 rpm) were varied to study their effect on properties of the composite and hybrid composite.

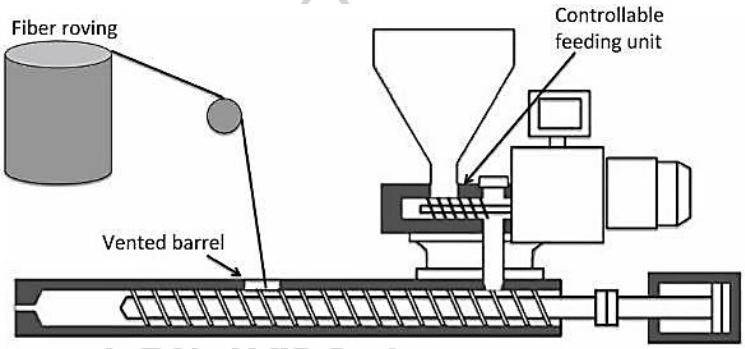

Figure 3.9 Schematic drawing of DFF injection molding process [74].

3.3.3. Preparation of tensile specimen of reactive PLA/Jute Composites and reactive PLA/Jute/CF fiber Hybrid Composites

Firstly, 0.05 g MAH (1.0 phr of jute fiber content) was dissolved in 20 ml acetone and 5 g jute fiber was added into the solution. After that, maleated jute fiber was dried at 80 °C in a hot air oven for 24 hrs while PLA was dried at 60 °C for 6 hrs. Long jute fiber with and without CF fiber was directly fed into vent area of injection barrel with constant 215 screw speed. Meanwhile, PLA pellet, which premixed with 0.2 phr peroxide and 0.5 phr CEGMA, was normally fed through a hopper of injection molding machine at 30, 40 and 50 rpm matrix feeding speed. The temperature profile in the screw barrel was 190/200/200/195 °C from feed to die zone.

3.3.4. Testing and characterizations

3.3.4.1. Tensile testing

The tensile specimen of neat PLA, PLA/Jute composites and PLA/Jute/CF hybrid composites with and without a reactive agent were investigated using a universal testing machine (Instron 5969) in accordance with ASTM D638, specimen type IV using 5 kN load cell. The specimens were carried out under ambient conditions using a cross-head speed of 5 mm/min. All the reported values were obtained by averaging over five specimens.

3.3.4.2. Fiber Content Measuring by dissolution method

Firstly, the weight of PLA/Jute composites and PLA/Jute/CF hybrid composites sample were measured (designated as W_{comp}). After that, PLA in composites and hybrid composites samples was dissolved in excess chloroform solvent. After three days, jute and/or CF fiber could be separated from PLA solution and removed out. Each fiber sample was retransferred to chloroform and stirred and washed three times to ensure the complete removal of PLA. The fiber was collected via filtration by vacuum suction. Afterward, the fibers were dried in an oven at 80 °C for 24 hrs to complete solvent removal. After drying, the weight of dried jute and CF fiber was measured (W_{fiber}). The fiber content in composite and hybrid composite was calculated by equation (1)

$$\text{Fiber content (wt.\%)} = (W_{fiber}/W_{comp})\times 100 \quad (1)$$

The average length and diameter of jute fiber were also analyzed by Fiber Quality Analyzer (FQA) assisted by SCG packaging PLC.

3.3.4.3. Morphological Observation

In order to observe the interfacial adhesion between fiber and PLA matrix, the tensile fracture surface morphology of PLA composite and hybrid composite specimens were observed using a Field Emission Scanning Electron Microscope (FE-SEM) (TESCAN MIRA3 LMH Schottky, Brno, Czech Republic) at an accelerating voltage of 5 kV. Prior to observations, the samples were sputter coated with a thin layer of gold/palladium to avoid charging.

3.3.4.4. Fourier transformation infrared spectroscopy (FT-IR)

In order to investigate the reaction between MAH and jute fiber during the drying process at 80 ℃, jute fiber was dispersed in MAH and then dried at 80 ℃ for 24 hrs. After that jute fiber with MAH was washed with acetone to remove of unreacted MAH and then dried again at 80 ℃ for 24 hrs. The jute fiber with and without MAH was analyzed by using FT-IR spectrometer (VERTEX70) at a resolution of 4 cm^{-1} with background and sample 32 scans in the spectral range of 4000-400 cm^{-1}. The extracted jute fiber from the non-reactive and reactive hybrid composites was also characterized to reveal the reaction.

Charpter 4 Results and discussion

In this chapter, the properties of PLA biocomposites and hybrid composites were disscussed. A series of experiments were performed to study the rheological, mechanical, dynamic mechanical thermal properties and morphology of PLA biocomposites and hybrid composites. In the first part, the effect of reactive agent types and contents as *in situ* compatibilizer in PLA/BEKP fiber biocomposites were discussed. In the second part, the properties of PLA/BEKP fiber/Talc hybrid composites with and without the selected reactive agent from the first part were discussed. In addition, the maleic anhydride was grafted onto the BEKP fiber in order to provide more reactive BEKP fiber on the surface. The MAH-treated BEKP/talc reinforced hybrid composites with reactive agent were prepared by a twin-screw extruder. The third part, reactive PLA hybrid composite with another natural fiber as jute and synthetic fiber as carbon fiber were prepared in direct fiber feeding injection molding. The effect of Jute-g-MAH and reactive agent content on direct fiber feeding composites were studied. Experimental and analysis results were described in detail below.

4.1. Properties of PLA/BEKP fiber biocomposites with and without reactive agents

The properties of PLA/BEKP fiber biocomposites containing BEKP fiber; 0, 10, 20 and 30 wt.% were investigated. The effect of reactive agent types, such as multifunctional epoxide-based and anhydride-based reactive agents, and contents as *in situ* compatibilizer were also studied.

4.1.1. Rheological properties of PLA biocomposites

4.1.1.1. Effect of fiber concentrations and reactive agent types

The torque value was monitored and evaluated for the reaction of PLA biocomposites during mixing in the molten state. The plot of torque against mixing time in the molten state of neat PLA and PLA/BEKP biocomposites containing various BEKP contents ranging from 10 to 30 wt.% was shown in Figure 4.1. The first torque

peak or maximum torque corresponded to the maximum mechanical shear forces required for causing PLA resin to flow. The torque was suddenly decreased when PLA became completely molten. After the initial mixing for each of PLA/BEKP biocomposite, a secondary torque peak was observed due to the presence of the fiber in the melt. The results showed that as the BEKP content was increased, the torque increased. The increase in secondary torque with the addition of BEKP fiber was ascribed to an increase in shear force that was needed to mix BEKP with molten PLA. This occurred towards the end of the mixing process where the equilibrium torque was noticed, which was depended on the BEKP content loading. It was observed that neat PLA and PLA loaded with 10 and 20 wt.% fibers showed the equilibrium torque after mixing for 10 minutes whereas PLA loading 30 wt.% fiber showed the equilibrium torque after mixing for 15 minutes due to a high volume of fiber content. PLA/BEKP biocomposite containing 30 wt.% exhibited the highest secondary and equilibrium torque values.

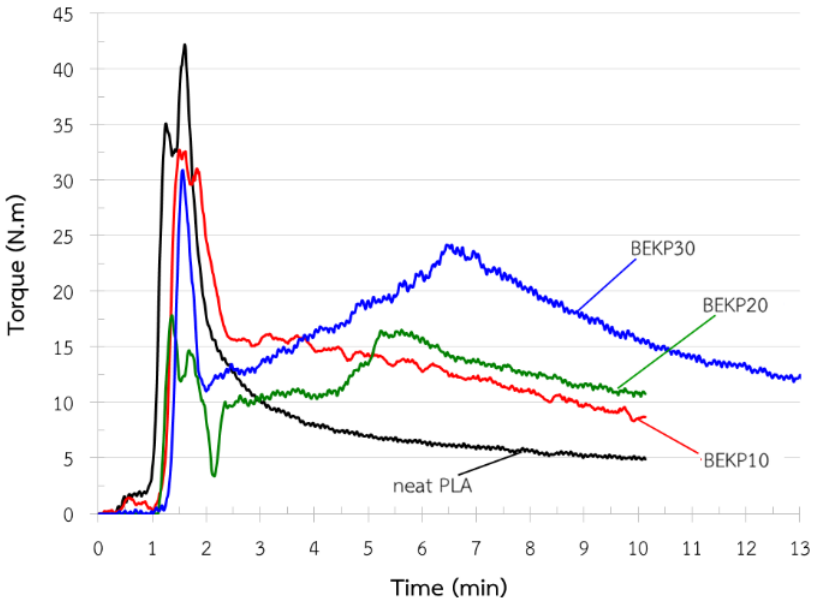

Figure 4.1 Plot of torque as a function of mixing time in the molten state for neat PLA and PLA containing 10, 20 and 30 wt.% of BEKP.

The plots of torque against mixing time in the molten state for neat PLA and PLA/BEKP biocomposites containing various BEKP contents ranging from 10 to 30

wt.% with a constant loading 0.5 phr of different reactive agent types (CEGMA, EAGMA, and EAMAH) were shown in Figure 4.2 and Figure 4.3. After mixing for 10 minutes, it was observed that PLA incorporated with CEGMA, EAGMA and EAMAH showed an equilibrium torque increase of 85, 34 and 8%, respectively, which were higher than that of neat PLA as shown in Figure 4.2. It was well known that an increase in torque value was associated with an increase in molten polymer viscosity, due to an increase in molecular weight [75]. For all BEKP contents loading into PLA as shown in Figure 4.3, it was shown that the equilibrium torque values were significantly increased with the presence of CEGMA in biocomposite compared to non-reactive PLA biocomposite. In contrast, the presence of EAGMA or EAMAH showed a slight decrease in torque values and an insignificant change in the equilibrium torque values compared to non-reactive PLA biocomposite. It was also reported that torque value increased with the presence of several bonding agents in composites because of stronger fiber-matrix interfacial adhesion, leading to a stronger, stiffer and harder of the composite [76].

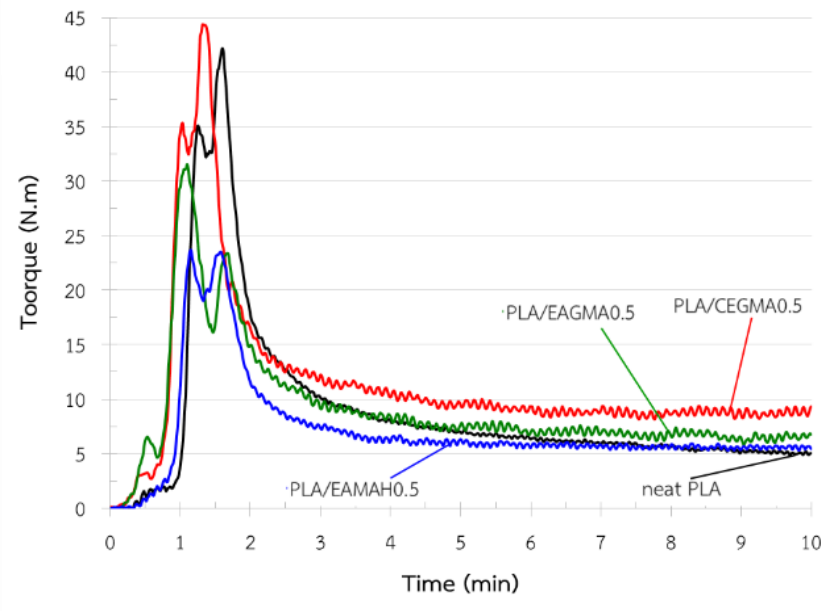

Figure 4.2 Plot of torque as a function of mixing time in the molten state for neat PLA and PLA with different reactive agents loading at 0.5 phr.

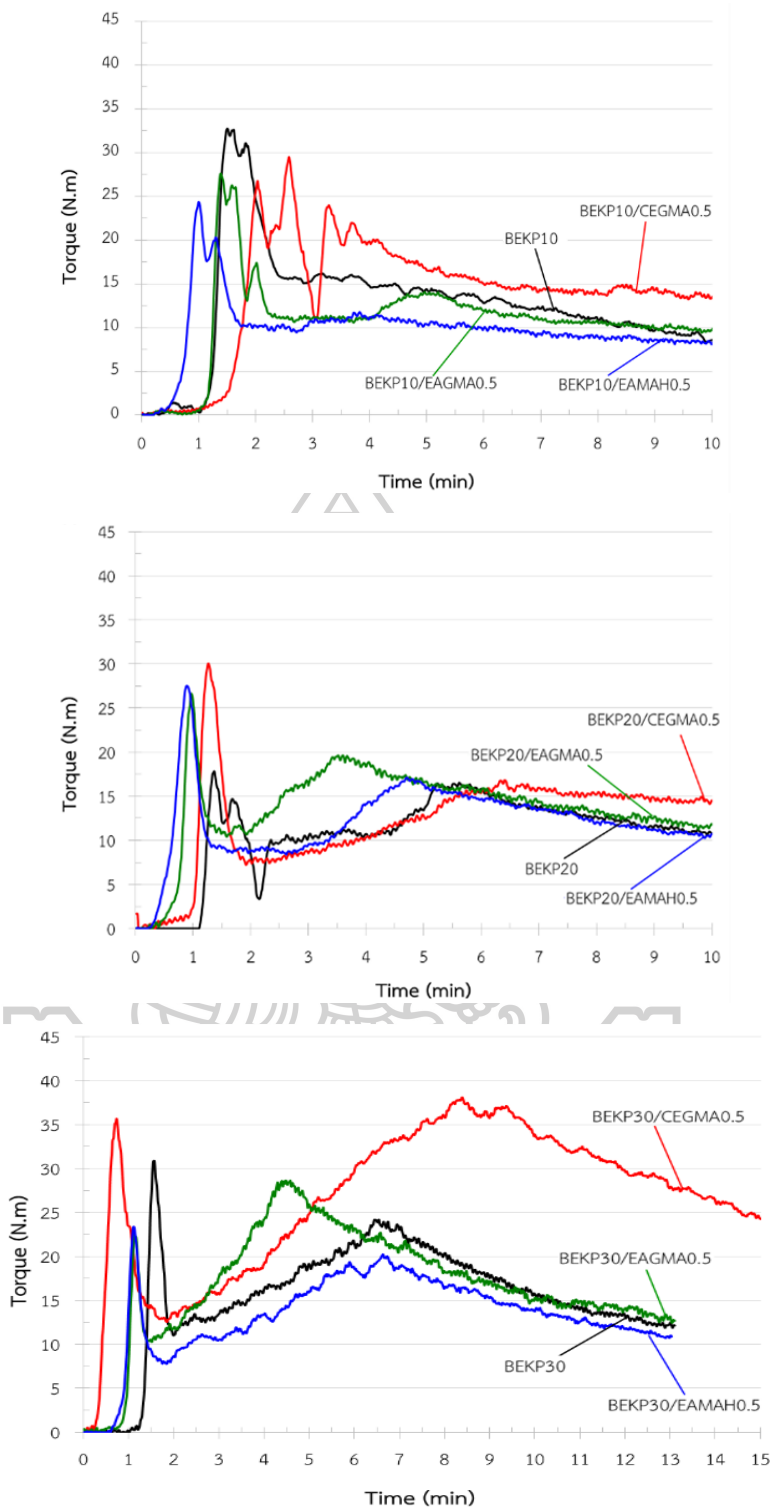

Figure 4.3 Plot of torque as a function of mixing time in the molten state for PLA containing 10, 20 and 30 wt.% with different reactive agents loading at 0.5 phr.

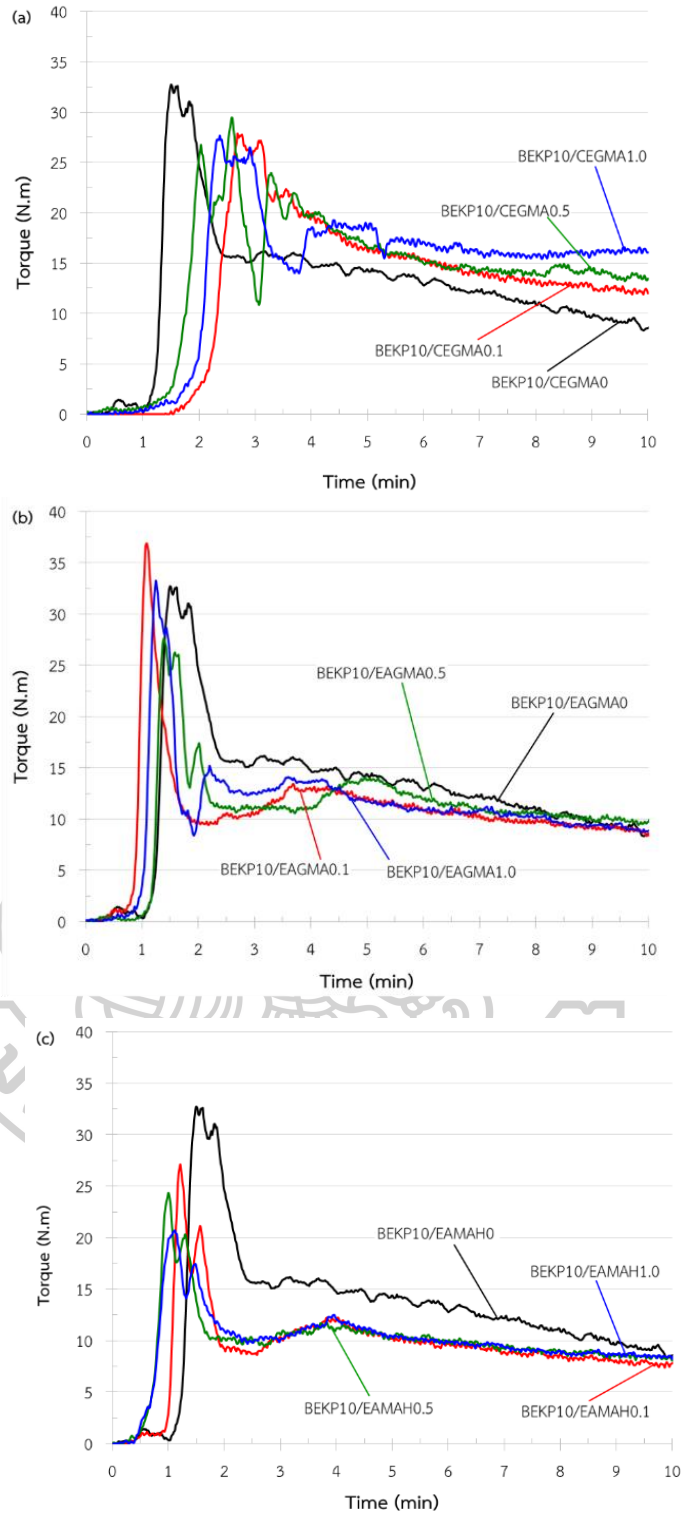

Figure 4.4 Plot of torque as a function of mixing time in the molten state for PLA containing 10 wt.% BEKP with various reactive type; CEGMA (a), EAGMA (b) and EAMAH (c) at 0.1, 0.5 and 1.0 phr content.

4.1.1.2.Effect of reactive agent concentrations

The plots of mixing torque against time in the molten state for PLA containing 10 wt.% BEKP with and without various reactive agent type (CEGMA, EAGMA, and EAMAH) and content (0.1, 0.5 and 1.0 phr) were shown Figure 4.4. After mixing for 10 minutes, it was noticed that the equilibrium torque of PLA with 0.1, 0.5 and 1.0 phr CEGMA was increased by 40, 57 and 88%, respectively, compared to the torque of non-reactive PLA biocomposite. On the other hand, PLA with 0.1, 0.5 and 1.0 phr EAGMA or EAMAH showed equilibrium torque values were similar to non-reactive PLA biocomposite. The addition of EAMAH to PLA resulted in a large decrease in the melt viscosity than of that non-reactive PLA biocomposite during the processing period. This indicated that CEGMA was more chain reactive with PLA than EAGMA and EAMAH, respectively.

4.1.2. Mechanical properties of PLA biocomposites

4.1.2.1. Effect of fiber concentrations and reactive agent types

Mechanical properties of neat PLA and PLA containing 0.5 phr of different reactive agent types; CEGMA, EAGMA, and EAMAH with and without 10, 20 and 30 wt.% of BEKP, were shown in Figure 4.8 - Figure 4.7. The open bars represented neat PLA (without BEKP) and PLA added various BEKP contents without the addition of the reactive agent. The dotted, diagonal, and solid bars represented PLA biocomposites incorporated with CEGMA, EAGMA, and EAMAH, respectively. Considering Young's modulus as shown in Figure 4.8, Young's modulus was an important characteristic to measure the stiffness of the materials [77]. It was seen that all PLA biocomposites showed a higher Young's modulus upon increase of BEKP content, which indicated a stiffer and more brittle behavior than that of neat PLA. Young's modulus of PLA biocomposites containing 10, 20 and 30 wt.% without a reactive agent was increased by 16.6, 26.6 and 41.2%, respectively, compared to that of neat PLA (1602.8 MPa). On the other hand, Young's modulus of PLA without BEKP was decreased when CEGMA, EAGMA or EAMAH was added, compared to neat PLA because there was a soft part in EAGMA and EAMAH. In contrast, Young's modulus of PLA added BEKP

with CEGMA or EAGMA was maintained while it was still decreased with the presence of EAMAH, compared to those non-reactive biocomposites.

Considering tensile strength as shown in Figure 4.6, the tensile strength of PLA with 10 wt% BEKP loading without a reactive agent was slightly increased by 2.0% compared to that of neat PLA, caused by the reinforcing effect of the fillers [35]. Reactive PLA biocomposites containing 10 wt% BEKP with CEGMA, EAGMA, and EAMAH was a higher increased by 13.5, 6.2 and 3.3%, respectively, compared to that of neat PLA. This indicated that the addition of any reactive agent with 10 wt% BEKP loading led to better stress transfer across the interphase of PLA to the BEKP fiber, caused by their better interfacial adhesion. In case of the 20 wt% BEKP loading, PLA biocomposite with CEGMA and EAGMA showed an increase in tensile strength by 7.1 and 8.2%, respectively, compared to that of neat PLA while the non-reactive biocomposite and PLA biocomposite with EAMAH showed a decrease in tensile strength by 7.6 and 25.7%, respectively. However, the tensile strength of PLA biocomposites with a higher loading of BEKP (30 wt.%) with and without reactive agent did not remarkably increase any further, probably due to the fact that the mobility of PLA chains was restricted by the aggregates of excess BEKP.

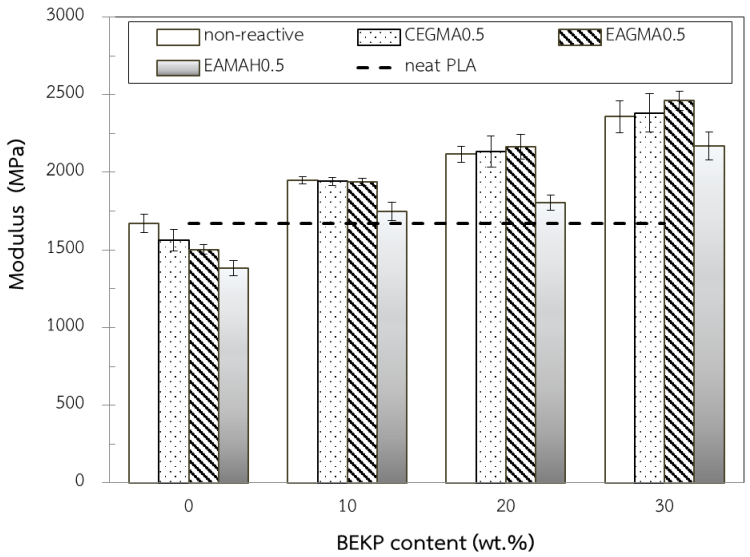

Figure 4.5 Young's modulus of neat PLA and PLA containing 10, 20 and 30 wt.% of BEKP with various reactive type; CEGMA, EAGMA, and EAMAH at 0.5 phr content.

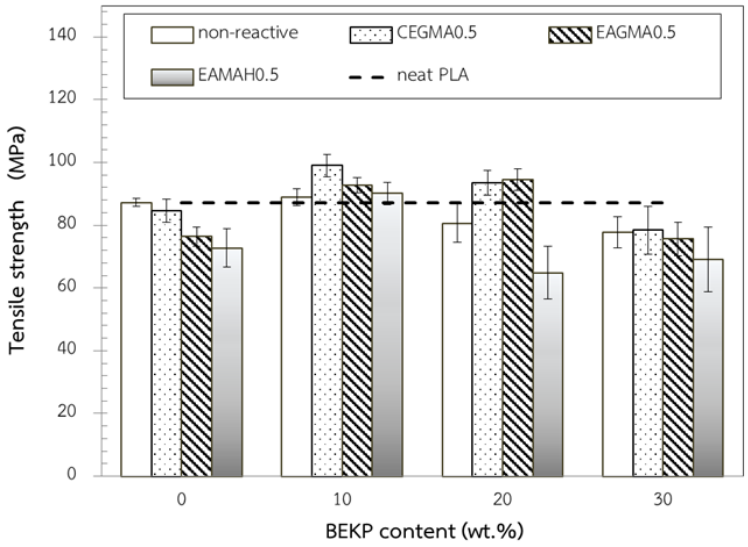

Figure 4.6 Tensile strength of neat PLA and PLA containing 10, 20 and 30 wt.% of BEKP with various reactive type; CEGMA, EAGMA, and EAMAH at 0.5 phr content.

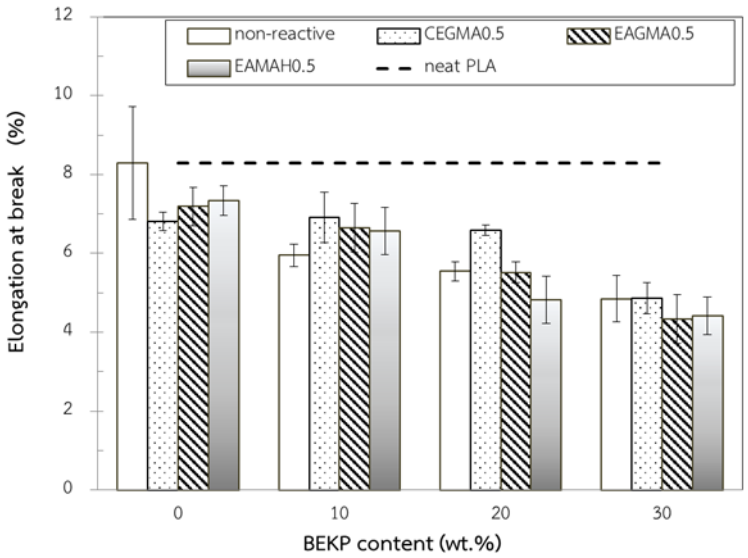

Figure 4.7 Elongation at break of neat PLA and PLA containing 10, 20 and 30 wt.% of BEKP with various reactive type; CEGMA, EAGMA, and EAMAH at 0.5 phr content.

Considering elongation at break as shown in Figure 4.7, a decreased elongation at break was found, with an increasing trend in BEKP loadings in PLA composites with and without reactive agents due to the decrease in the mobility of PLA matrix chains. Considering PLA biocomposite at 10 wt.% BEKP loading, the

presence of any reactive agent displayed a higher elongation at break value than PLA biocomposite without a reactive agent (called non-reactive biocomposite). The result was in good agreement with the improvement in tensile strength of PLA biocomposite added 10 wt.% BEKP with a reactive agent, suggesting that all reactive agent type could promote the stress transfer from PLA matrix to the BEKP fiber. However, at 20 wt.% BEKP loading, it was seen that only CEGMA addition showed a higher elongation at break value than that of non-reactive biocomposite. The possible reason for an increase in tensile strength and elongation at break might be the proper adhesion between fiber and matrix in case of PLA biocomposite incorporated with CEGMA.

4.1.2.2. Effect of reactive agent types and concentrations

The Young's modulus, tensile strength, and elongation at break of PLA biocomposites containing 10 wt.% BEKP with and without CEGMA, EAGMA or EAMAH at 0.1, 0.5 and phr 1.0 content, were demonstrated in Figure 4.8. PLA biocomposites with CEGMA loading at any contents showed an insignificant change in Young's modulus, as seen in Figure 4.8(a). It was known that the improvement of the quality of the polymer interface did not significantly affect Young's modulus or stiffness of the materials [71]. PLA biocomposites with EAGMA loading showed only a slight decrease in Young's modulus compared to non-reactive biocomposite. On the other hand, the presence of EAMAH in PLA biocomposite showed a lower Young's modulus upon increasing of EAMAH contents. This might be due to the fact that EAGMA and EAMAH contained ethylene copolymer acted as a soft segment of their molecule. Considering the tensile strength as showed in Figure 4.8(b), the tensile strength of PLA biocomposites with CEGMA showed a pronounced improvement than that of non-reactive biocomposite (PLA/BEKP10). In contrast, the tensile strength of PLA biocomposites with EAGMA and EAMAH was slightly higher than that of non-reactive biocomposite.

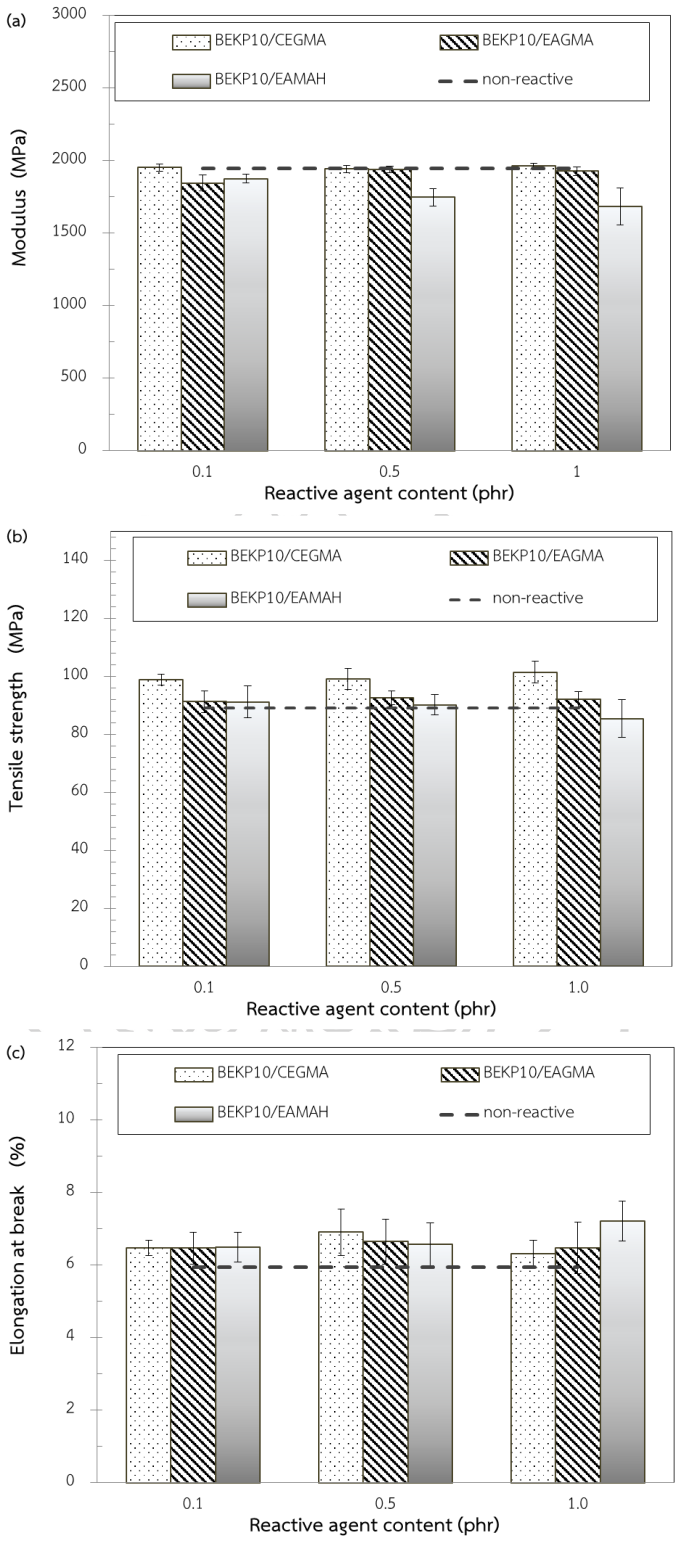

Figure 4.8 Young's modulus (a), tensile strength (b) and elongation at break (c) of PLA biocomposites containing 10 wt.% of BEKP with various reactive types (CEGMA, EAGMA, and EAMAH) and contents (0.1, 0.5 and 1.0 phr).

Both of PLA biocomposites with EAGMA and EAMAH loading showed a higher elongation at break than that of non-reactive biocomposite, particularly at 1.0 phr EAMAH loading as seen in Figure 4.8(c). Although CEGMA did not have ethylene copolymer in their chain, the elongation at break of PLA biocomposite with CEGMA loading was higher than that of non-reactive biocomposite. CEGMA could change the molecular weight distribution of PLA matrix due to its chain extension effect [78], which might lead to the improvement of the elongation at break. Increasing elongation at break without the decline of Young's modulus and tensile strength of PLA biocomposite with CEGMA loading. This may be due to better interfacial adhesion between BEKP fiber and PLA matrix.

4.1.3. Morphology of PLA biocomposites

4.1.3.1. Effect of fiber concentrations

In order to observe the fiber distribution and PLA/fiber interfacial adhesion in PLA biocomposite, SEM micrographs of the tensile fractured surface of PLA biocomposites containing 10, 20 and 30 wt.% BEKP without reactive agents were depicted in Figure 4.9. The addition of 10 and 20 wt.% BEKP with PLA showed a fair distribution of fiber in PLA matrix. In contrast, PLA biocomposite with 30 wt.% BEKP loading showed a poor distribution and some aggregations of fiber, suggesting that 30 wt.% BEKP was too much. Moreover, there were many pores and cavities for all BEKP loading contents due to the pull-out of fibers, because of the lack of interfacial adhesion between the BEKP fiber and PLA matrix.

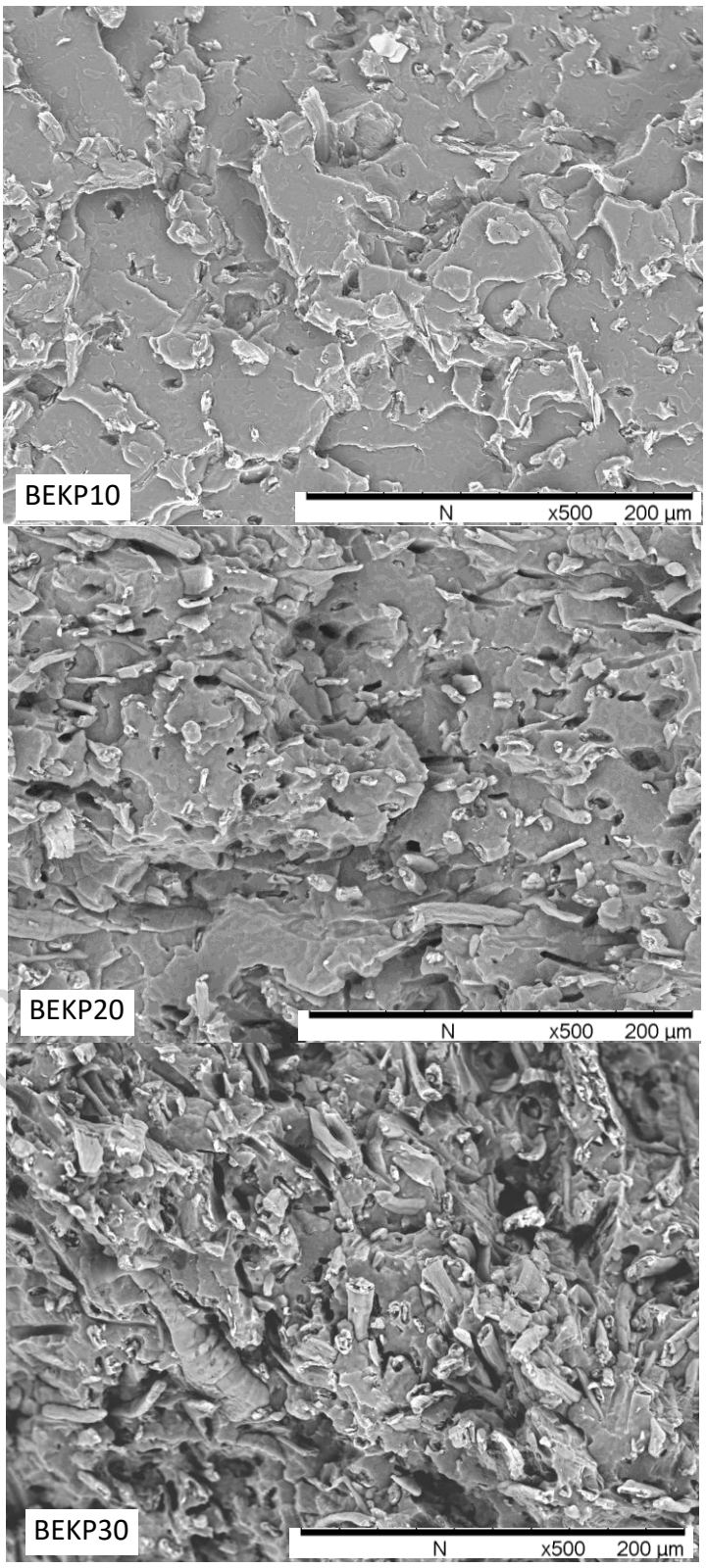

Figure 4.9 SEM micrographs (×500) of PLA biocomposites containing 10, 20 and 30 wt.% BEKP without a reactive agent.

4.1.3.2. Effect of reactive agent types and concentrations

FE-SEM micrographs of the tensile fractured surface of PLA biocomposites containing 10 wt.% BEKP with and without reactive agent were shown in Figure 4.10.

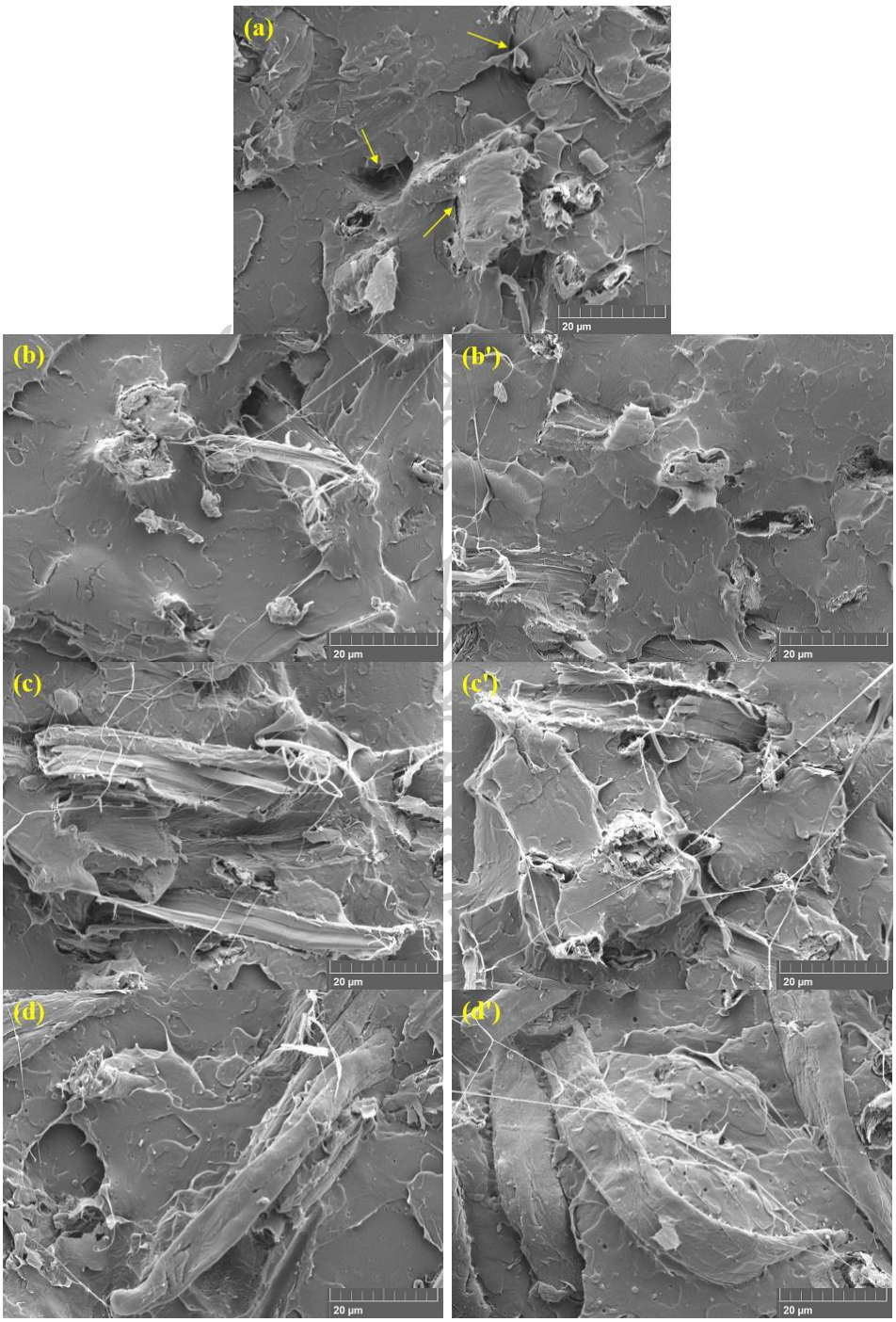

Figure 4.10 FE-SEM micrographs of tensile fractured surface of PLA biocomposites containing 10 wt.% BEKP; PLA/BEKP (a), PLA/BEKP/CEGMA 0.5 (b) and 1.0 phr (b'), PLA/BEKP/EAGMA 0.5 (c) and 1.0 phr (c'), PLA/BEKP/EAMAH 0.5 (d) and 1.0 phr (d').

The micrograph of non-reactive biocomposite in Figure 4.10.(a) exhibited space between the fiber and PLA matrix and remaining pores due to fiber pull-out, suggesting a poor interfacial adhesion. On the other hand, the micrographs of PLA biocomposites incorporated with CEGMA (Figure 4.10.(b, b')) or EAGMA (Figure 4.10.(c, c')) demonstrated the fiber breakage and disappearance of space between PLA and fibers rather than pull-out, indicating the better interfacial adhesion between the BEKP fiber and PLA matrix. On the other hand, the micrographs of PLA biocomposites incorporated with EAMAH showed the smooth fiber surface without polymer adhered to the surface indicated no adhesion at the interface as seen in Figure 4.10.(d, d'). From FE-SEM results, it could be concluded that PLA biocomposites with epoxide-based reactive agents (CEGMA and EAGMA) helped to promote the better interfacial adhesion, essentially resulting in a more efficient transfer of stress from PLA matrix to the BEKP fiber than that with the anhydride-based reactive agent (EAMAH). It was generally well known that the fiber reinforced polymer composites had exhibited fiber breakage rather than pull-out indicating the better stress transfer between fiber and matrix [79]. The results were in good agreement with the improved mechanical properties of PLA composites with the epoxide-based reactive agent (CEGMA) discussed earlier.

4.1.4. Dynamic mechanical thermal (DMTA) properties of PLA biocomposites

The temperature dependence of storage moduli of neat PLA and PLA biocomposites with and without reactive agents were presented in Figure 4.11. In the glassy region (from 30 to 50°C), all PLA biocomposite samples displayed the higher values of storage modulus (G') than that of neat PLA. The storage modulus of PLA with 10 wt% fiber loading was increased compared to that of neat PLA due to the reinforcement effect. It was observed in Figure 4.11(a) that PLA biocomposites incorporated with 0.5 phr of all reactive agents had higher storage moduli than non-reactive PLA biocomposite. The addition of CEGMA into PLA and fibers exhibited higher storage modulus than EAGMA and EAMAH, respectively. However, in the case of adding 1.0 phr of the anhydride-based reactive agent, the storage modulus was

comparable to non-compatibilized PLA biocomposite. Upon increasing temperature, the storage modulus of neat PLA and all PLA biocomposites dropped at around 60°C, which corresponded to their glass transition temperature. As the temperature continued to increase from 70 to 90°C, the storage moduli decreased as PLA matrix became soft at higher temperatures. In the rubbery region, all PLA biocomposites exhibited significantly higher storage modulus than that of neat PLA, especially for the addition of the epoxide-based reactive agent. From Figure 4.11(b), the storage moduli of neat PLA and PLA incorporated with 1.0 phr EAGMA started to increase again at about 98°C. These storage moduli were recovered due to the cold crystallization of PLA tested specimen in DMA temperature sweep [80].

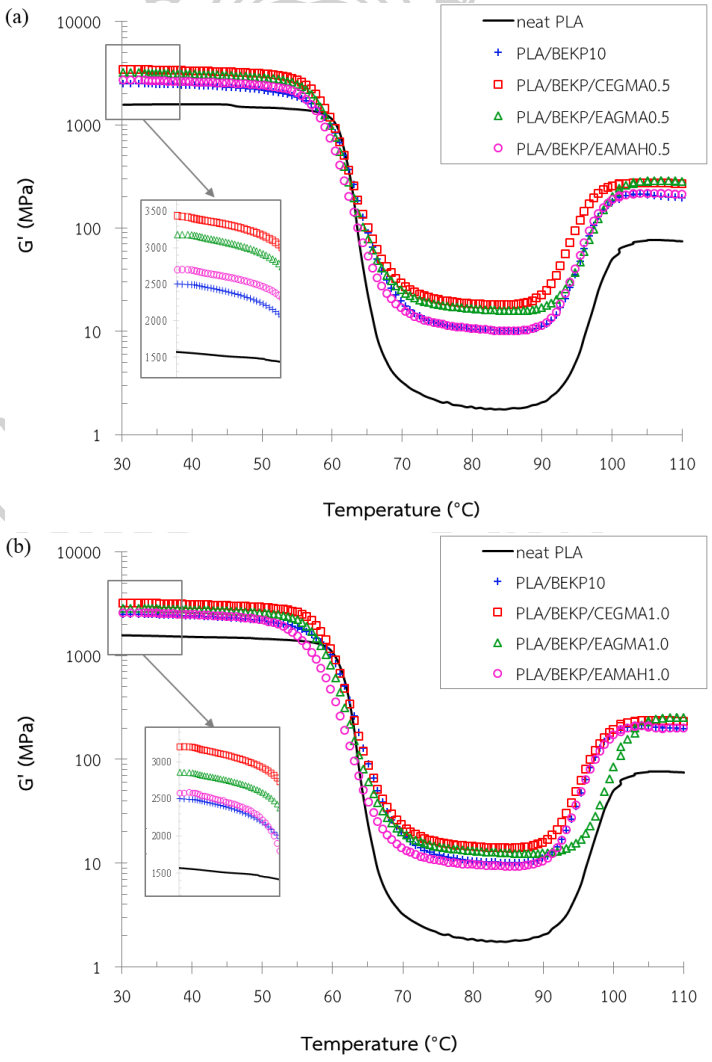

Figure 4.11 Storage modulus of neat PLA and PLA biocomposites with and without reactive agents 0.5 (a) and 1.0 phr (b).

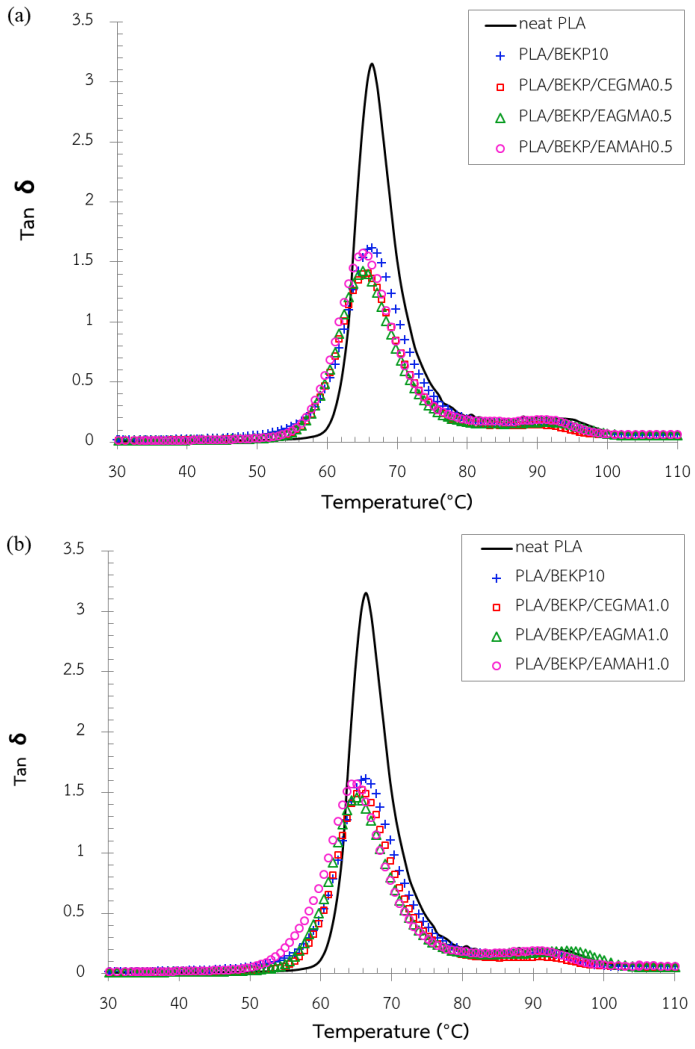

Figure 4.12 Tan δ of neat PLA and PLA biocomposites with and without reactive agents .5 (a) and 1.0 phr (b).

Figure 4.12 depicted the curves of damping or tan δ, which was described as the ratio of loss to the storage modulus. The loss and storage modulus were referred to an ability for dissipating energy (viscous phase) and storing mechanical energy (elastic phase), respectively [2]. In the transition region, composites had essentially lower tan δ than neat PLA because the addition of fibers increased the mobility of the amorphous phase in the polymer matrix [2, 65]. For composites, tan δ was affected by the distribution of fibers, a concentration of shear stress, viscoelastic energy dissipation as well as the fiber and matrix interfacial adhesion [57, 81].

Therefore, tan δ peak height might be used in order to investigate the interfacial adhesion between fiber and polymer matrix [82-85]. As reported elsewhere [83, 85, 86], the higher tan δ values indicated a weak interfacial adhesion whereas the lower tan δ values indicated a good interfacial adhesion due to a reduction in mobility of the polymer chain. From Figure 4.12, tan δ curves of all PLA biocomposites with reactive agents shifted toward lower values than non-reactive PLA biocomposite, implying the better interface between the components compared to non-reactive PLA biocomposite. However, the incorporating of 0.5 phr anhydride-based reactive agent showed the similar tan δ value to non-reactive PLA biocomposite.

One of the parameters used to evaluate a degree of interfacial adhesion between fiber and polymer matrix due to the reduction of molecular mobility of polymer around the fiber surface compared to the matrix is called an adhesion factor (A). The adhesion factor (A) is determined using equation (1) [86], where V_f was the volume fraction of the fiber (0.1), tan δ_c was the relative damping of PLA biocomposites and tan δ_p was the relative damping of the pure PLA (3.15). The relative damping of the materials was determined by the maximum tan δ peak [85]. The results were presented in Table 4.1.

$$A = \left(\frac{1}{1-V_f} \frac{\tan \delta_c}{\tan \delta_p} \right) - 1 \qquad (1)$$

As seen in Table 4.1, PLA/BEKP/CEGMA0.5 and PLA/BEKP/EAGMA0.5 showed the lowest adhesion factor, which implied the strong interfacial adhesion between the fiber and PLA matrix. Furthermore, the effectiveness of stress transfer between PLA and filler could be demonstrated by effectiveness coefficient parameter (C) [86]. The effectiveness coefficient was defined as the ratio of storage modulus of the composite in the glassy region and the rubbery region in relation to the pure resin [86]. The effectiveness coefficient (C) was computed using equation (2) [86], where G'_g and G'_r were storage modulus in the glassy region and rubbery region, respectively.

$$C = \frac{G'_g/G'_r\,(composite)}{G'_g/G'_r\,(resin)} \qquad (2)$$

Table 4.1 Tan δ peak values, Adhesion factor (*A*) and Effectiveness coefficient (*C*) parameters of neat PLA and PLA biocomposites

Sample code	Max tan δ peak value	Adhesion factor (A)	Effectiveness coefficient (C)
neat PLA	3.15	0	1.00
PLA/BEKP10	1.61	-0.43	0.27
PLA/BEKP10/CEGMA0.5	1.40	-0.50	0.21
PLA/BEKP10/CEGMA1.0	1.52	-0.46	0.25
PLA/BEKP10/EAGMA0.5	1.43	-0.50	0.22
PLA/BEKP10/EAGMA1.0	1.46	-0.49	0.25
PLA/BEKP10/EAMAH0.5	1.57	-0.45	0.29
PLA/BEKP10/EAMAH1.0	1.57	-0.45	0.30

From Table 4.1, PLA/BEKP/CEGMA0.5 exhibited the lowest C, which indicated the most effectiveness of stress transfer from PLA matrix to the fiber, similar to PLA/BEKP/EAGMA0.5 while PLA/BEKP/EAMAH1.0 showed the highest C compared to all PLA biocomposites. For the comparison, the incorporation the epoxide-based reactive agent exhibited more improved interfacial adhesion or compatibility between PLA and the fiber than the anhydride-based reactive agent. This could result from reactive epoxide group, which was more selective to the fiber and PLA system.

4.1.5. Molau test of PLA biocomposites

Molau test was performed by dissolving PLA biocomposite samples in chloroform and left to stand for 48 hrs in order to investigate changes in physical properties due to interfacial bonding or compatibility in PLA biocomposites with and without reactive agents. Photographs after Molau test of PLA biocomposites compared to neat PLA were presented in Figure 4.13. It was observed that neat PLA could be dissolved completely in chloroform, thus a transparent solution was obtained. In the case of non-reactive PLA biocomposite (PLA/BEKP10), the phase separation was clearly noticed. The lower layer contained the insoluble fiber and the

upper layer was PLA solution, indicating the lack of interaction between the fiber and PLA. When 1.0 phr of EAGMA or EAMAH was used as a reactive agent for PLA biocomposite, more turbidity of the solution was observed even though the phase separation was still observed. The addition of CEGMA in PLA biocomposites exhibited the most turbid suspension, which were maintained stable. This indicated that the addition of CEGMA could couple fibers and PLA caused by the reaction between epoxide groups in CEGMA and carboxyl or hydroxyl group in PLA chain and hydroxyl group in fiber. CEGMA might be more reactive with PLA and fiber at the interface than EAGMA because CEGMA has a lower molecular weight than EAGMA.

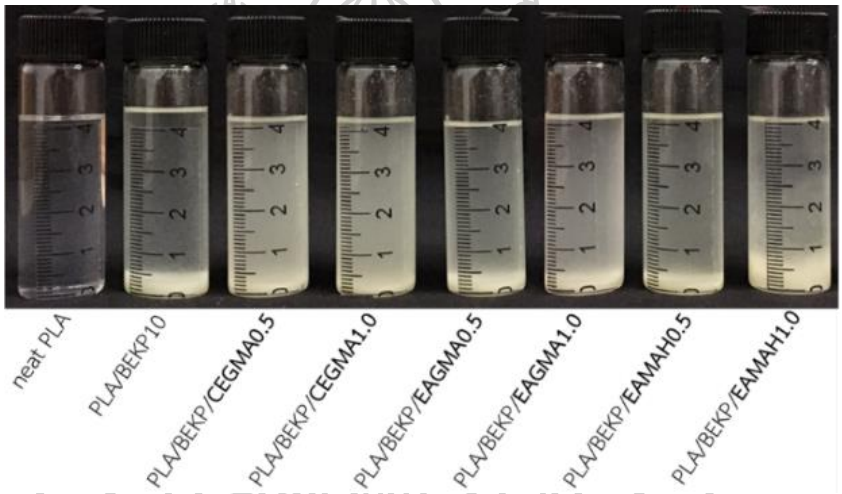

Figure 4.13 Digital photographs obtained by Molau test of neat PLA and PLA biocomposites with and without different reactive agents (0.5 and 1.0 phr).

4.1.6. FT-IR of PLA biocomposites

The BEKP fibers were extracted from PLA biocomposites after molau test was done. The interaction between extracted fiber and PLA in the biocomposites was further analyzed by FTIR. The significant peaks in those spectra were shown in Table 4.3. Figure 4.14 illustrated FT-IR spectra of virgin fiber and the extracted fibers of PLA biocomposites with and without reactive agents. The intensity of the broad peak at 3480 cm^{-1}, which assigned to the -OH stretching of cellulose fibers in all samples, was unchanged. Considering the characteristic at peak 1758 cm^{-1}, it was assigned to the remaining carbonyl groups (C=O) of PLA chains on the extracted fibers. It was

clearly seen the strong peak at 1758 cm^{-1} for extracted BEKP/CEGMA sample, indicating a strong interaction between the fiber and PLA matrix. It was also shown the weak peak at 1758 cm^{-1} for extracted BEKP/EAGMA sample while the peak at 1758 cm^{-1} was disappeared for virgin BEKP and the others. It was suggested that CEGMA was significantly improved the interfacial adhesion between the fiber and PLA matrix. Since CEGMA had multiple reactive epoxide groups, CEGMA might be chemically reacted with hydroxyl groups in fiber and also PLA chain ends (-OH and -C=O groups) during melt processing, resulting in the significant increase in the compatibility between the fiber and PLA matrix. Similarly, EAGMA could improve the interfacial adhesion between the fiber and PLA matrix but not as much as CEGMA. In contrast, the addition of anhydride-based reactive agent (EAMAH) resulted in the unimproved interaction between the fiber and PLA matrix.

Table 4.2 FT-IR of the fibers with and without MAH

Wavenumbers (cm^{-1})	**Assignments**	**References**
897	Glucose ring stretching, C-H deformation	[87]
1033, 1059	C-O stretching	[87]
1113	Glucose ring stretch (asymmetric)	[87]
1165	C-O-C asymmetric vibration	[87]
1240	C-O stretching of acetyl groups in the hemicellulose	[88]
1372	CH_2 symmetric deformation	[89]
1431	CH_3 asymmetric deformation	[87]
1639	O–H of adsorbed water in pulp	[90]
1736	C=O stretching, carboxyl groups in hemicelluloses, lignin	[89]
1758	C=O stretching (strong), carboxyl group	[89]
2855	CH_2, CH_3, symmetric stretching	[89]
2918	CH_2 asymmetric stretching	[89]
3300-3600	O-H stretch (broad)	[89]

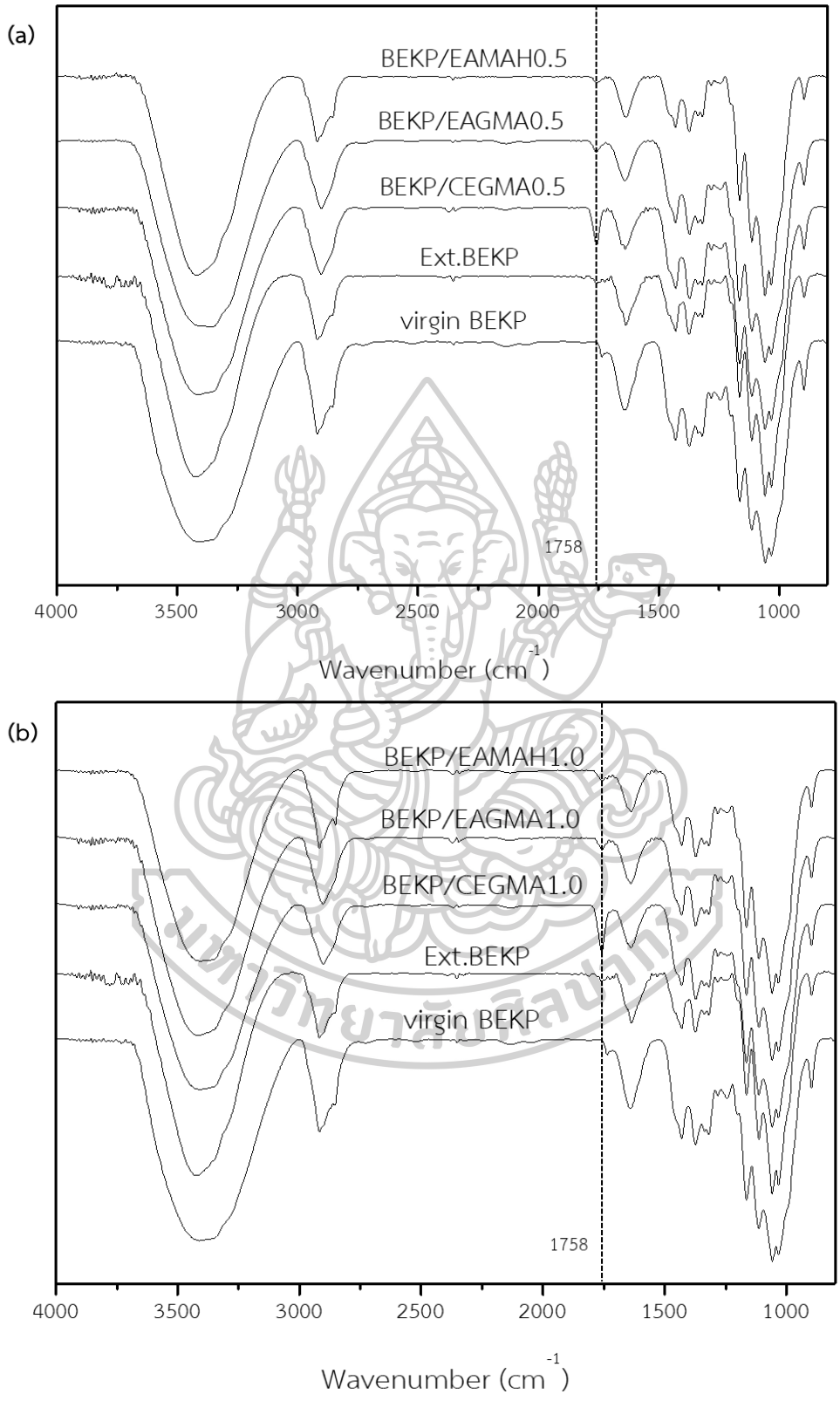

Figure 4.14 FT-IR spectra of virgin BEKP and BEKP with and without reactive agents 0.5 (a) and 1.0 phr (b) after extraction from PLA biocomposites.

Table 4.3 FT-IR of the fibers with and without MAH

Wavenumbers (cm^{-1})	Assignments	References
897	Glucose ring stretching, C-H deformation	[87]
1033, 1059	C-O stretching	[87]
1113	Glucose ring stretch (asymmetric)	[87]
1165	C-O-C asymmetric vibration	[87]
1240	C-O stretching of acetyl groups in the hemicellulose	[88]
1372	CH_2 symmetric deformation	[89]
1431	CH_3 asymmetric deformation	[87]
1639	O–H of adsorbed water in pulp	[90]
1736	C=O stretching, carboxyl groups in hemicelluloses, lignin	[89]
1758	C=O stretching (strong), carboxyl group	[89]
2855	CH_2, CH_3, symmetric stretching	[89]
2918	CH_2 asymmetric stretching	[89]
3300-3600	O-H stretch (broad)	[89]

4.1.7. Possible chemical reaction between PLA and BEKP composites and CEGMA or EAGMA during the melt-blending processing.

The possible chemical reactions occurring between PLA and BEKP via *in situ* reaction with CEGMA or EAGMA during the melt-blending were shown in Figure 4.15. The hydroxyl and carboxyl groups in PLA chain and also the hydroxyl groups in BEKP fiber might react with epoxide rings in the CEGMA or EAGMA through ring opening reactions forming covalent bonds at a high temperature (190-210 ℃) [71, 91]. However, CEGMA might be more reactive with PLA and fiber than EAGMA as confirmed by FE-SEM observation and FT-IR spectra. This might be because CEGMA was a lower molecular weight than EAGMA, which CEGMA could react more readily with PLA and fiber than EAGMA at the interface.

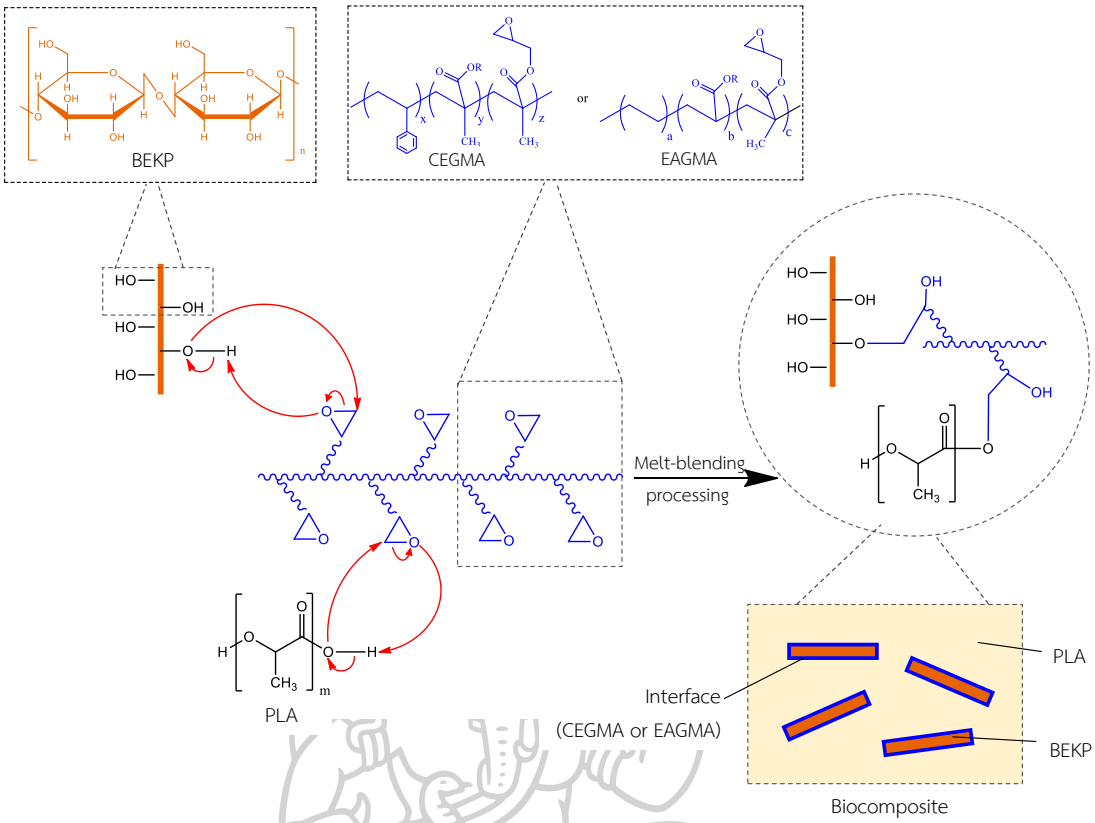

Figure 4.15 Possible reactions between PLA and BEKP fiber via *in situ* reaction with CEGMA or EAGMA during the melt-blending processing.

4.2. Properties of PLA/BEKP fiber/talc hybrid biocomposites with and without reactive agents

According to the first part, CEGMA was the most effective reactive agent as *in situ* compatibilizer for PLA/BEKP biocomposite. The addition of CEGMA showed a significant improvement in mechanical properties and interfacial adhesion of PLA/BEKP biocomposite. In this section, the properties of PLA/BEKP fiber/Talc hybrid composites with and without CEGMA were investigated. In addition, the effect of maleated BEKP/talc loading with PLA, CEGMA, and peroxide was also studied.

4.2.1. Effect of BEKP fiber and talc ratios with and without CEGMA

4.2.1.1. Modulus, tensile strength, and elongation at break of PLA hybrid composites

Modulus, tensile strength and elongation at break of neat PLA and PLA/BEKP fiber/Talc hybrid composites at various BEKP fiber/Talc ratios; 30/0, 20/10, 15/15, 10/20 and 0/30, with and without various 1.5 phr CEGMA, were shown in Figure 4.16. All PLA hybrid composites showed much higher Young's modulus and lower elongation at break than that of neat PLA, indicating the enhanced stiffness due to the presence of fillers [92, 93]. In addition, the tensile strength of all PLA hybrid composites increased when compared to that of neat PLA, caused by the reinforcing effect of the fillers. In case of non-reactive hybrid composites, Young's modulus tended to increase slightly by 49, 52, 60, 70 and 68% for 30/0, 20/10, 15/15, 10/20 and 0/30 of BEKP fiber/Talc ratios, respectively, compared to that of neat PLA. In case of PLA hybrid composites incorporated with CEGMA, Young's modulus tended to increase by 53, 59, 64, 75 and 82% for 30/0, 20/10, 15/15, 10/20 and 0/30 of BEKP fiber/Talc ratios, respectively, compared to that of neat PLA. Both PLA hybrid composites with and without CEGMA showed an increase in Young's modulus with increasing talc's ratios. These results indicated more enhanced stiffness of PLA hybrid composites due to the presence of talc. It seemed that talc acted as the main reinforcing filler in PLA hybrid composite. PLA/fiber composite added talc showed an increase in Young's modulus of hybrid composite compared to PLA/fiber composite, as reported by many researchers [3, 94]. The tensile strength and elongation at break of the hybrid composites were similar, which independent from talc's ratios. However, PLA hybrid composites incorporated with CEGMA showed slightly higher Young's modulus, tensile strength, and elongation at break than those of their non-reactive hybrid composites. This indicated that a better stress transfer between the fillers and PLA matrix due to better interfacial adhesion caused by multifunctional epoxides.

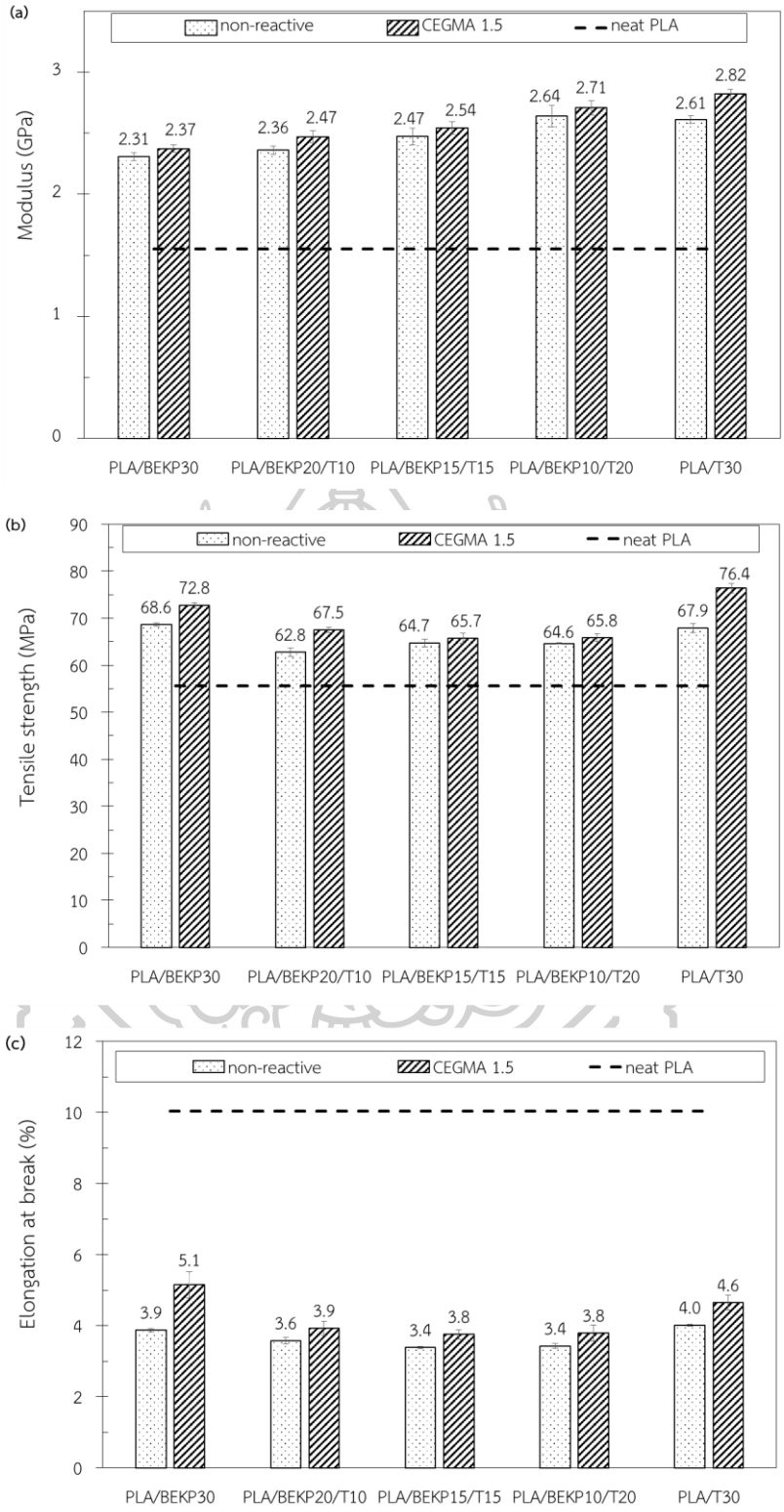

Figure 4.16 Young's modulus, tensile strength, and elongation at break for PLA hybrid composites with various BEKP fiber/Talc ratios; 30/0, 20/10, 15/15, 10/20 and 0/30 with and without 1.5 phr CEGMA.

4.2.1.2. Morphology of PLA hybrid composites

The tensile fracture surfaces of PLA/BEKP/Talc hybrid composites at different BEKP fiber/Talc ratios; 30/0, 20/10, 15/15, 10/20 and 0/30 with and without 1.5 phr CEGMA, were observed at 8000x magnification times using FE-SEM, as shown in Figure 4.17, respectively. The different BEKP fiber/Talc ratios did not affect the interfacial adhesion of the components in hybrid composites. According to Figure 4.17(a1-d1), PLA hybrid composites without CEGMA exhibited space between PLA matrix and fiber or talc, and some pull-outs of talc because of the poor interfacial adhesion between the fillers and PLA matrix. In contrast, for PLA hybrid composites with CEGMA as seen in Figure 4.17(a2-d2), it was obviously seen that the BEKP fiber was broken and tended to be torn up in the hybrid composites. These results reflected that the presence of CEGMA improved the interfacial adhesion between fiber or talcum and PLA matrix due to better compatibility by reaction of *in situ* multifunctional epoxides (CEGMA).

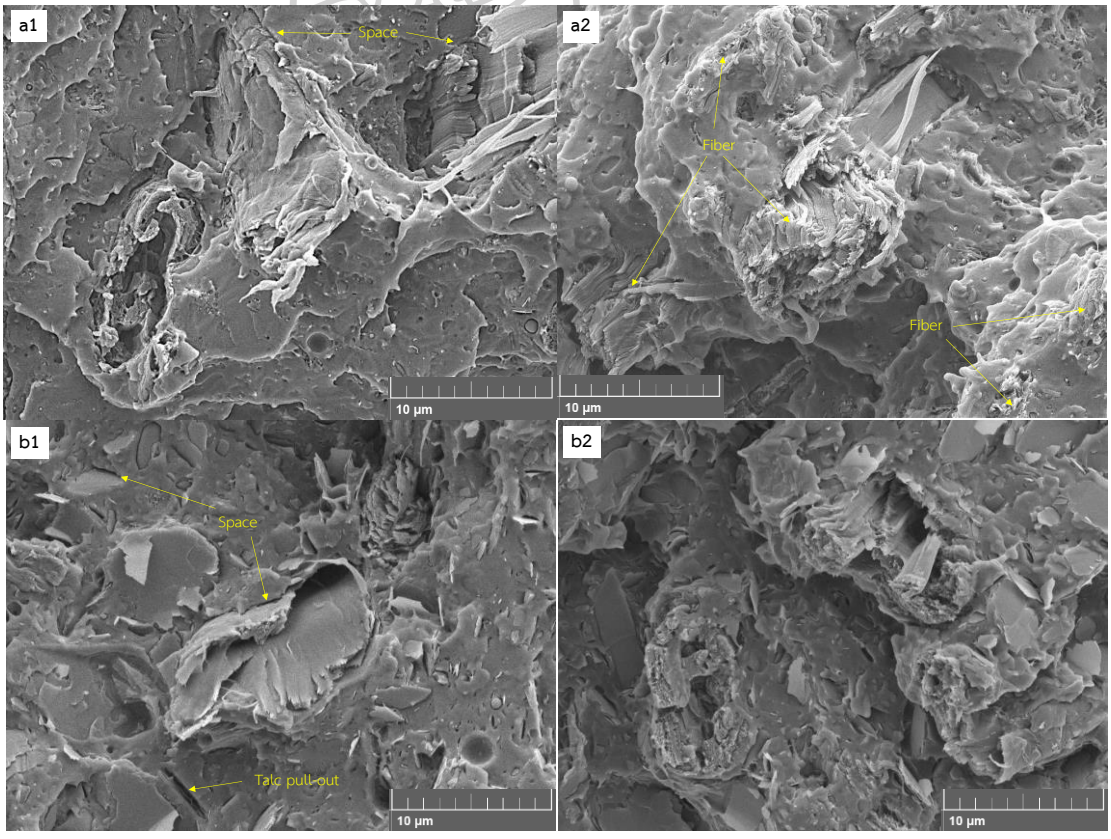

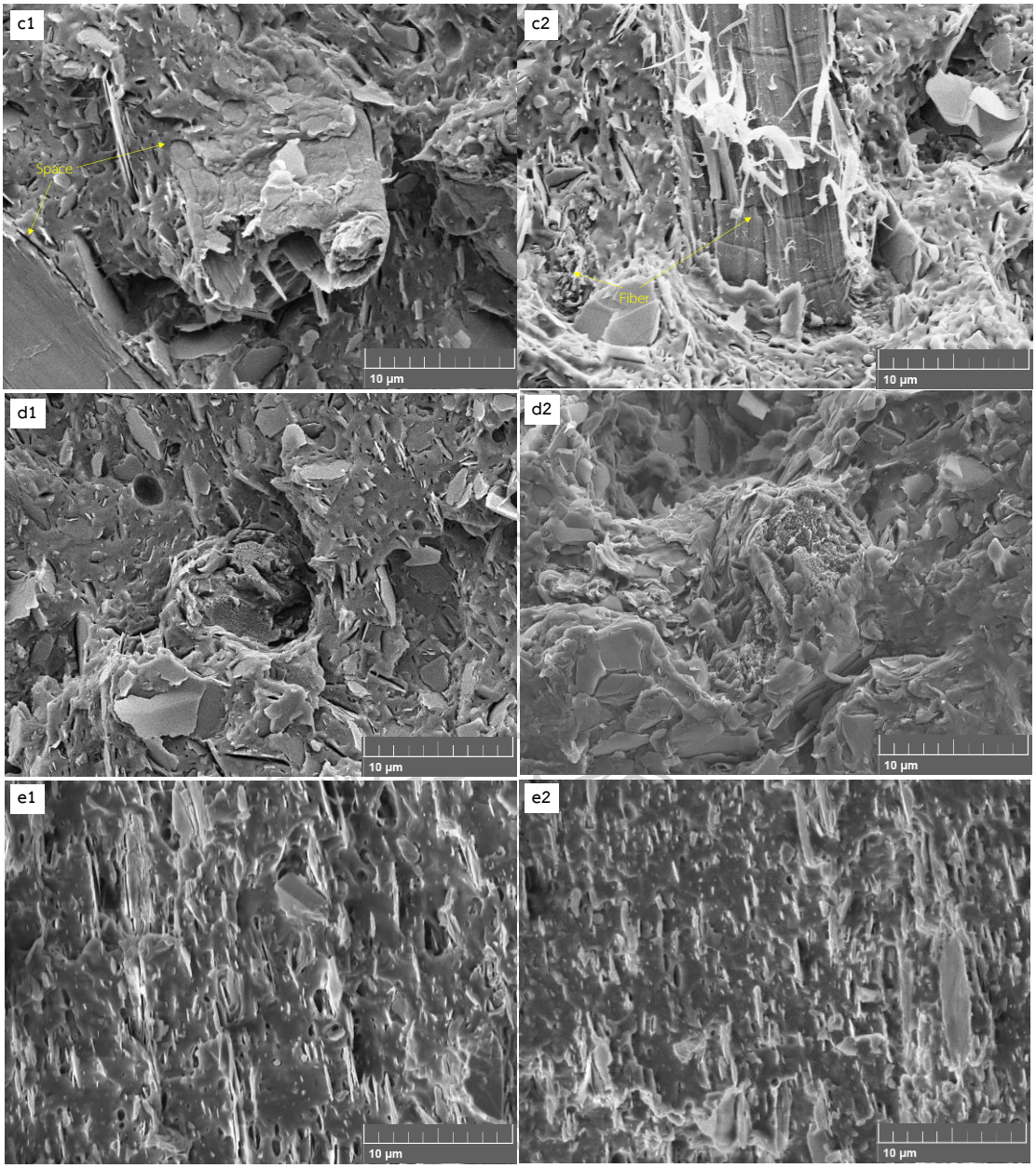

Figure 4.17 FE-SEM micrographs for PLA hybrid composites at various BEKP fiber/Talc ratios without CEGMA; 30/0 (a1), 20/10 (b1), 15/15 (c1), 10/20 (d1) and 0/30 (e1) and with and 1.5 phr CEGMA; 30/0 (a2), 20/10 (b2), 15/15 (c2), 10/20 (d2) and 0/30 (e2).

Micrographs in Figure 4.17 (a2-d2), the BEKP fiber in PLA matrix containing CEGMA was evidenced more broken rather than pulled out after the tensile tests. This phenomenon could be attributed to the reaction among the multifunctional epoxide groups in CEGMA, hydroxyl groups in the fibers or talc structure, and

carbonyl or hydroxyl groups at the end group of PLA molecular chain during the melt-blending process, as proved by FT-IR analysis of the extracted fibers in the first part.

4.2.1.3. Impact strength of PLA hybrid composites

The impact strength for PLA hybrid composites with various BEKP fiber/Talc ratios; 30/0, 20/10, 15/15, 10/20 and 0/30 with and without 1.5 phr CEGMA compared to neat PLA was shown in Figure 4.18. The dotted and diagonal bars represented the non-reactive PLA hybrid composites and PLA hybrid composites incorporated with 1.5 phr CEGMA, respectively. The non-reactive hybrid composites at the ratio of BEKP fiber/Talc 30/0 showed the same range of impact strength as that of neat PLA. However, the ratios of BEKP fiber/Talc at 20/10, 15/15 and 10/20 showed a slight decrease in impact strength compared to that of neat PLA. In case of non-reactive hybrid composite sample, the mechanical shock could generate a large concentration of stress at the talc or fiber/PLA interface, which was poor adhesion, causing subsequent disadhesion and crack formation. PLA hybrid composites with 0/30 of BEKP/Talc ratio loading showed the highest impact strength. Generally, an increase in impact strength with the incorporation of talc is in agreement with the report made by M.S. Huda et al [9]. The impact strength of all reactive PLA hybrid composites compatibilized with CEGMA was increased by 6 – 9 % compared to that of their non-reactive hybrid composite. The improvement in impact strength of PLA hybrid composites incorporating of CEGMA was considered to have two effects, improving the matrix/filler interfacial adhesion and formatting of long-branched PLA chains, which stress concentrated chain ends were reduced [95]. A. Jaszkiewicz and co-workers reported that the increasing of Joncryl content led to no detectable improvement in the impact strength of PLA [95]. Furthermore, since the impact strength of the composites tended to increase with the decrease of average particle size and uniform dispersion in matrix [30]. Therefore, the improvement in the impact strength of reactive PLA hybrid composites was due to better interfacial adhesion between the fillers and PLA matrix, caused by multifunctional epoxides and this interaction reinforced the interface against crack propagation. A high matrix/filler

interfacial adhesion provided an effective resistance to crack propagation during the impact test as suggested by Sahu and Broutman [96].

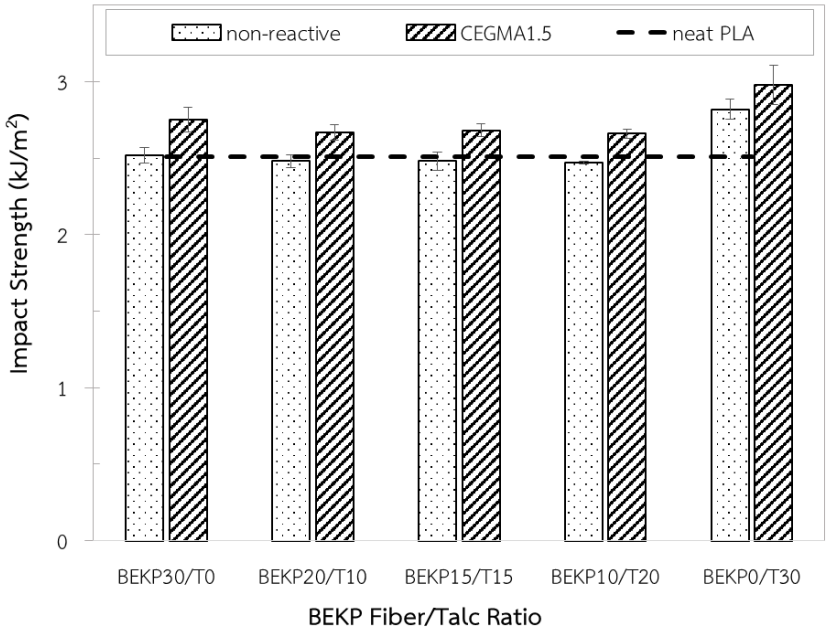

Figure 4.18 The impact strength for PLA hybrid composites with various BEKP fiber/Talc ratios; 30/0, 20/10, 15/15, 10/20 and 0/30 with and without 1.5 phr CEGMA.

4.2.1.4. Dynamic mechanical thermal (DMTA) properties of PLA hybrid composites

The plots of storage modulus as a function of temperature for neat PLA and PLA hybrid composites at different BEKP fiber and talc ratio with and without CEGMA were shown in Figure 4.21 and Figure 4.20, respectively. Considering in glassy region (30-50°C), PLA hybrid composites without CEGMA (Figure 4.20) showed an increasing trend of storage modulus as the talc's ratio was increased, which was associated to the lower temperature relaxation [97]. The increasing storage modulus in the glassy region of PLA hybrid composite with and without CEGMA was in agreement with Young's modulus as discussed earlier in Figure 4.16(a). However, storage modulus in the rubbery region (70-80°C) of PLA hybrid composite with and without CEGMA was observed a different behavior from that of the glassy region. For PLA hybrid composite without CEGMA in the rubbery region, it was found that the storage

modulus was increased when talc's ratio was increased up to equal in BEKP's ratio (BEKP15/T15) and then decreased when more talc's ratio (BEKP10/T20 and BEKP0/T30). This might be due to the effect of hybridization of BEKP fiber presented in a rich particle of talc. The presence of BEKP fiber with talc leading the motion of PLA chains was restricted, which could not happen in the single filler composites. The sketch of BEKP fiber with talc in PLA matrix was demonstrated in Figure 4.19. In other words, it showed increasing storage modulus in the rubbery region, suggesting the improvement in the heat distortion temperature (HDT) [98]. Therefore, PLA hybrid composites showed an improvement in HDT in BEKP15/talc15 ratios, compared to that of neat PLA.

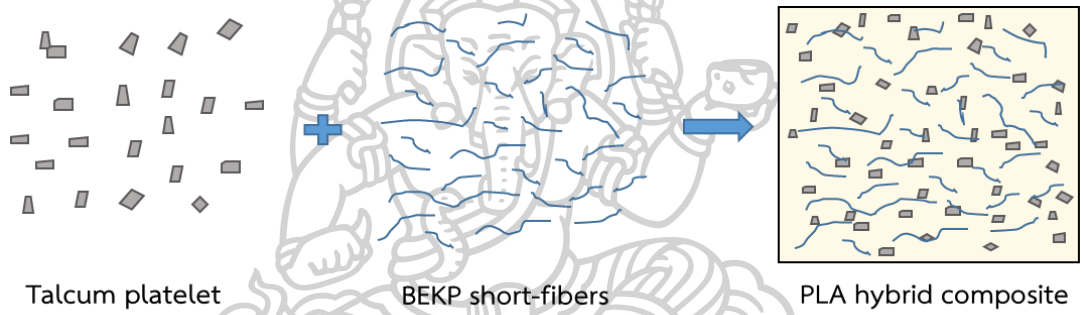

Figure 4.19 Sketch of BEKP fiber with talc in PLA matrix

PLA hybrid composites with and without CEGMA (Figure 4.21), the storage modulus in the glassy region was not greatly affected by the presence of CEGMA. However, in the rubbery region was observed that the storage modulus of PLA hybrid composites with CEGMA was lower than that of without CEGMA. As previously mentioned, the addition of CEGMA into PLA hybrid composites was considered to have two effects, improving the matrix/filler interfacial adhesion and formation of long-branched PLA chains. Therefore, some of long-branched PLA chains caused by CEGMA might increase the free volume and mobility of PLA chains in the rubbery region.

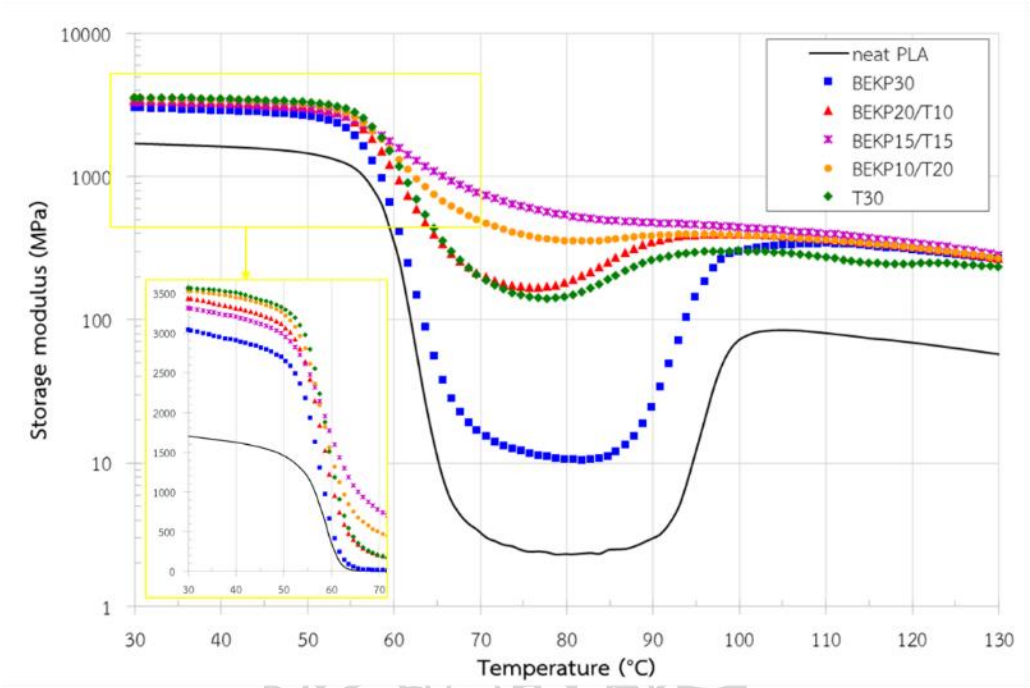

Figure 4.20 Storage modulus as a function of temperature for neat PLA and PLA hybrid composites at different talc and BEKP fiber ratio.

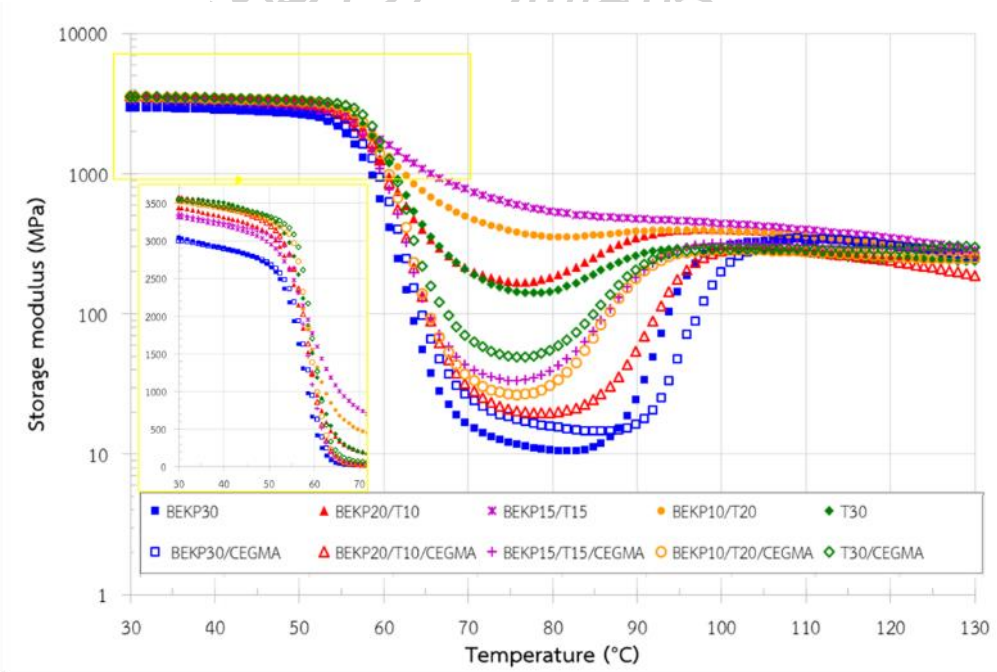

Figure 4.21 Storage modulus as a function of temperature for neat PLA and PLA hybrid composites at different talc and BEKP fiber ratio with and without 1.5 phr CEGMA loading.

4.2.2. Effect of MAH treatment with CEGMA and peroxide

It has been reported that the epoxide groups could react more rapidly with carboxyl groups than with hydroxyl groups [70, 99-101]. Therefore, the hydroxyl groups of BEKP fiber might not be sufficiently reacted with epoxide groups of CEGMA. Most of the researchers have focused on the grafting of MAH onto the polymeric backbone using different methods [6, 47, 48]. These highly reactive functional group of MAH could react with the hydroxyl groups of cellulose fiber (BEKP) macromolecules to form covalent bonds, therefore, it provided better control of the reactive site at the interface of the BEKP fiber. The MAH-treatment on BEKP surface might help the faster reaction between BEKP fiber and PLA chain, which coupled by CEGMA with the carboxyl groups at the end of MAH-treated BEKP. On the other hand, the double bond of MAH on BEKP fiber could also react with PLA backbone by peroxide.

4.2.2.1. Characterization of MAH-treated BEKP/Talc

The reaction between MAH and BEKP fiber or talc, occurred in a dry condition at 80°C in an oven for 24 hrs without a catalyst was characterize by using FTIR as resulted in Figure 4.22. The peak band at 1639 cm^{-1} was assigned to O-H bending vibration in BEKP fiber and overlapped with the C=C stretching of anhydride. As could be seen, FTIR spectrum of BEKP-MA showed the presence of the peak at 1726 cm^{-1}, corresponding to the -C=O stretching, which confirmed the success of esterification reaction between hydroxyl groups of BEKP fibers and anhydride groups of the MAH without using a catalyst. It was known that the carbonyl stretch band of C=O of α, β-unsaturated esters appeared from 1730-1715 cm^{-1} [102]. As expected, the absence of absorption in the multiple peaks at 1706, 1783 and 1858 cm^{-1}, which indicated that C=O band of unreacted maleic anhydride [103]. These confirmed that the -OH in BEKP fiber structure could react with –COOH of MAH during drying condition in the oven at 80 °C and left the alkene group in MAH. These results were in agreement with Yingfeng Zuo that maleic anhydride could react with hydroxyl groups of starch by the dry condition at 80°C of reaction temperature and 3 hrs of reaction time and the reaction efficiency reached to 85.1% [104]. The Possible reaction of surface

modification mechanism of MA moiety onto the BEKP fiber was shown in Figure 4.23. In the case of talc-MA, the significant peaks that confirmed esterification reaction were not presented. However, it was reported that the hydroxyl groups on the edge surface of the talc particle would react with the anhydride group on the functionalized PLA via an esterification reaction, which was implied by an increase in maleated-PLA/talc interfacial adhesion as shown in SEM micrographs [72].

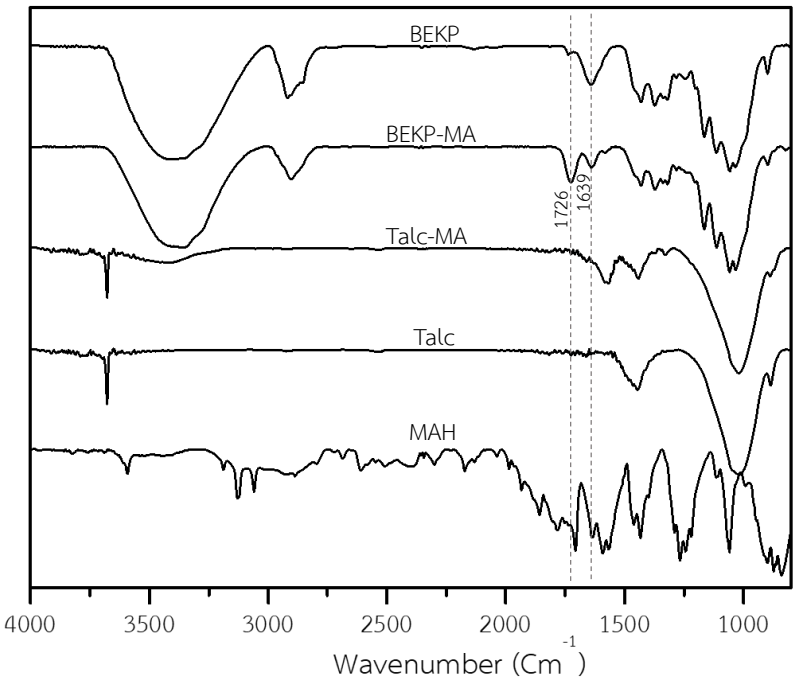

Figure 4.22 FTIR spectra of BEKP fiber, talc with and without MAH.

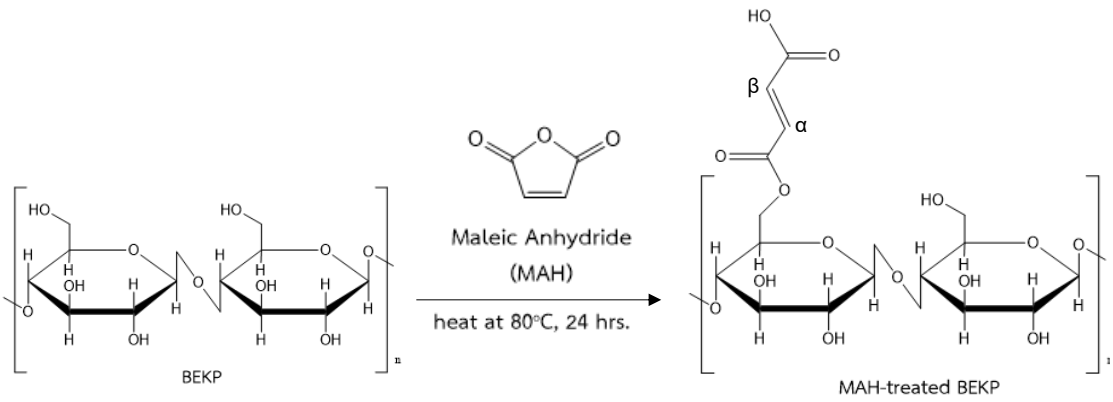

Figure 4.23 Surface grafting mechanism of MA moiety onto the BEKP fiber.

4.2.2.2. Modulus, tensile strength, and elongation at break of PLA hybrid composites

Young's modulus, tensile strength, and elongation at break of PLA hybrid composites in the presence of 1.0 and 1.5 phr CEGMA with and without 0.4 phr perkadox and various MAH content; 0.1, 0.2, 0.3 and 0.4 phr were demonstrated in Figure 4.24. It was shown that Young's modulus of PLA hybrid composites tended to slightly increase when MAH content was increased, compared to that of non-reactive hybrid composite (the dashed line). However, Young's modulus of PLA hybrid composites was insignificant changed by MAH content, compared to that of without MAH. It was known that the improvement of the quality of the polymer interface did not significantly affect Young's moduli or stiffness of the materials [105]. In case of tensile strength, all PLA hybrid composites with and without MAH showed an increase in tensile strength, compared to that of non-reactive hybrid composite (the dashed line). For the presence in 1.0 phr CEGMA, the tensile strength of PLA hybrid composites with MAH loading up to 0.2 phr was slightly increased by 6% higher than of that without MAH due to better fiber/PLA interfacial adhesion. However, PLA hybrid composites with increasing MA content showed slight decrease in tensile strength, which value was similar to that of without MAH. A similar result was reported by Yu and co-workers [97] that the reduction in the tensile strength was due to degradation of PLA caused by free radical reaction with unreacted MAH remaining in PLA matrix after PLA-g-MA reaction; however, PLA chain scission in this study maybe caused by remaining unreacted MAH on BEKP surface. In contrast, for the presence in 1.5 phr CEGMA, the tensile strength of PLA hybrid composites with all MAH loading content was increased about 8% and no decline in the tensile strength despite loading more MAH. One reason for the addition MAH higher than 0.2 phr without sacrificing tensile strength of PLA hybrid composites was, at a higher content of CEGMA (1.5 phr) could act as a chain extender for short-PLA chain caused by remaining unreacted MAH on BEKP surface, so PLA chain was reconnected [78]. In case of elongation at break of PLA hybrid composites, it showed a tendency as similar as tensile strength.

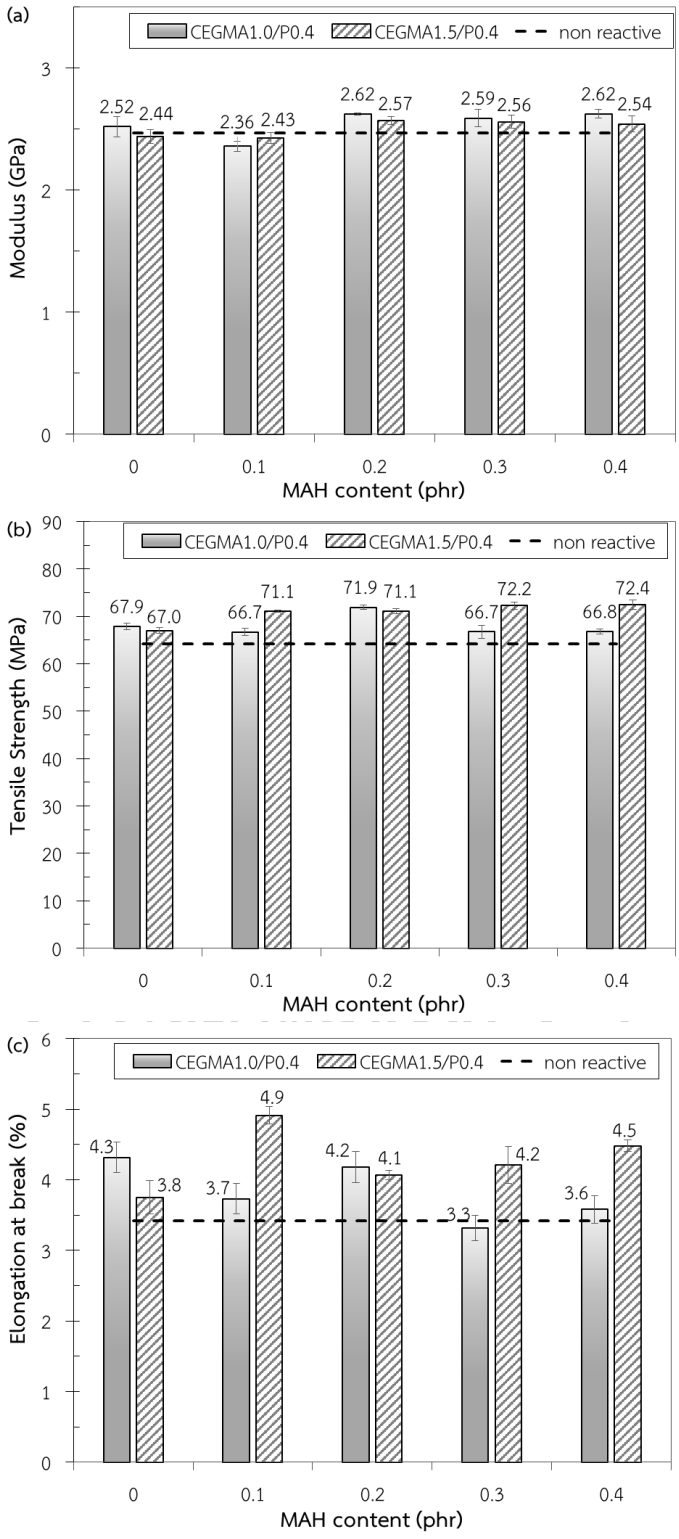

Figure 4.24 Young's modulus (a), tensile strength (b) and elongation at break (c) of PLA hybrid composites in the presence of 1.0 and 1.5 phr CEGMA with and without 0.4 phr perkadox and various MAH content; 0.1, 0.2, 0.3 and 0.4 phr.

The reactive PLA hybrid composite with CEGMA and MAH/peroxide showed the higher tensile strength and the elongation at break than non-reactive hybrid composite without sacrificing Young's modulus. This indicated a strong interfacial adhesion between PLA matrix and filler, which would result in effective stress transfer across the interface and allow the reactive hybrid composite to withstand higher stresses upon loading. This could be seen in the FE-SEM micrographs obtained from the fracture surfaces of the specimens broken after the tensile tests.

4.2.2.3. Morphology of PLA hybrid composites

The tensile fracture surfaces of PLA/maleated BEKP/talc hybrid composites with CEGMA (1.0 and 1.5 phr) and peroxide were observed at 8000x magnification times using FE-SEM, as shown in Figure 4.25. It was evidently seen that the maleated BEKP fibers were tightly connected with PLA matrix and broken within the matrix for both CEGMA loading contents. Whereas the talc surface was smooth and it showed some space between talc surface and the matrix. Furthermore, the adhered PLA resin exhibited a small fibril deformation and a little change in the morphology the fracture surface, which slightly rougher than that of non-reactive PLA/BEKP/talc hybrid composites (Figure 4.17 (c1)). The enhancing interfacial compatibility between BEKP and PLA matrix via *in situ* reaction was considered to cause by two effects, the coupling between maleated BEKP and PLA chain by the multifunctional epoxide and/or by free radical reaction.

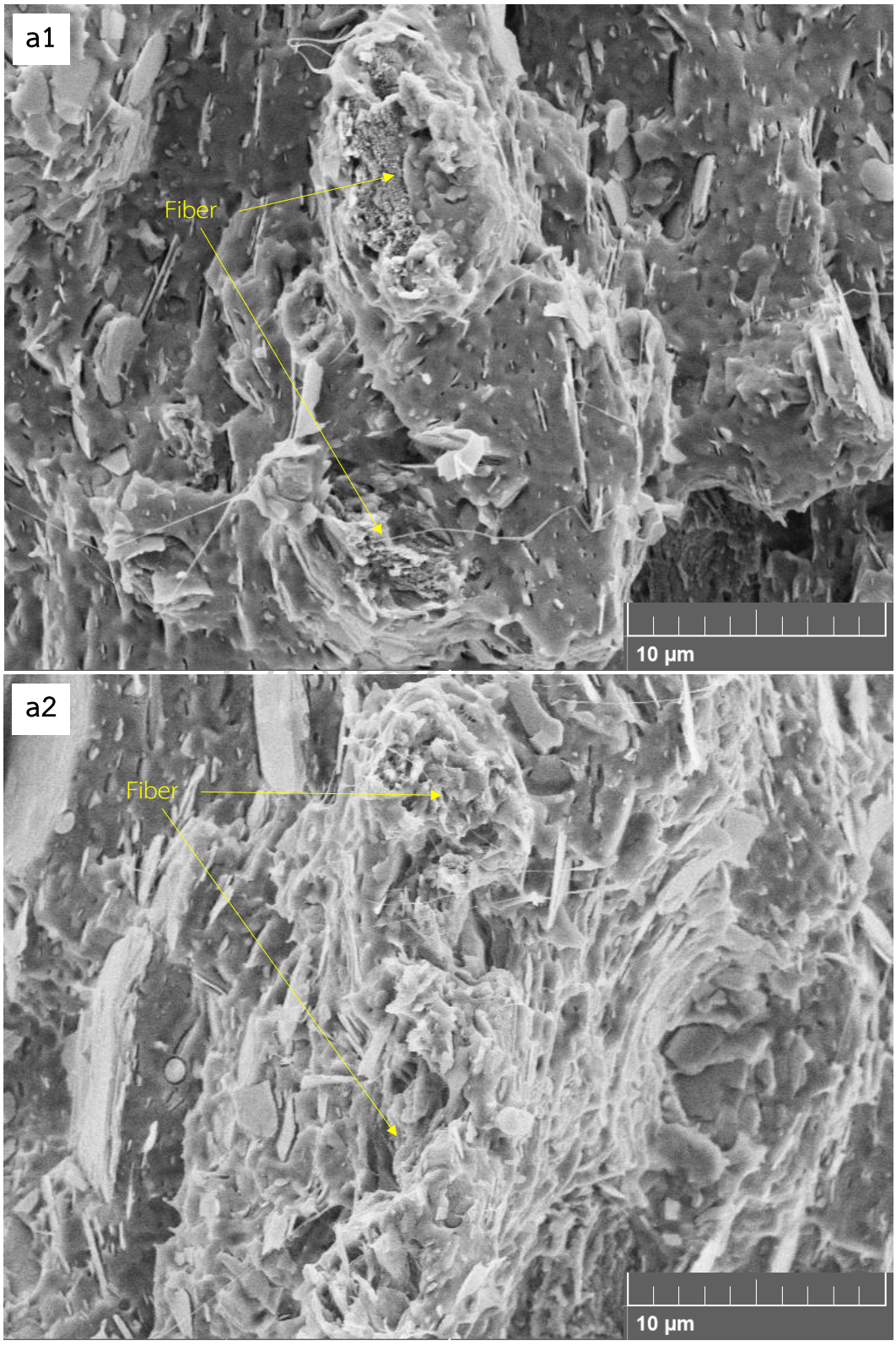

Figure 4.25 FE-SEM micrographs (8000×) for PLA hybrid composites with CEGMA1.0/MAH0.2 (a1), CEGMA1.5/MAH0.2 (a2).

4.2.2.4. Impact strength of PLA hybrid composites

The impact strength of PLA hybrid composites in the presence of 1.0 and 1.5 phr CEGMA with and without 0.4 phr perkadox and various MAH content; 0.1, 0.2, 0.3 and 0.4 phr was illustrated in Figure 4.26. All PLA hybrid composites in the presence of CEGMA with and without peroxide and MAH exhibited the impact strength greater than that of non-reactive hybrid composite. The addition of different CEGMA content did not significantly affect the impact strength of PLA hybrid composite upon increasing MAH content. On the other hand, the impact strength of PLA hybrid composites tended to increase when MAH content was increased up to 0.2 phr for both CEGMA content loading indicating more effective resistance to crack propagation. This might be due to better interfacial adhesion between the BEKP fiber and PLA matrix. The impact strength of PLA hybrid composite in the presence of 1.0 phr CEGMA with peroxide/MAH0.2 was increased by 25 and 11%, compared to that of non-reactive hybrid composite and PLA hybrid composite added only CEGMA, respectively. In addition, PLA hybrid composite in the presence of 1.5 phr CEGMA with peroxide/MAH0.2 gave the highest impact strength that increased by 35 and 25%, compared to that of non-reactive hybrid composite and PLA hybrid composite added only CEGMA, respectively. High impact strength could arise from the matrix/filler interfacial adhesion, which might be described by the reaction among the multifunctional epoxide groups, carboxyl groups of the MAH-treated BEKP structure, and carboxyl or hydroxyl groups at the end group of PLA molecular chain during the melt-blending process. However, when MAH loading was increased more than 2 phr, it was found that the impact strength of PLA hybrid composites was decreased at a similar level as only CEGMA loading. According to the BEKP was previously treated with MAH and the MAH-treated BEKP was used without the removal of unreacted maleic anhydride. One reason for that was, at a higher content of MAH, the chain scission reaction of PLA might occur similar to those found by elsewhere [106].

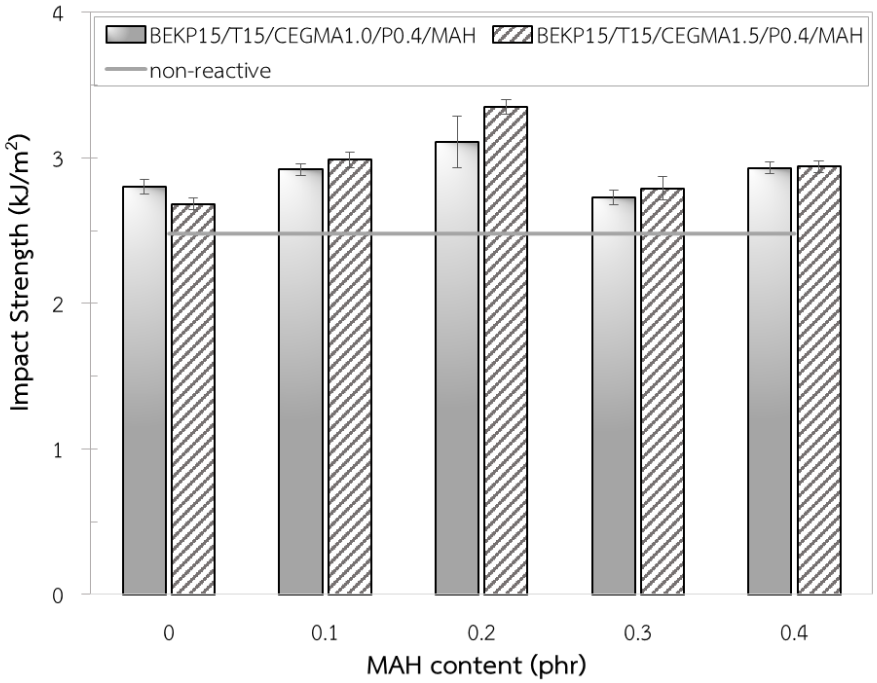

Figure 4.26 Impact strength of PLA hybrid composites in the presence of 1.0 and 1.5 phr CEGMA with and without 0.4 phr perkadox and various MAH content; 0.1, 0.2, 0.3 and 0.4 phr.

4.2.2.5. Dynamic mechanical thermal (DMTA) properties of PLA hybrid composites

The plot of storage modulus as a function of temperature for PLA hybrid composite containing 30 wt.% filler (1:1 BEKP: talc) incorporated with 1.0 and 1.5 phr CEGMA, peroxide and various MAH loadings: 0, 0.1, 0.2, 0.3 and 0.4 wt.% as shown in Figure 4.27. The storage modulus of PLA hybrid composites incorporated with both 1.0 and 1.5 phr CEGMA shows an increasing trend when MAH content was increased up to 0.2 phr and then decreased with further increasing MAH content, which was in agreement with tensile property result but it was significantly affected on dynamic stress [72].

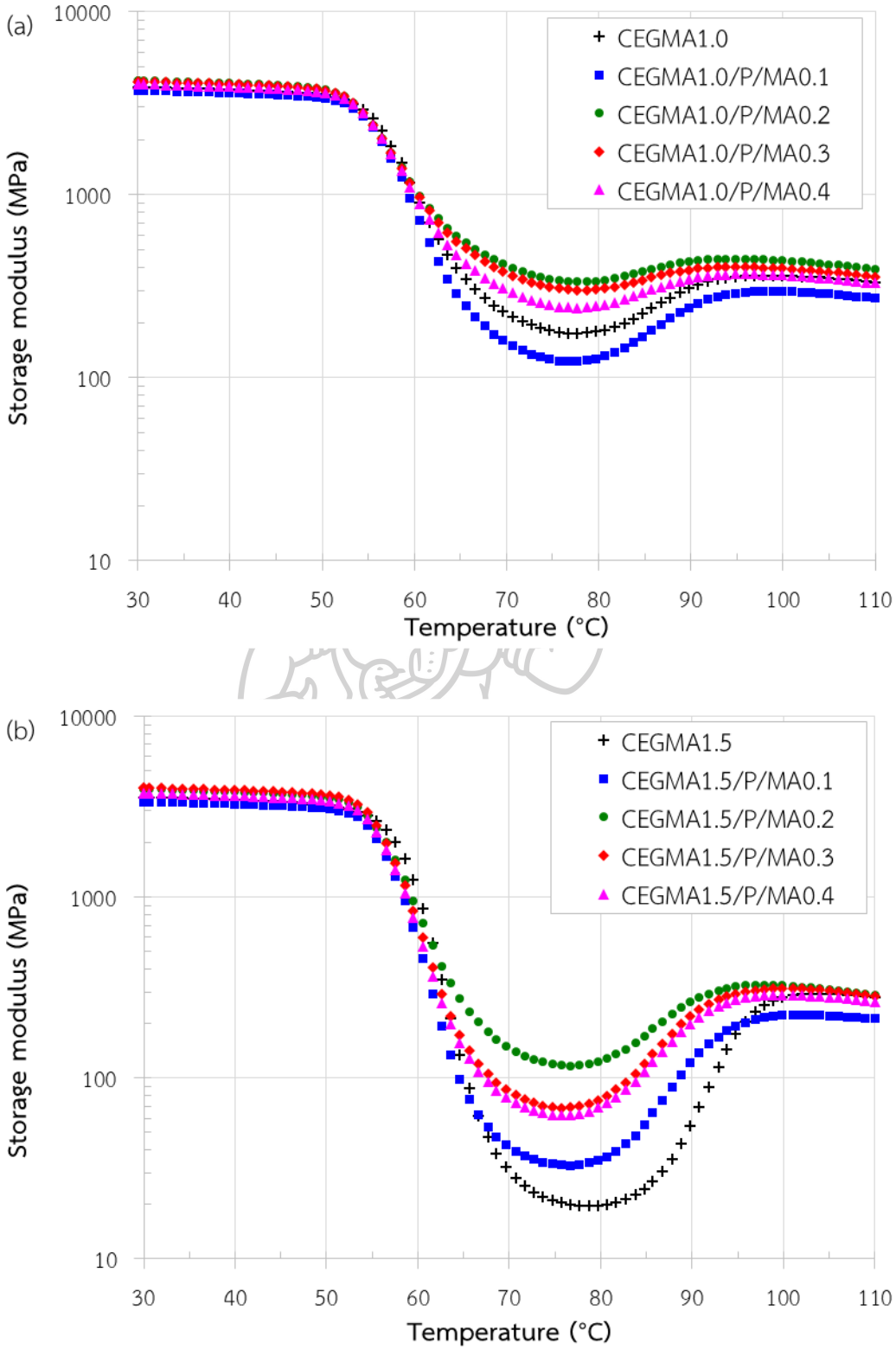

Figure 4.27 Storage modulus as a function of temperature for PLA hybrid composite containing 30 wt% filler (1:1 BEKP:talc) incorporated with 1.0 (a) and 1.5 (b) phr CEGMA, peroxide and various MAH loadings: 0, 0.1, 0.2, 0.3 and 0.4 phr.

4.2.2.6. Characterization of the extracted filler from PLA hybrid composites

FTIR spectra of extracted BEKP fiber and talc from the non-reactive (PLA/BEKP/Talc) and reactive hybrid composite (PLA/maleated BEKP/Talc/CEGMA/peroxide) were illustrated in Figure 4.28. It was found that the great difference was the two ester stretching peaks at 1758 and 1740 cm^{-1} in the reactive hybrid composite sample, which were assigned to carbonyl stretch (-C=O) of saturated and α, β-unsaturated esters, respectively. The C=O stretch of saturated corresponded to the remaining carbonyl groups (C=O) of PLA chains in extracted BEKP fibers. In case of another report, the two ester carbonyl vibrations were ascribed the splitting either to the symmetric and antisymmetric coupling of the two C=O stretching vibrations or to their resonance coupling with an overtone [107]. Abramovitch, RA. reported that the two ester carbonyl vibrations were the spectra of the malonate esters or diethyl malonate [107]. Furthermore, the peak wavenumber at around 1641 cm^{-1} for non-reactive hybrid composite was slightly shifted to a lower value for reactive hybrid composite. This may be explain that the decrease in wavenumber is due to the increase of the bond length caused by the change in electronegativity of the neighboring atom [108]. It could be suggest that H-bonding of carboxylic group on maleated fiber may be change to be ester bond by epoxide group leading to increase of bonds between two atoms.

Proposed *in situ* reaction mechanism in the reactive hybrid composite (PLA/maleated BEKP/Talc/CEGMA/peroxide) during the melt-blending process was considered to two mechanisms as shown in Figure 4.29. According to FT-IR results from the earlier (Figure 4.22), it confirmed that BEKP fiber could be reacted with MAH and left the alkene group in the structure, which could be grafted onto PLA chains via free radical reactions using peroxide in the melt state. In another proposed *in situ* reaction mechanism was, CEGMA could reactively react with the carboxyl group on maleated BEKP and chain-end of PLA via an *in situ* melting-process. As it was reported that the reaction of the epoxide group with the anhydride group occurred as well as the acid group resulting in an ester linkage [109].

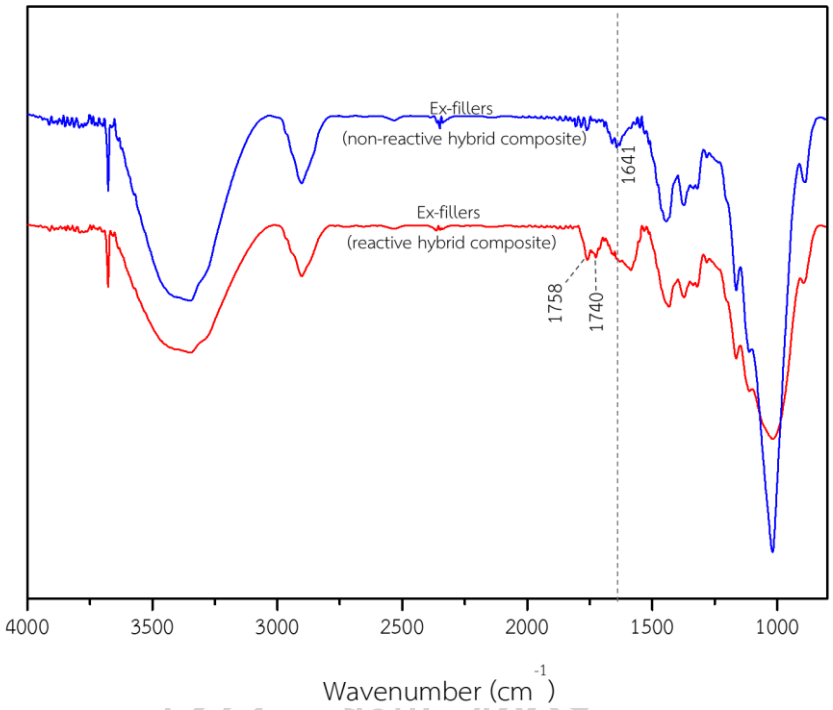

Figure 4.28 FTIR spectra of extracted BEKP fiber and talc from the non-reactive and reactive hybrid composites.

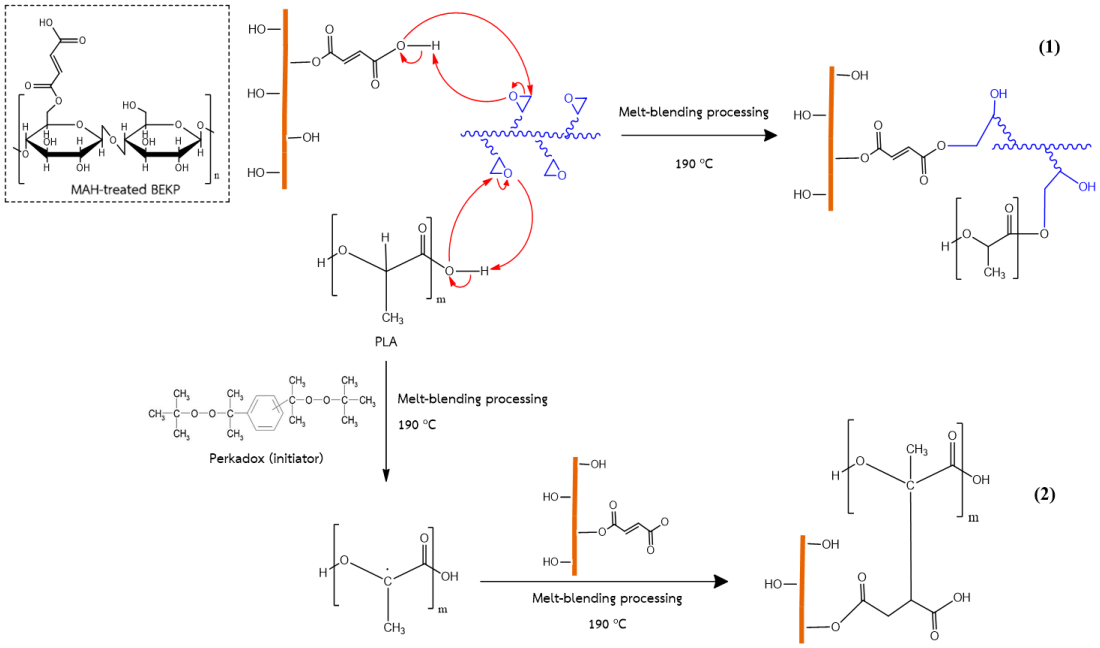

Figure 4.29 Proposed *in situ* reaction mechanisms in the reactive hybrid composite during the melt-blending process.

4.2.3. Effect of talc and BEKP contents in the reactive hybrid composites (PLA/maleated- BEKP/Talc/CEGMA/peroxide)

4.2.3.1. Modulus, tensile strength, and elongation at break of the reactive hybrid composites

Young's modulus, tensile strength, and elongation at break of the reactive hybrid composites (PLA/maleated BEKP/Talc/CEGMA/peroxide) containing various filler (1:1 of BEKP: Talc) contents; 20, 30 and 40 wt.% were shown in Figure 4.30. As expected, a higher filler loading led to the increase in Young's modulus and the decrease in elongation at break of the reactive hybrid composites. An interesting feature of the results was the increase in tensile strength of the reactive hybrid composites without sacrificing Young's modulus upon increasing filler loading. Generally, a drop of tensile strength could be seen at 30 wt% to 40 wt% of fiber or filler loading due to weak interfacial adhesion and poor distribution as discussed in the previous part in this work and others [110, 111]. These results revealed that the surface modification of BEKP fiber using MAH improved the tensile strength of the reactive PLA hybrid composites with CEGMA.

4.2.3.2. Morphology of the reactive hybrid composites

FE-SEM micrographs of the reactive PLA hybrid composites containing various filler (1:1 of BEKP: Talc) contents; 20, 30 and 40 wt.% were demonstrated in Figure 4.31. It was seen that all reactive hybrid composites exhibited strong interfacial adhesion between PLA matrix and BEKP fiber as discussed earlier. The reactive hybrid composites containing 20 and 30 wt.% filler loading displayed a good distribution of BEKP fiber and talc in PLA matrix. On the other hand, The reactive hybrid composites containing 40 wt.% filler loading revealed some agglomerates of BEKP fibers.

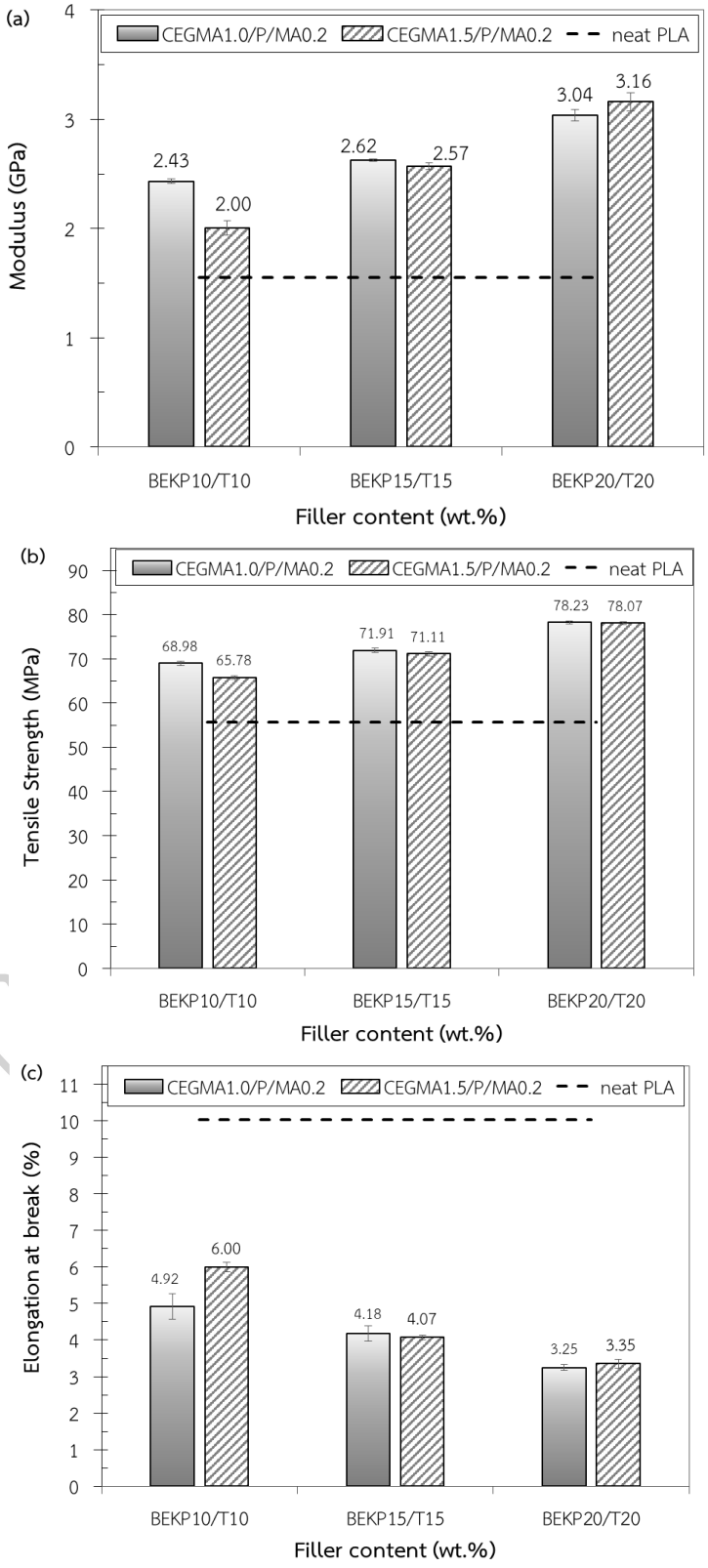

Figure 4.30 Young's modulus (a), tensile strength (b) and elongation at break (c) of the reactive PLA hybrid composites with various filler contents; 20, 30 and 40 wt.%

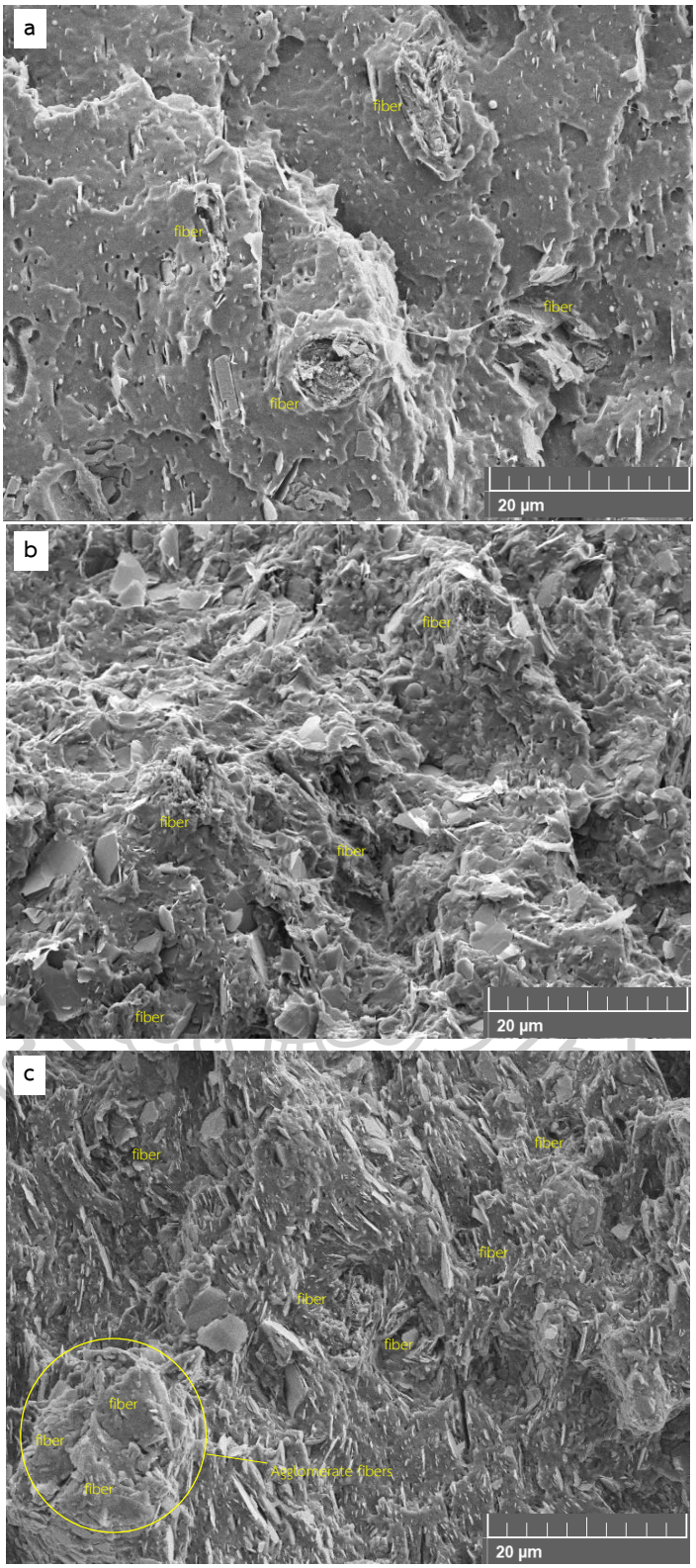

Figure 4.31 FE-SEM micrographs of the reactive PLA hybrid composites containing various filler (1:1 of BEKP: Talc) contents; (a) 20, (b) 30 and (c) 40 wt.%

4.2.3.3. Impact strength of the reactive hybrid composites

Impact strength of the reactive PLA hybrid composites containing various filler (1:1 of BEKP: Talc) contents; 20, 30 and 40 wt.% as shown in Figure 4.32. As expected, the impact strength of the reactive PLA hybrid composites was decreased when filler contents were increased from 20 to 40 wt.% but still higher than that of neat PLA. The impact strength of the reactive PLA hybrid composites with 1.0 phr CEGMA increased by 25, 24 and 9% for 20, 30 and 40 wt.% filler loading, respectively, compared to that of neat PLA. In case of the reactive PLA hybrid composites with 1.5 phr CEGMA, the impact strength increased by 42, 33 and 14% for 20, 30 and 40 wt.% filler loading, respectively, compared to that of neat PLA. These results were the difference from another report that the impact strength of silane-treated-talc/Newspaper/PLA hybrid composite containing 40 wt.% filler loading (Newspaper30/talc10) was improved only 2.3% compared to that of neat PLA [30]. In this work, although, the high filler content up to 40 wt.% was loaded in the reactive PLA hybrid composites, it showed a higher impact strength than that of neat PLA, indicating strong interfacial adhesion between PLA matrix.

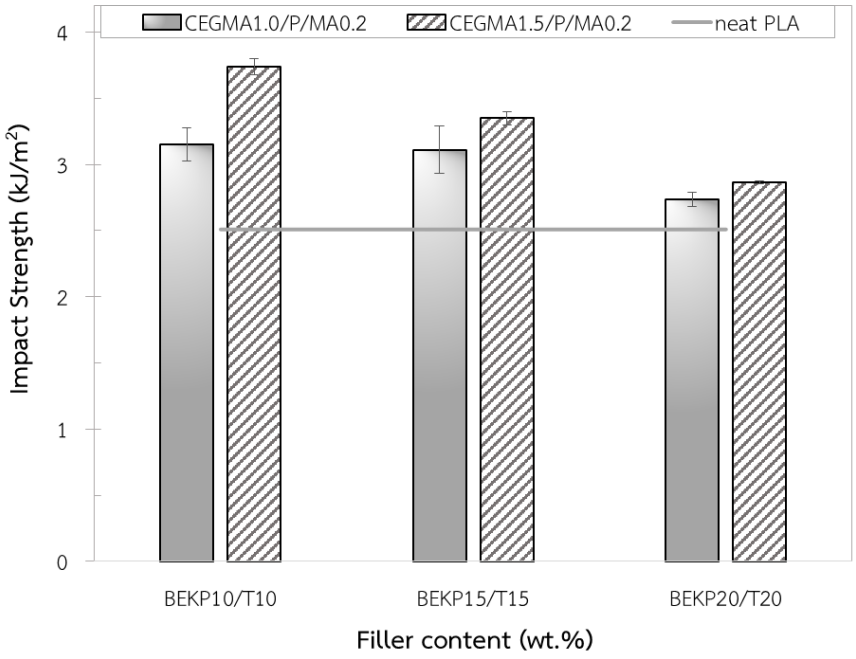

Figure 4.32 Impact strength of the reactive PLA hybrid composites containing various filler (1:1 of BEKP: Talc) contents; 20, 30 and 40 wt.%

4.2.3.4. Dynamic mechanical thermal (DMTA) properties of the reactive hybrid composites

From Figure 4.33, as expected the storage modulus of all reactive hybrid composites was greater than that of neat PLA due to the presence of the rigid part of BEKP fiber and talc, indicating the stress transfer from PLA matrix to the filler [112]. It was found that the storage modulus of all reactive hybrid composites decreased with increasing CEGMA content, which was explained previously.

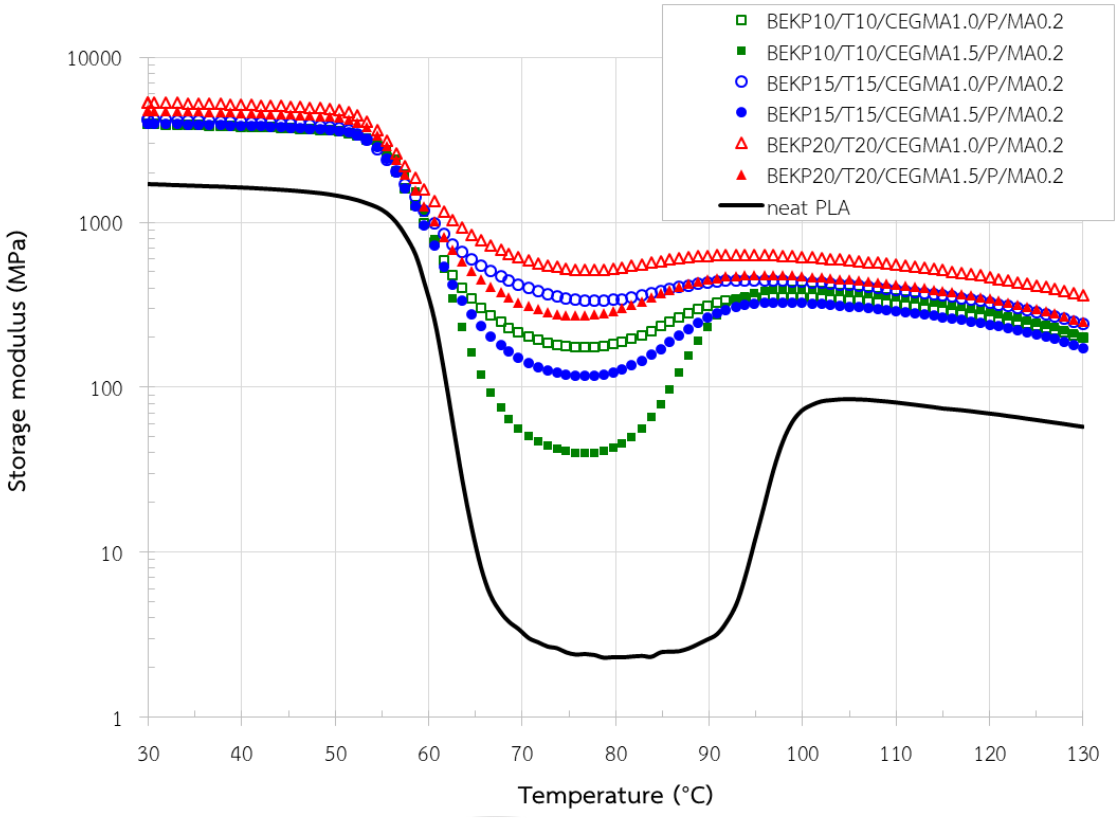

Figure 4.33 Storage modulus as a function of temperature for PLA hybrid composite containing 20, 30 and 40 wt.% filler (1:1 BEKP: talc) incorporated with 1.0 and 1.5 phr CEGMA, peroxide and 0.2 phr MAH loadings.

4.3. Properties of reactive PLA/Jute/Carbon fiber hybrid composites.

The *in situ* reactive MAH-treated BEKP/talc reinforced PLA hybrid composites with CEGMA and peroxide showed an effective improvement in interfacial adhesion between PLA matrix and fillers, particularly BEKP fiber as previously proved. In this respect, the same reactive *in situ* reactive agents might be used for another fiber such as jute fiber reinforced PLA composite using direct fiber feeding injection molding (DFFIM) process. This technique was practical process for injection molding products of PLA shot fiber composites with short reaction and preparation time. Furthermore, Carbon fiber (CF) was superimposed with jute fiber into PLA in order to improve the performance of PLA/jute/CF hybrid composite.

4.3.1. Fiber length and dimension of PLA/Jute fiber composites

Effect of matrix feeding speed and screw speed on the average (arithmetic mean) length and dimension of jute fiber in PLA/Jute fiber composite was shown in Figure 4.34. For non-reactive composites (○, □ symbols), it was found that a lower matrix feeding speed and higher screw speed led to shorter fiber length and smaller dimension. This could be ascribed to more fiber breakage due to a higher amount of fiber loading content caused by higher screw speed and lower matrix feeding speed [41]. At 20 rpm matrix feeding speed, the fiber length in reactive composites (●, ■ symbols) using low screw speed was shorter than non-reactive composite while it was no change at using high screw speed. This might be due to the increase in PLA matrix viscosity caused by the presence of CEGMA, which was more affected by using lower screw speed (more matrix content). However, the fiber dimension in reactive composites was higher than non-reactive composites. Furthermore, their fiber length distribution and details were in Appendix A.

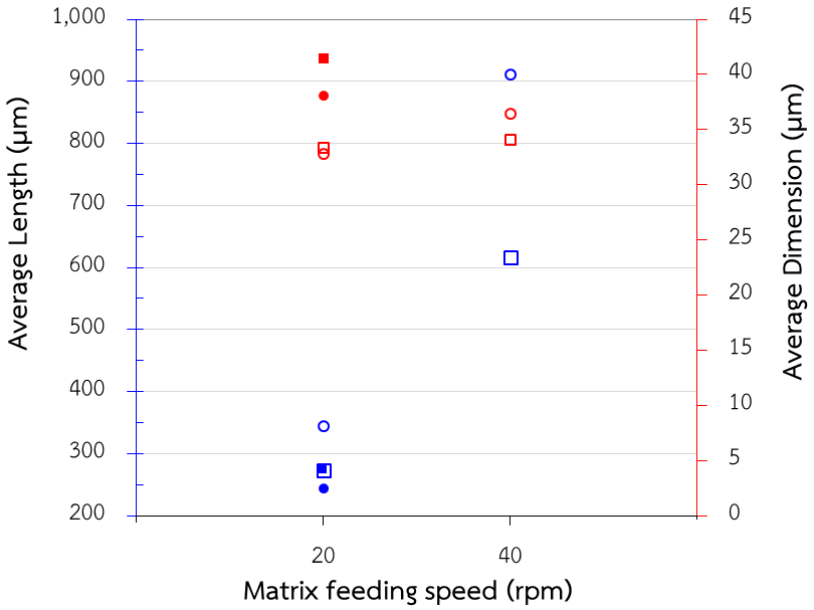

Figure 4.34 Average length (primary axis) and average dimension (secondary axis) of extracted jute fiber from PLA composites using various matrix feeding speeds; 20 and 40 rpm and different screw speeds; 215 (○=non-reactive composite and ●=reactive composite) and 301 (□=non-reactive composite and ■=reactive composite) rpm.

4.3.2. Effect of Fiber contents of Mechanical properties on PLA/Jute composites and PLA/Jute/Carbon fiber hybrid composite

Effect of fiber content and reactive agents on mechanical properties of PLA/Jute fiber composites and PLA/Jute/Carbon fiber hybrid composite were shown in Figure 4.35 to Figure 4.40. The increasing of matrix feeding speed and decreasing of screw speed led to the decrease in fiber content in composite. At low matrix feeding speed (20 rpm), the maximum fiber contents were 20.3 and 15.9 wt.% for high and low screw speed, respectively. The minimum fiber contents were 8.7 and 6.2 wt.% for using high and low screw speed using, respectively. In the case of the reactive composite, fiber loading content was slightly lower than that of the non-reactive composite, which might be due to the increase in PLA matrix viscosity caused by the presence of CEGMA. As expected, the modulus of PLA composites was increased when matrix feeding speed was decreased due to high fiber loading content. At 20

rpm matrix feeding speed, the highest modulus of non-reactive composites was increased by 78.2 and 61.5 % compared to that of neat PLA (1.68 GPa) for using high and low screw speed, respectively. However, modulus of the reactive composites was slightly higher, although fiber content was lower than non-reactive composites. The modulus of the reactive composite was increased by 97.1 and 10.6 %, compared to that of neat PLA (1.68 GPa) and non-reactive composite, respectively (2.23 GPa).

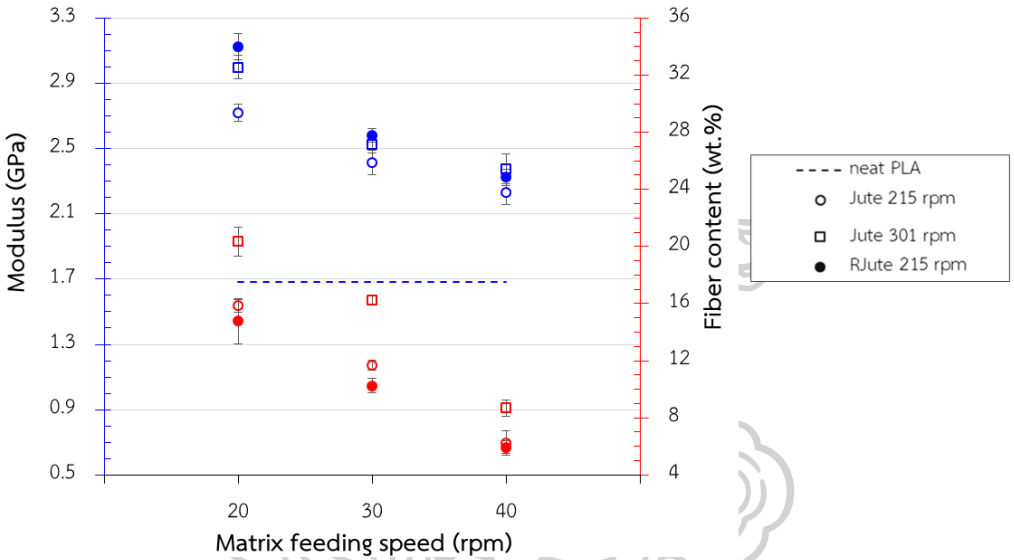

Figure 4.35 Modulus (primary axis) and fiber content (secondary axis) of PLA composites with and without reactive agents using various matrix feeding speeds; 20, 30 and 40 rpm and different screw speeds; 215 (○=non-reactive composite and ●=reactive composite) and 301 (□=non-reactive composite) rpm.

The tensile strength of PLA composites was showed the same trend as modulus as seen in Figure 4.36. At 20 rpm matrix feeding speed, the highest tensile strength of non-reactive composites was increased by 10.0 and 9.0 % compared to that of neat PLA (63.2 MPa) for using high and low screw speed, respectively. The tensile strength was a significantly higher than neat PLA (63.2 MPa) and non-reactive composite (75.2 MPa) by 36.5 and 14.9 %, respectively, although fiber content in the reactive composites was lower than that of non-reactive composites.

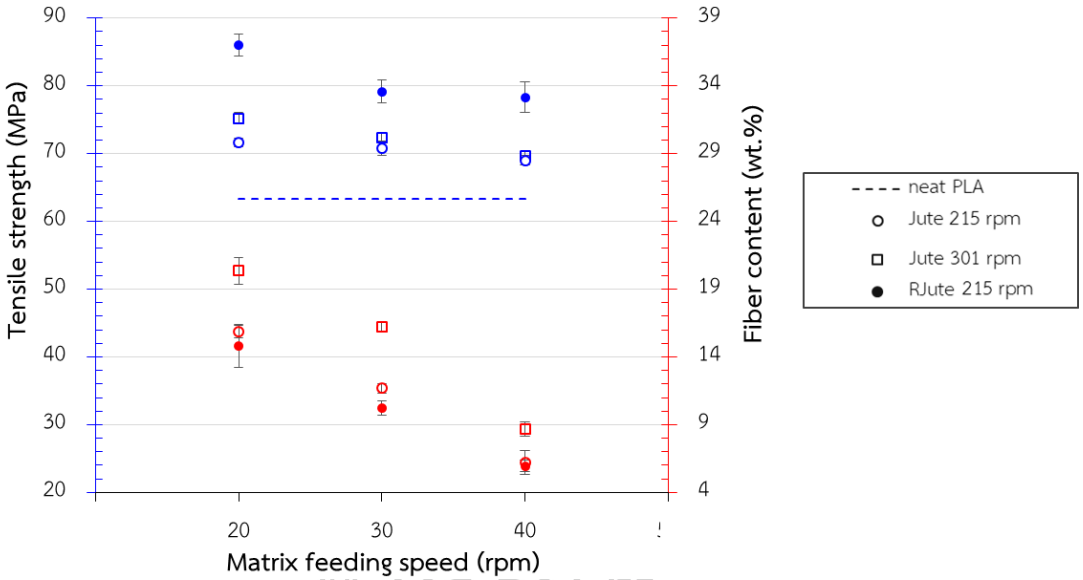

Figure 4.36 Tensile strength (primary axis) and fiber content (secondary axis) of PLA composites with and without reactive agents using various matrix feeding speeds; 20, 30 and 40 rpm and different screw speeds; 215 (○=non-reactive composite and ●=reactive composite) and 301 (□=non-reactive composite) rpm.

Elongation at break of PLA composites was decreased when matrix feeding speed was decreased due to a high fiber loading content as shown in Figure 4.37. Furthermore, elongation at break of reactive composites was also higher than that of non-reactive composites. The reactive composites showed more improvement in mechanical properties, although, they had lower fiber content than that of non-reactive composites. These indicated the strong interfacial adhesion between maleated jute and PLA matrix due to *in situ* reaction. These could be concluded that the mechanical properties of PLA/Jute composited were more affected by PLA/Jute interfacial adhesion than fiber loading content.

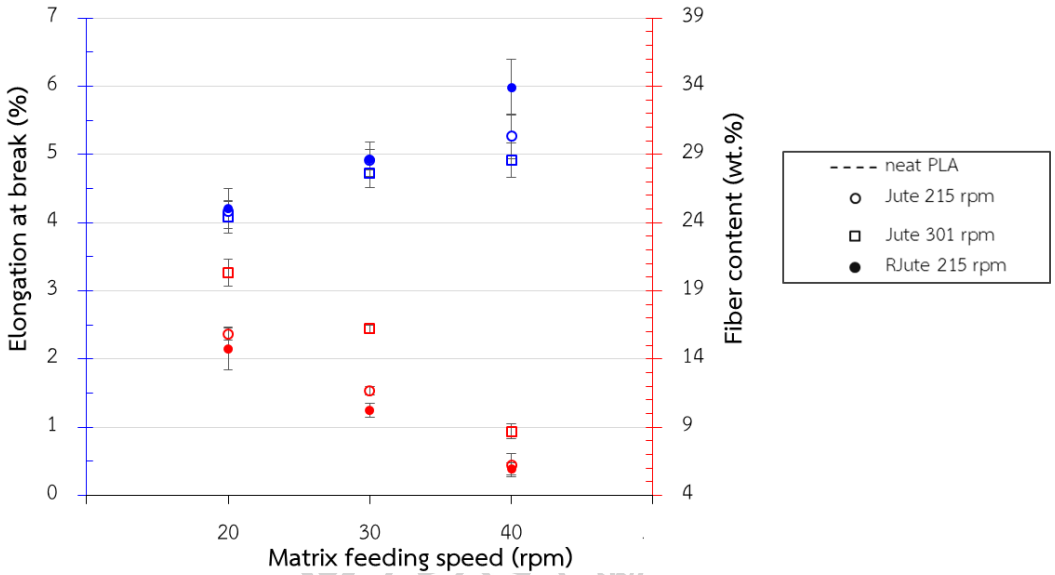

Figure 4.37 Elongation at break (primary axis) and fiber content (secondary axis) of PLA composites with and without reactive agents using various matrix feeding speeds; 20, 30 and 40 rpm and different screw speeds; 215 (○=non-reactive composite and ●=reactive composite) and 301 (□=non-reactive composite) rpm.

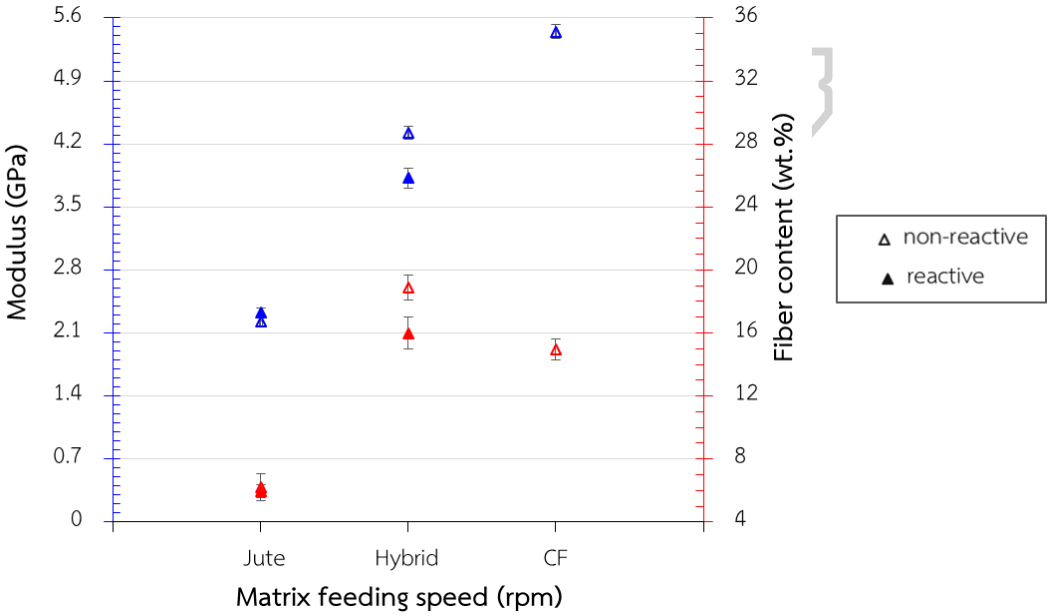

Figure 4.38 Modulus (primary axis) and fiber content (secondary axis) of PLA composites and hybrid composite with (△) and without reactive agents (▲) using matrix feeding speed 40 rpm and screw speed 215 rpm.

In the case of PLA hybrid composite reinforced with jute and carbon fiber, the effect of fiber content and reactive agents on mechanical properties were shown in Figure 4.38 to Figure 4.40. It could be observed that modulus and tensile strength increment has followed as order: PLA/CF > PLA/Jute/CF > PLA/Jute. However, the fiber content increment was followed the order: PLA/Jute/CF > PLA/CF > PLA/Jute. PLA/CF composite showed the highest modulus and tensile strength because CF has higher modulus and strength than jute fiber. In the case of the reactive hybrid composite, it showed a lower modulus than that of non-reactive hybrid composite due to the influence of fiber content as seen in Figure 4.38. However, from Figure 4.39, the tensile strength of reactive hybrid composite was higher than non-reactive hybrid composite, explained by good interfacial adhesion of PLA and fibers. Elongation at break of the reactive hybrid composite was as similar as the non-reactive hybrid composite (Figure 4.40).

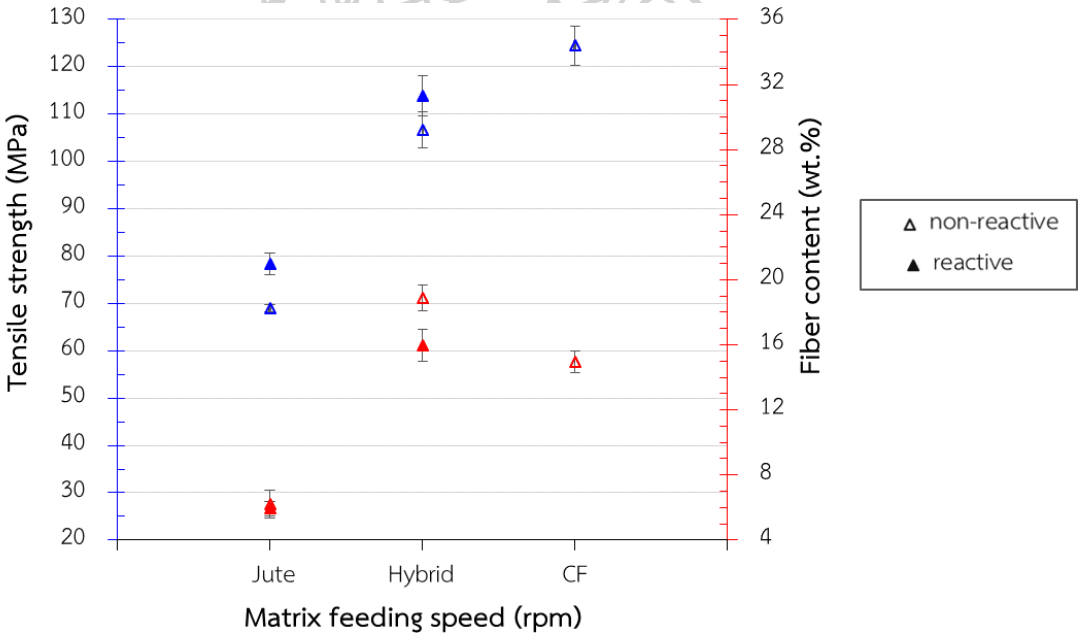

Figure 4.39 Tensile strength (primary axis) and fiber content (secondary axis) of PLA composites and hybrid composite with (△) and without reactive agents (▲) using matrix feeding speed 40 rpm and screw speed 215 rpm.

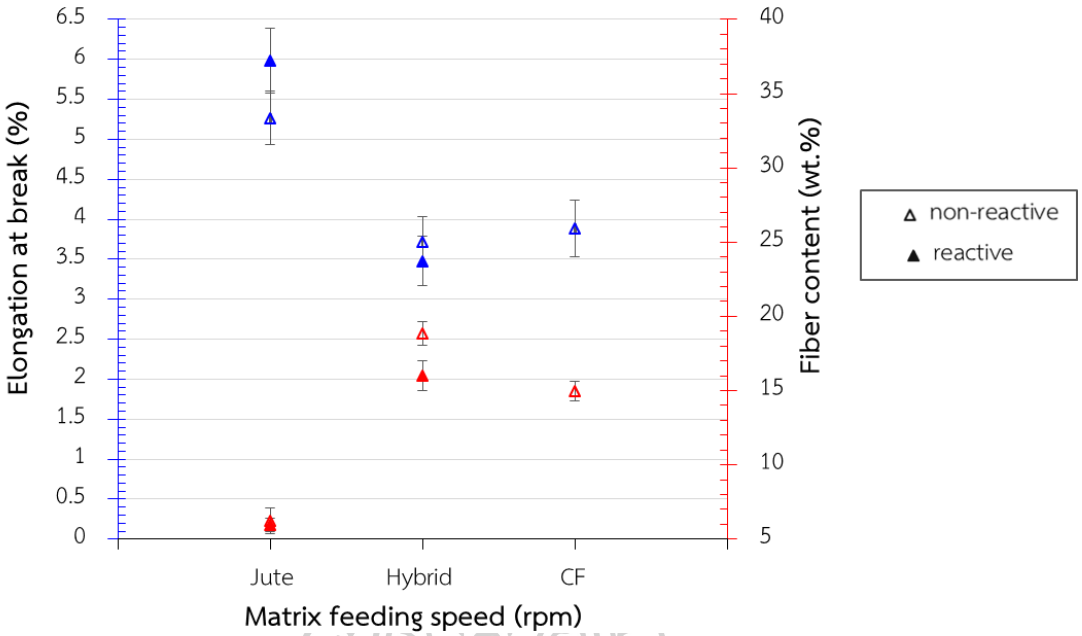

Figure 4.40 Elongation at break (primary axis) and fiber content (secondary axis) of PLA composites and hybrid composite with (△) and without reactive agents (▲) using matrix feeding speed 40 rpm and screw speed 215 rpm.

4.3.3. Morphology of PLA/Jute fiber composites

In order to observe the fiber distribution in PLA matrix, tensile fractured surface was observed at low magnification (40x). Morphology of tensile fractured surface of PLA composites and hybrid composite of different matrix feeding and screw speed with and without reactive agents was displayed in Figure 4.41. The morphology of non-reactive PLA/Jute composites using low screw speed as seen in Figure 4.41(c) - (d) showed a good fiber distribution while the others showed some aggregation of fibers at the edge of the specimen. This suggested that the distribution of fiber was more affected by high screw speed. Considering non-reactive PLA/Jute composites, they exhibited a lot of remaining pores due to the pull-out of fibers in PLA matrix, indicating a lack of PLA/fiber interfacial adhesion. Moreover, they showed a variety of fiber orientation plane in PLA matrix as seen from the presence of some fibers were parallel to the fracture surface. In contrast, the micrograph of reactive PLA/Jute composites (Figure 4.41 (e)) showed a decrease in remaining pores suggesting better PLA/fiber interfacial adhesion, compared to non-reactive PLA/Jute

composites. In case of PLA hybrid composites with and without a reactive agent (Figure 4.41(g) - (h)), it was not clearly seen the difference at low magnification observation due to the smaller diameter of CF.

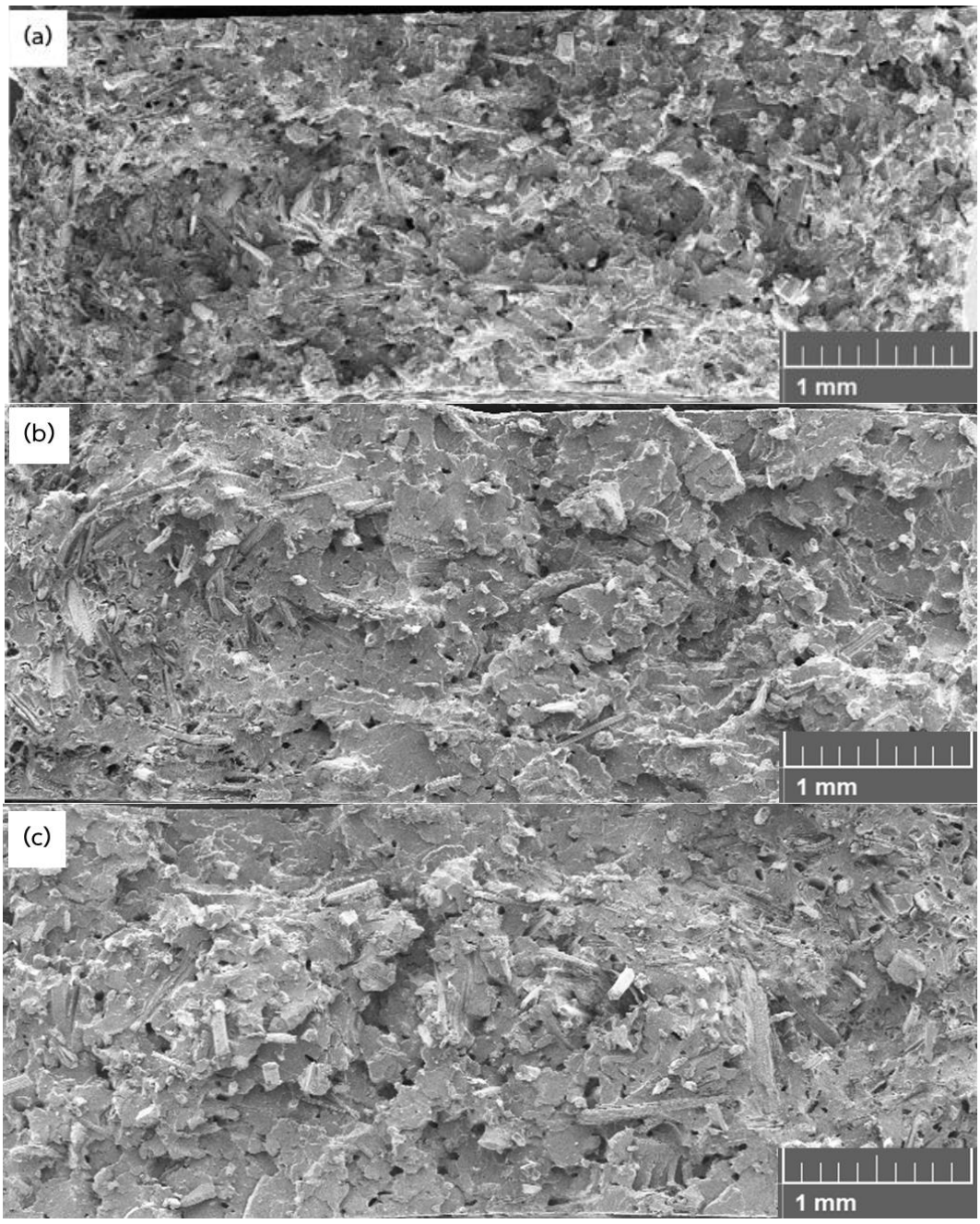

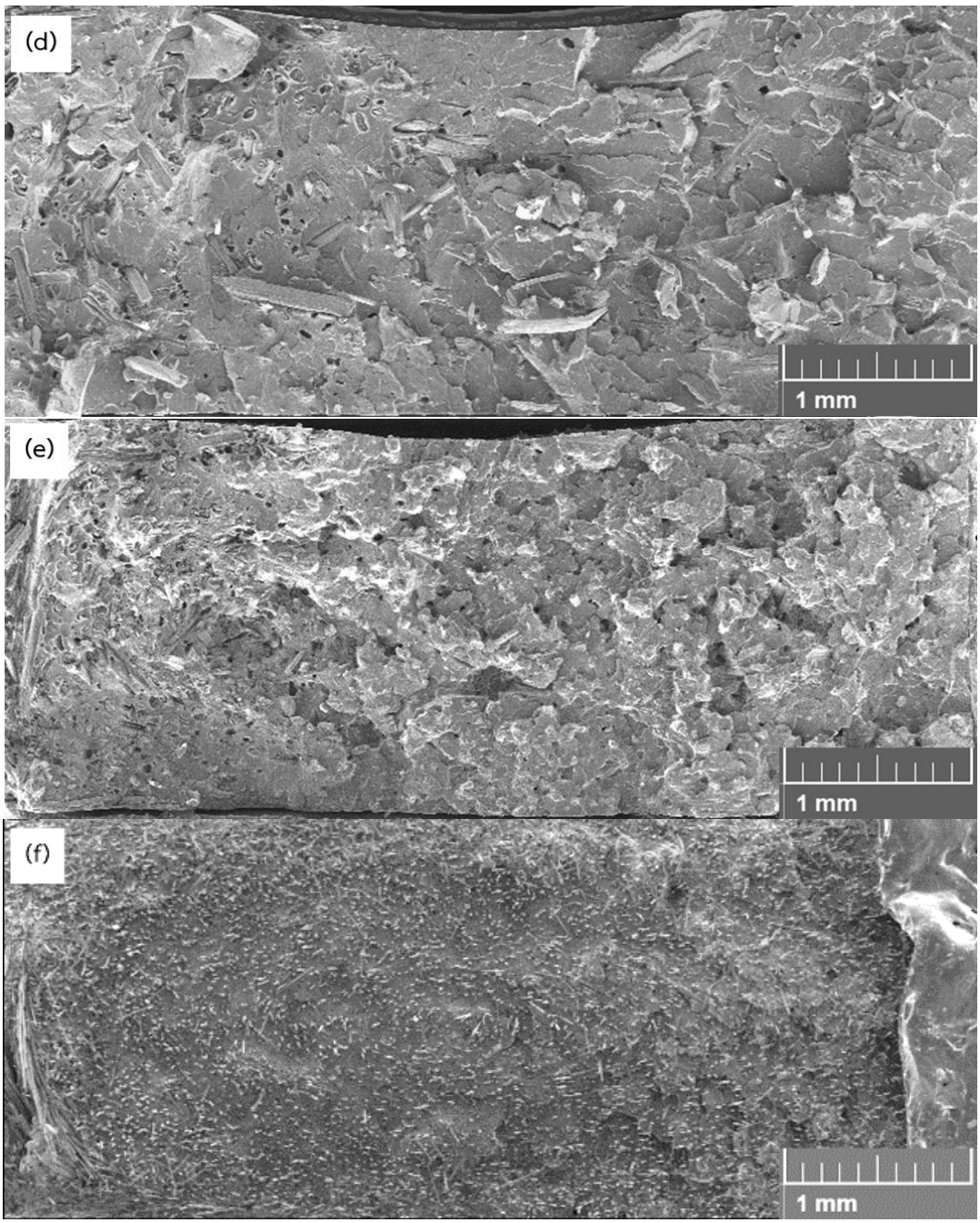
(d)
1 mm
(e)
1 mm
(f)
1 mm

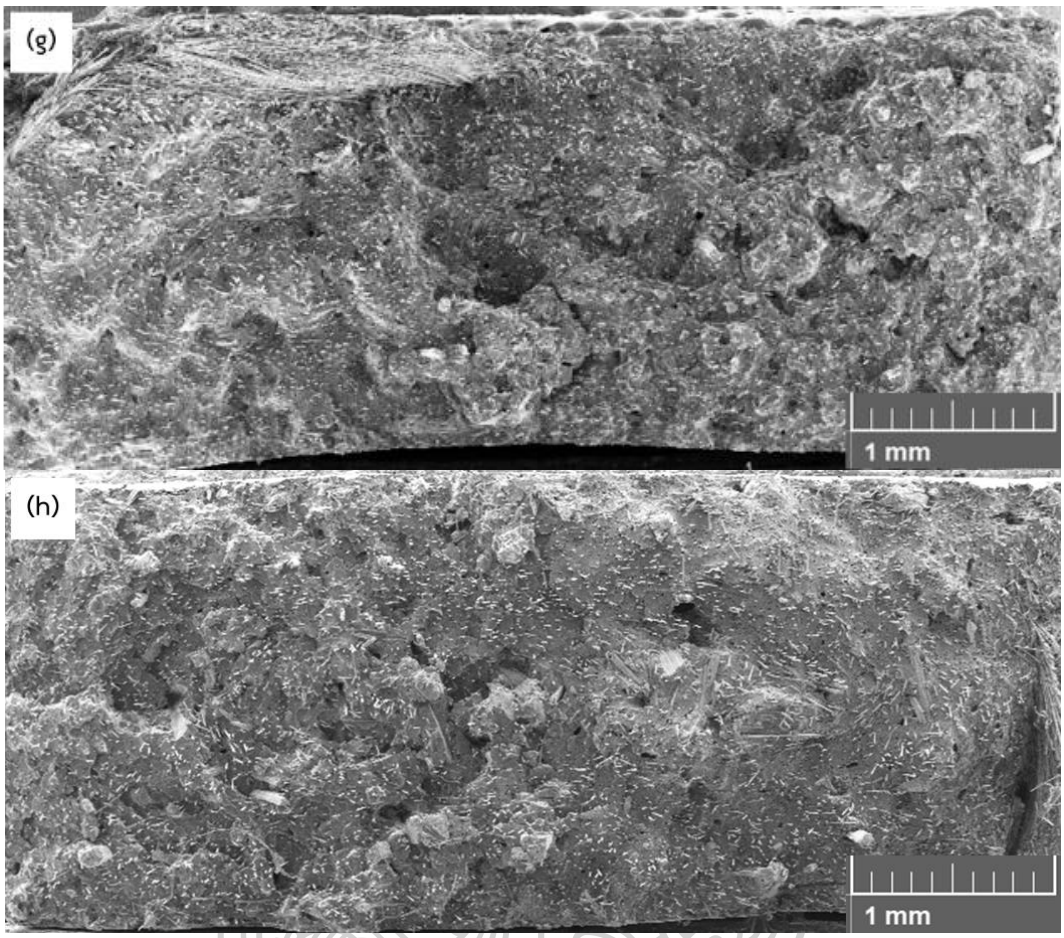

Figure 4.41 FE-SEM micrographs of tensile fractured surface of PLA composites using different matrix feeding/screw speed with Jute; 20/301 (a), 40/301 (b), 20/215 (c), 40/215 (d), reactive Jute; 20/215 (e), CF 40/215 (f), reactive hybrid Jute/CF 40/215 (g) and non-reactive hybrid Jute/CF 40/215 (h).

For a clear observation of PLA/fiber interfacial adhesion, the micrographs of tensile fractured surface PLA/Jute composites and PLA/Jute/CF hybrid composites with and without a reactive agent at high magnification were presented in Figure 4.42. Considering PLA/Jute composites, it was noticed that the non-reactive composite (Figure 4.42 (a)) demonstrated some fiber pull-out and space between PLA and fibers indicating poor PLA/fiber interfacial adhesion. On the other hand, it was clearly seen that the reactive composite (Figure 4.42 (b)) exhibited the fiber breakage along PLA matrix fractured surface rather than pull-out and no space between PLA and fibers. This indicated the strong PLA/fiber interfacial adhesion in the reactive composite that

was a reason for the increase in tensile strength. Considering non-reactive PLA/Jute/CF hybrid composites (Figure 4.42 (a)), it showed a lot of remaining pores of CF located by jute fiber and space between PLA and CF, indicating poor PLA/CF interfacial adhesion. In contrast, reactive PLA/Jute/CF hybrid composites (Figure 4.42 (b)) showed less pores and more CF breakage and interfacial adhesion, which might be due to the influence of MAH-treated jute located nearby and the reactive agent.

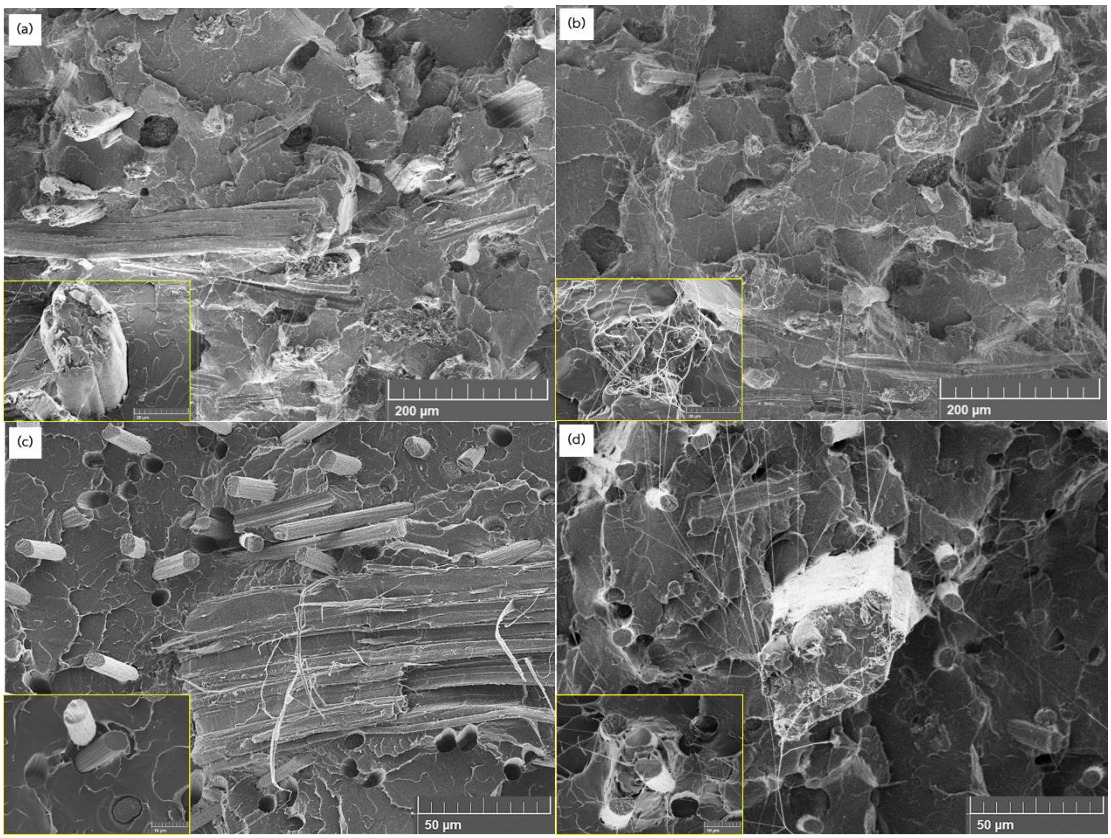

Figure 4.42 FE-SEM micrographs of tensile fractured surface non-reactive PLA/Jute composites (a), reactive PLA/Jute composites (b), non-reactive PLA/Jute/CF hybrid composites (c) and reactive PLA/Jute/CF hybrid composites (d).

4.3.4. FT-IR of extracted fiber from composites

In order to elucidate the reaction between jute fiber and MAH and also PLA molecule, FT-IR spectra of virgin jute, maleated jute and extracted jute fiber from composites was presented in Figure 4.43. The strong peak at 1738 cm^{-1} was observed in all samples corresponding to C=O stretching vibration of an ester components of hemicellulose in jute fiber [18]. It was found that the intensity of the ester band at 1738 cm^{-1} of maleated jute was increase due to an increase in ester groups, thus, it confirmed that MAH was successfully grafted on jute fiber. Likewise, the peak intensity at 1738 cm^{-1} of extracted jute fiber from reactive composite was higher than that of from non-reactive composite, which confirmed that the *in situ* compatibilization between maleated jute fiber and PLA chain occurred in a short reaction time via a reactive injection molding process.

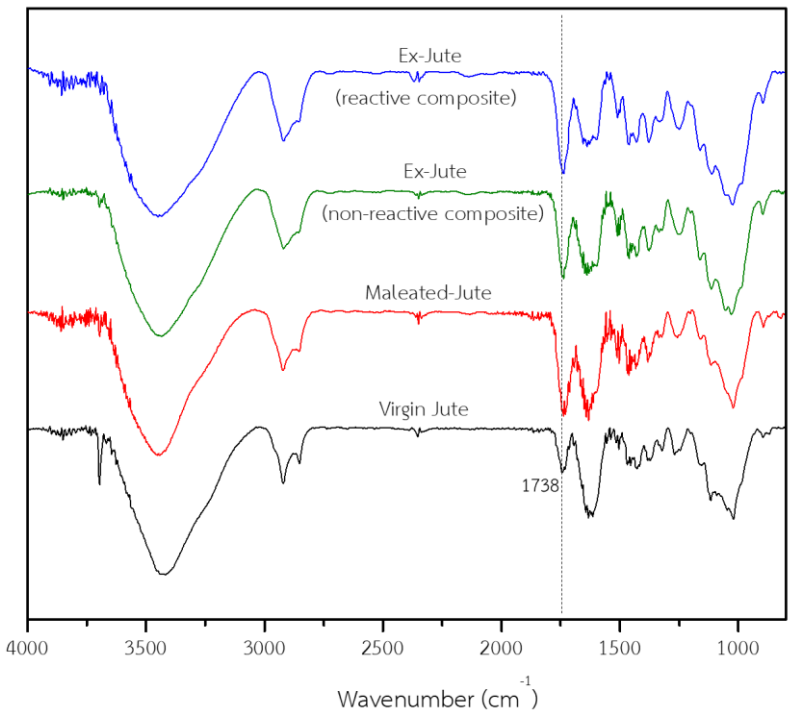

Figure 4.43 FTIR spectra of virgin jute, maleated jute and extracted BEKP fiber from non-reactive and reactive composites.

Charpter 5 Conclusions and suggestions

5.1. Conclusions

The aim of this work was to simply prepare PLA composite and hybrid composites reinforced with natural fibers, inorganic filler and/or synthetic fiber. PLA composite was successfully prepared by very simple method by *in situ* reactive melt-blending in a one-step process on twin-screw extrusion and direct fiber feeding injection molding (DFFIM) process. The properties of PLA composite and hybrid composites were improved. The general conclusions from this study were summarized as follows:

5.1.1. PLA/BEKP fiber biocomposites with and without reactive agents

The *in situ* reactive compatibilization of short-fiber BEKP reinforced PLA biocomposites were successfully prepared by melt-mixing. Reactive agents with a multifunctional group such as CEGMA, EAGMA, and EAMAH were selected as *in situ* reactive compatibilizers for PLA/BEKP biocomposites. It was found that the interfacial adhesion between PLA and BEKP fiber was improved as proved by FE-SEM micrographs, the adhesion factor, and effectiveness of PLA biocomposites. The improvement of PLA/BEKP interfacial adhesion was ascribed by chemical bonding between BEKP fiber and PLA chain. PLA chemical bonded with BEKP fiber by multifunctional epoxide-based reactive agents (CEGMA and EAGMA) as revealed by FTIR spectra and Molau test. Furthermore, PLA biocomposites loaded with 1.0 phr of CEGMA showed the most improvement on tensile strength about 16.3% and 13.9% compared to neat PLA and non-compatibilized PLA biocomposite, respectively. However, the effect of different reactive agents was not so dominant in terms of Young's modulus. The presence of all reactive agents also improved the elongation at break of PLA due to existing acrylic ester as soft part in their molecules. The storage modulus of PLA biocomposites showed the most increased when loading 0.5 phr of CEGMA followed by EAGMA and EAMAH, respectively. The present results indicated that CEGMA was the most effective *in situ* compatibilizer for PLA/BEKP biocomposite.

5.1.2. PLA/BEKP fiber/talc hybrid composites with and without CEGMA

The *in situ* reactive compatibilization of PLA reinforced with BEKP/talc and MAH-treated BEKP/talc hybrid composites were successfully prepared by one-step process via a twin-screw extruder. It was found that Young's modulus and tensile strength of PLA hybrid composites tended to increase with the increasing of talc' ratio. PLA hybrid composite with 1:1 of BEKP: talc ratio showed the highest storage modulus in the rubbery region, which was related to HDT property. PLA hybrid composites showed a rise of storage modulus in the order of 15:15 > 10:20 > 20:10 = 0:30 > 30:0 BEKP:talc ratios. PLA/fiber/talc interfacial adhesion was significantly improved with the presence of CEGMA as observed from FE-SEM micrographs. The tensile strength and impact strength of PLA hybrid composites incorporated with 1.5 phr CEGMA showed a slight improvement by 6% than that of non-reactive hybrid composite. In case of introducing a more reactive site on BEKP fiber surface, MAH was successfully grafted onto BEKP fiber surface via esterification reaction n during the drying process as revealed by FT-IR spectra. The interfacial adhesion between PLA and MAH-treated fiber in the hybrid composite was dramatically improved in reactive PLA hybrid composite. For MAH-treated fiber/talc reinforced PLA with CEGMA and peroxide loading, 0.2 phr MAH treatment showed the most improvement on tensile and impact strength of the reactive hybrid composite. The tensile and impact strength of the reactive hybrid composite with 1.0 – 1.5 phr of CEGMA was increased by 11 - 12 and 29 – 36 %, respectively, compared to non-reactive hybrid composite. Moreover, the treatment by 0.2 phr MAH with peroxide and CEGMA loading showed the highest storage modulus in the rubbery region. From these results, it could be concluded that PLA reinforced with MAH-treated BEKP/talc hybrid composites showed an effective improvement in PLA/fillers interfacial adhesion than the addition only CEGMA in the reactive extrusion process.

5.1.3. PLA/Jute/Carbon fiber hybrid composites with and without a reactive agent in term of practical application

Jute fiber and Carbon fiber (CF) reinforced PLA with the same *in situ* reactive agents were produced in direct fiber feeding injection molding (DFFIM) process, which was shorter reaction time. CF was added with jute fiber in order to improve the performance of PLA hybrid composite. It was found that the mechanical properties of non-reactive composites and hybrid composite were affected by fiber loading content. In contrast, the mechanical properties of reactive composites and the hybrid composite were more affected by PLA/fiber interfacial adhesion than fiber loading content. Although fiber content in the reactive composites was lower than that of non-reactive composites, the tensile strength of PLA/Jute composite was a significantly higher than neat PLA and non-reactive composite by 36.5 and 14.9 %, respectively. Likewise, the tensile strength of reactive hybrid composite was higher than non-reactive hybrid composite by 6.8%. Although the MAH was treated onto only jute surface, CF surface was also influenced during melt processing. The improvement on fibers/PLA interfacial adhesion was obviously seen in FE-SEM micrographs that exhibited fiber breakage rather than pull-out. These indicated that the reactive composites and the hybrid composite were better stress transfer between PLA matrix and fiber due to their strong interfacial adhesion. It was confirmed that the *in situ* compatibilization between MAH-treated jute fiber and PLA chain occurred in a short reaction time via reactive injection molding process as also confirmed by FT-IR spectra.

5.2. Suggestions

1. For interfacial adhesion improvement, *in situ* reactive system (MAH-treated cellulose fiber, CEGMA and peroxide) is suitable for cellulosic natural fiber and PLA through composite approach. For biodegradable polyesters with different polarities such as PBS, PBAT and so on, the interfacial adhesion with the fibers can be quite different, so it is interesting to investigate how this is affected by the reactive agents when reinforced with natural fiber. Furthermore, another natural fiber should be also

considered for fabricating composites using this *in situ* reactive system due to different composition of cellulose, hemicelluloses, lignin in natural fiber.

2. As reported in this research, MAH treatment for natural fiber occurred during drying process at 80 °C without any catalyst. Since there are different compositions of cellulose, hemicelluloses, lignin in natural fiber leading to different treatment efficiency. Therefore, the reaction time and temperature of MAH treatment for natural fiber should be studied for a balance in term of treatment efficiency and time.

3. Since this reactive system (MAH-treated cellulose fiber, CEGMA and peroxide) is suitable for improving interfacial adhesion between natural fiber and PLA. There are two proposed *in situ* reaction mechanisms in the reactive composite during the melt-blending process. First, alkene group in MAH-treated fiber structure could be grafted onto PLA chains via free radical reactions using peroxide. Second, epoxide group in CEGMA could reactively react with carboxyl group on MAH-treated fiber and chain-end of PLA. Therefore, using MAH-treated cellulose fiber and peroxide without CEGMA should be studied for improving interfacial adhesion for PLA/fiber composite as well as cost-effectiveness. In addition, without using CEGMA, MAH content for fiber treatment could be reduced in order to avoid PLA degradation due to remaining unreacted MAH on fiber during melt-blending process.

4. Since the reaction time occurred during fabrication composite and hybrid composite in DFFIM is very short, it is possible that the *in situ* reaction might be not completed. Therefore, the post-curing of samples obtained by DFFIM should be studied to ensure the completion of *in situ* reaction.

Appendix A Fiber length distribution

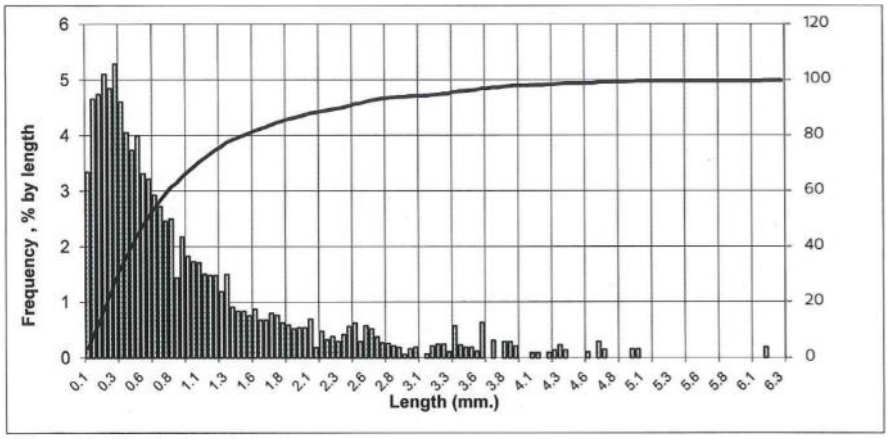

Test results by FQA (Fiber Quality Analyzer)

Arithmatic AV	0.3445	mm.	Width	32.80	µm.
L Weighted AV	0.7940	mm.	Total fibers	11,602	pcs.
Fines by number	45.83	%			
Fines by length (Less than 0.2 mm.)	17.32	%			
Curl index	0.136				
Kink index	1.688				

Figure A.0.1 Fiber length and width distribution of non-reactive PLA/Jute composite using 20 rpm matrix feeding speed and 215 rpm screw speed.

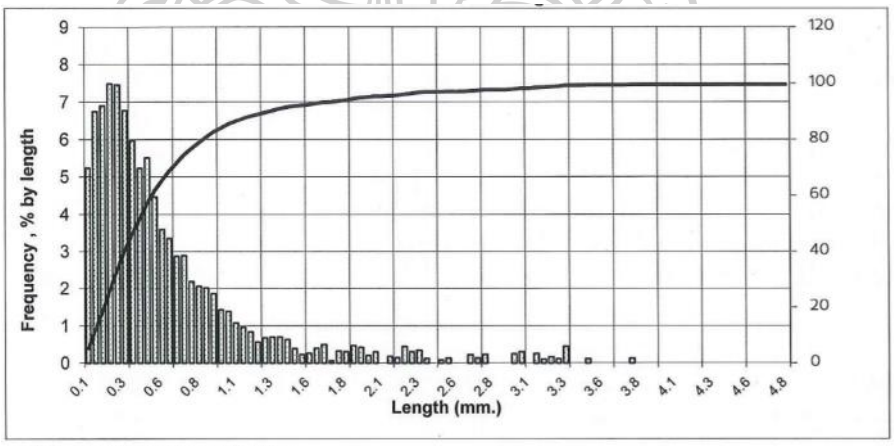

Test results by FQA (Fiber Quality Analyzer)

Arithmatic AV	0.2725	mm.	Width	33.35	µm.
L Weighted AV	0.5235	mm.	Total fibers	11,568	pcs.
Fines by number	53.31	%			
Fines by length (Less than 0.2 mm.)	24.77	%			
Curl index	0.134				
Kink index	1.621				

Figure A.0.2 Fiber length and width distribution of non-reactive PLA/Jute composite using 20 rpm matrix feeding speed and 301 rpm screw speed.

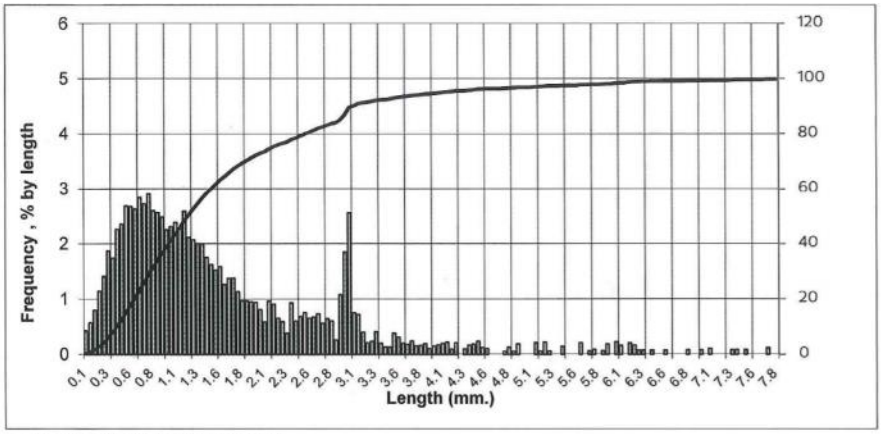

Test results by FQA (Fiber Quality Analyzer)

Arithmatic AV	0.9105	mm.	Width	36.40	µm.
L Weighted AV	1.6490	mm.	Total fibers	5,378	pcs.
Fines by number	13.29	%			
Fines by length (Less than 0.2 mm.)	1.86	%			
Curl index	0.140				
Kink index	1.663				

Figure A.0.3 Fiber length and width distribution of non-reactive PLA/Jute composite using 40 rpm matrix feeding speed and 215 rpm screw speed.

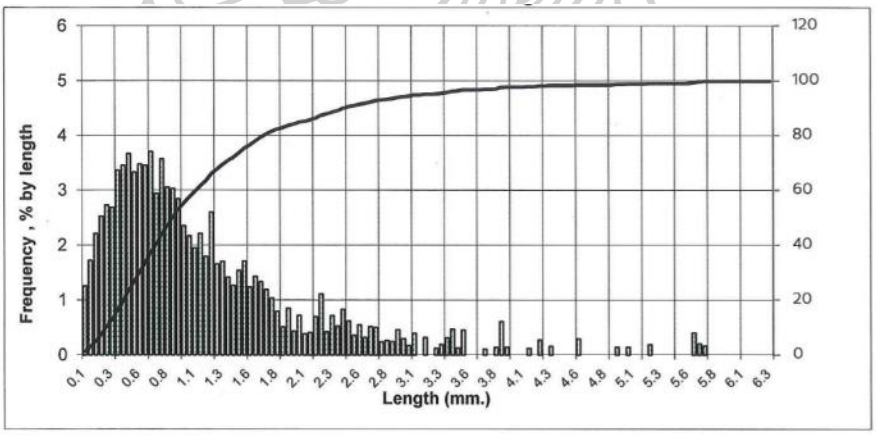

Test results by FQA (Fiber Quality Analyzer)

Arithmatic AV	0.6160	mm.	Width	34.10	µm.
L Weighted AV	1.1665	mm.	Total fibers	3,729	pcs.
Fines by number	20.36	%			
Fines by length (Less than 0.2 mm.)	4.42	%			
Curl index	0.134				
Kink index	1.785				

Figure A.0.4 Fiber length and width distribution of non-reactive PLA/Jute composite using 40 rpm matrix feeding speed and 301 rpm screw speed.

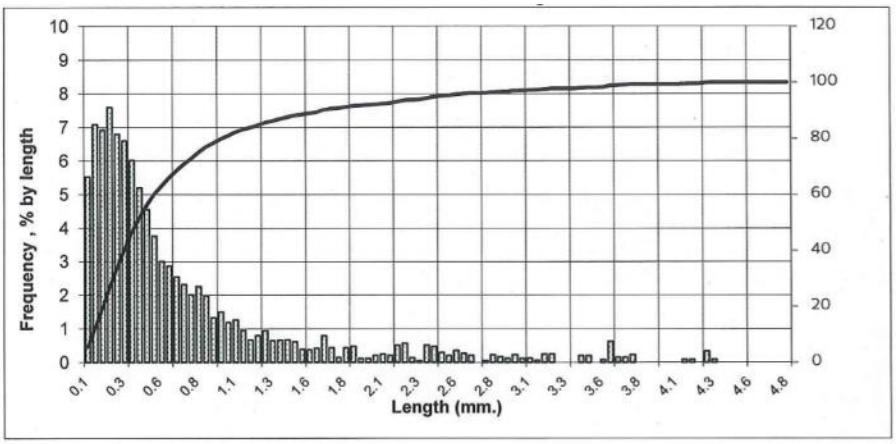

Test results by FQA (Fiber Quality Analyzer)

Arithmatic AV	0.2440	mm.	Width	38.05	µm.
L Weighted AV	0.5145	mm.	Total fibers	17,868	pcs.
Fines by number	61.15	%			
Fines by length (Less than 0.2 mm.)	30.85	%			
Curl index	0.155				
Kink index	1.332				

Figure A.0.5 Fiber length and width distribution of reactive PLA/Jute composite using 20 rpm matrix feeding speed and 215 rpm screw speed.

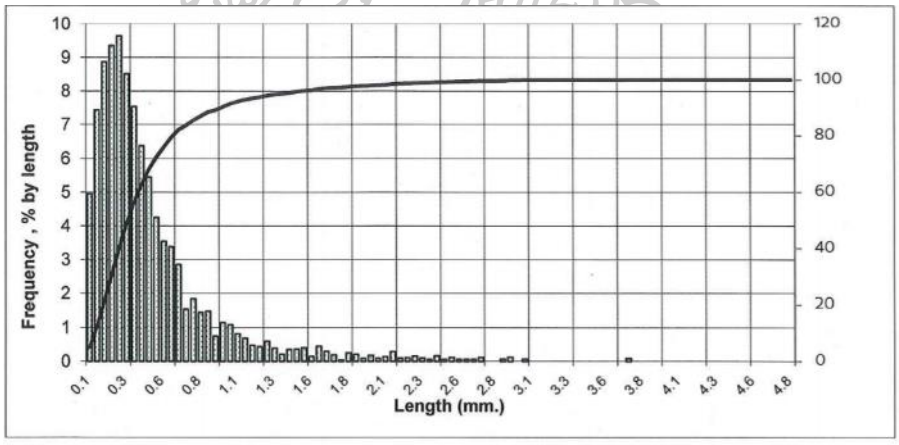

Test results by FQA (Fiber Quality Analyzer)

Arithmatic AV	0.2745	mm.	Width	41.45	µm.
L Weighted AV	0.4670	mm.	Total fibers	14,264	pcs.
Fines by number	50.56	%			
Fines by length (Less than 0.2 mm.)	22.58	%			
Curl index	0.173				
Kink index	1.092				

Figure A.0.6 Fiber length and width distribution of reactive PLA/Jute composite using 20 rpm matrix feeding speed and 301 rpm screw speed.

Appendix B Publications

Paper publications

1. Nanthananon, P., Seadan, M., Pivsa-Art, S., Hamada, H. and Suttiruengwong, S. (2017): Biodegradable Polyesters Reinforced with Eucalyptus Fiber: Effect of Reactive Agents, AIP Conference Proceedings, p. 070012

2. Nanthananon, P., Seadan, M., Sripethdee, C., Pivsa-Art, S., Hamada, H. and Suttiruengwong, S. (2018): Reactive Compatibilization of Short-Fiber Reinforced Poly(lactic acid) Biocomposites, Journal of Renewable Materials, p. 573-583

Proceeding publication

1. Nanthananon, P., Seadan, M., Sripethdee, C., Pivsa-Art, S., Hamada, H. and Suttiruengwong, S. (2018): Facial Preparation and Characterization of Short-Fiber and Talc Reinforced Poly(lactic acid) Hybrid composite with In Situ Reactive Compatibilizers, Materials, 11(7), p. 1183-1195

materials

MDPI

Article

Facile Preparation and Characterization of Short-Fiber and Talc Reinforced Poly(Lactic Acid) Hybrid Composite with In Situ Reactive Compatibilizers

Phornwalan Nanthananon [1], Manus Seadan [2], Sommai Pivsa-Art [3], Hiroyuki Hamada [4] and Supakij Suttiruengwong [1,*]

1 Department of Materials Science and Engineering, Faculty of Engineering and Industrial Technology, Silpakorn University, Nakhon Pathom 73000, Thailand; p.nanthananon@hotmail.com
2 Department of Physics, Faculty of Science, Silpakorn University, Nakhon Pathom 73000, Thailand; manus_sc.su@hotmail.com
3 Department of Material and Metallurgical Engineering, Faculty of Engineering, Rajamangala University of Technology Thanyaburi, Pathumthani 12110, Thailand; sommai.p@en.rmutt.ac.th
4 Kyoto Institute of Technology, Matsugasaki, Sakyo-ku, Kyoto City 606-8585, Japan; hhamada10294@gmail.com
* Correspondence: suttiruengwong_s@su.ac.th; Tel.: +66-34-241-708

Received: 15 June 2018; Accepted: 4 July 2018; Published: 10 July 2018

check for updates

Abstract: Hybrid composites of fillers and/or fibers reinforced polymer was generally produced by masterbatch dilution technique. In this work, the simplified preparation was introduced for the large volume production of 30 wt % short-fiber and talcum reinforced polymer hybrid composite by direct feeding into twin-screw extruder. Multifunctional epoxide-based terpolymer and/or maleic anhydride were selected as in situ reactive compatibilizers. The influence of fiber and talcum ratios and in situ reactive compatibilizers on mechanical, dynamic mechanical, morphological and thermal properties of hybrid composites were investigated. The morphological results showed the strong interfacial adhesion between fiber or talcum and Poly(lactic acid) (PLA) matrix due to a better compatibility by reaction of in situ compatibilizer. The reactive PLA hybrid composite showed the higher tensile strength and the elongation at break than non-compatibilized hybrid composite without sacrificing the tensile modulus. Upon increasing the talcum contents, the modulus and storage modulus of hybrid composites were also increased while the tensile strength and elongation at break were slightly decreased compared to PLA/fiber composite. Talcum was able to induce the crystallization of PLA hybrid composites.

Keywords: reactive hybrid composite; in situ reactive compatibilizer; facile preparation; poly(lactic acid) (PLA); one-step twin-screw extrusion

1. Introduction

Hybrid composite is a system which contains two or more different types of reinforcing materials incorporated into a single matrix, for example, fillers and/or fibers reinforcement [1–8], or one type of reinforcing material presented in a blend of different matrices [3], or both approaches combined [9]. The main advantage of using hybrid composite could be supplemented with the lack of the other fillers, thus causing a balance in terms of cost and performance of composite materials [9]. The particles and short-fibers can be directly incorporated into thermoplastics by conventional processes, such as extrusion compounding and injection molding [1]. The effects of particle fillers and fibers on composite materials were investigated using a number of techniques, because they affected the mechanical

properties of the polymer matrix [1,2,8]. However, improved performance of the hybrid composites was needed to ensure more use of renewable resources and sustainability.

Poly(lactic acid) (PLA) has extensively been explored for various applications due to its large-scale commercial availability, renewability and biodegradability. There are, however, few works carried out using natural fibers and particles reinforced PLA hybrid composites, for instance, PLA/newspaper fibers/talc [4], PLA/cellulose fiber/montmorillonite [7], PLA/cellulose fiber/nano calcium carbonate [7], and PLA/cellulose fiber/clay [6]. In our previous work on PLA biocomposites, the natural fiber from Bleach Eucalyptus Kraft Pulps (BEKP) was used as a reinforcing agent for PLA biocomposites due to its cost-effectiveness, whiteness, light weight, high purity of cellulose, high aspect ratio (40–50) and uniform diameter [10]. The addition of inorganic particle to polymer effectively enhanced the mechanical properties of the polymer matrix [1]. The addition of talcum (talc) as a filled particle in thermoplastics is a common practice [4,11–13] for promoting the performance in term of the improvement of mechanical and thermal properties of plastics with cost-effectiveness [1,13]. Ease of processing is also possible with the addition of talc.

An important concern for composite systems is the poor interaction between the polymer matrix and natural fibers and talc because a polymer matrix is hydrophobic while natural fiber and talc are naturally hydrophilic [14]. The incompatibility between the polymer matrix and the natural fibers or talc often reduces the capability of fillers and, hence, limits their practical usage [4,14]. Coupling agents are usually used to improve bonding between the filler and the thermoplastic by modifying their interfacial regions. Organo-functional silane is the most common coupling agent for modifying the surface of fillers [4,14]. In the case of surface treatment for a polymer matrix, maleic anhydride treatment was usually achieved though graft reactions [15–17]. Barletta and colleagues modified microlamellar talc by functionalization via hydrolysis and condensation reaction of its surface hydroxyl groups with different kinds of organosilanes (glycidyl, amino and isocyanate groups) in order to potentially be able to react with the -OH terminal groups of the PLA matrix [12]. In addition, they also investigated PLA–talc biocomposites that involve two compatibilizing agents, maleic anhydride (MA) and glycidyl methacrylate (GMA)-grafted PLA [12]. However, such methods were time-consuming and difficult to scale up for large industrial production. Based on these aspects, in situ reactive processing can be introduced and applied for hybrid composite processing, allowing the possibility of increasing the interfacial adhesion with a cost-effectiveness in terms of the manufacturing technique [10]. Some of the current in situ compatibilizers used for each biopolymer blends have been investigated, such as Methylene diphenyl diisocyanate (MDI) used in Poly(lactic acid)/Polybutylene succinate [18] and Poly(L-lactic acid)/Polycaprolactone [19], Dicumyl peroxide (DCP) used in Poly(L-lactic acid)/Polybutylene succinate [20] and PHB/Polybutylene succinate [21], Joncryl used in Poly(lactic acid)/PBSA [22], Poly(lactic acid)/Polypropylene carbonate [23] and Poly(L-lactic acid)/PBAT [24], PLA-g-GMA (glycidyl methacrylate grafted Poly(lactic acid) used in PLA/Starch [25], PLA-g-MA (Maleic anhydride-grafted Poly(lactic acid)) used in Poly(lactic acid)/Polycaprolactone [26], Poly(lactic acid)/Starch [27] and Poly(L-lactic acid)/Polybutylene adipate terephthalate [28]. From our previous work, different types of reactive agents including multifunctional epoxide-based reactive terpolymer (CEGMA, EAGMA) and maleic anhydride-based reactive terpolymer (EAMAH) were introduced as in situ reactive compatibilizer in the processing of PLA biocomposites [10]. It was found that CEGMA was the most effective compatibilizer for PLA and natural fiber biocomposite, as the optimal mechanical properties could be realized [10]. Hao and colleagues studied the compatibilization between PLA and sisal fiber (SF) biocomposites using an epoxy-functionalized terpolymer elastomer (EGMA) as an in situ compatibilizer. They found that the addition of EGMA into PLA/SF composites, not only enhanced the interfacial compatibility of fiber and PLA matrix, but also improved the toughness of composites without much deterioration of the tensile strength [29].

To the best of our knowledge, there have not yet been reports about in situ reactive compatibilization of natural fibers and particle-reinforced PLA hybrid composites. Another challenge

was the processing of the hybrid composite, because it was difficult to load a high content of fillers with polymers into a conventional twin-screw extruder without side-feeding due to the different densities of the individual materials. The existing solution is masterbatch preparation, but this is a time and energy-consuming process and is difficult to scale up for large volumes. Therefore, the aim of this work is to introduce a simplified method for producing PLA hybrid composites consisting of 30 wt % of short-fiber and talc using one-step twin-screw extrusion using in situ reactive compatibilization. Multifunctional epoxide-based reactive terpolymer (CEGMA) was selected as an in situ single compatibilizer and incorporated with maleic anhydride (MAH) as multiple compatibilizers. The influence of the filler ratios (talc and fiber) and the in situ reactive compatibilizer on the morphological mechanical, dynamic mechanical, and thermal properties of hybrid composites were investigated.

2. Materials and Methods

2.1. Materials

Poly(lactic acid) (PLA), 3052D injection grade was purchased from NatureWorks® LLC (Minnetonka, MN, USA). Bleach Eucalyptus Kraft Pulps (0.538 mm in average length and 13.90 µm in diameter) were kindly supplied by SCG Packaging PLC., Ratchaburi, Thailand. Talcum, 1250 grade was purchased from Thai Poly Chemicals Co., Ltd., Samut Sakhon, Thailand. An epoxy-based chain extender Joncryl® ADR-4368F (designated as CEGMA) was obtained from BASF Chemical Co., Ltd., Bangkok, Thailand. Maleic anhydride, 99.0% purity, (designated as MAH) was purchased from Sigma-Aldrich, Bangkok, Thailand. Peroxide (Perkadox® 14-40B-pd) was purchased from AkzoNobel (Bangkok, Thailand). Ethanol and chloroform were purchased from Better Syndicate Co., Ltd., Bangkok, Thailand.

2.2. Preparation of PLA/NF Particles

The dried Bleach Eucalyptus Kraft Pulp (BEKP) was ground to obtain a natural fiber (NF) using a high-speed grinder. NF was dried at 80 °C in a vacuum oven for 24 h. To allow for ease of fiber feeding, the density of NF, PLA was firstly dissolved in chloroform using a mechanical stirrer at 60 °C for 30 min and then 60 wt % of NF was added to the solution containing 40 wt % of PLA. The PLA/NF mixed suspension was evaporated to remove chloroform solvent at room temperature for 1 h and then dried at 80 °C hot air oven for 6 h. Finally, the dried mixed PLA/NF was crushed into particles.

2.3. Facile Preparation of Hybrid Fillers between Natural Fiber and Talc

The preparation of the hybrid of NF and talc was divided into two routes. In the first route, talc was dispersed in ethanol and then NF, with and without CEGMA, was added into the talc suspension under NF-to-talc ratios of 2:1, 1:1, and 1:2. In the second route, MAH was firstly dissolved in ethanol and then talc was dispersed in the MAH solution under stirring. After that, NF followed by CEGMA were added into the mixed suspension, respectively, using the same fillers ratios of the first case, under constant stirring. The mixed suspension of each case was continuously stirred for 2 min using an electric mixer at room temperature to obtain the suspended hybrid fillers of NF and talc. After that, the mixed suspensions were dried at 80 °C in a hot air oven for 24 h to remove ethanol. Finally, hybrid fillers, with and without deposited reactive compatibilizers, were obtained as particles ranging between 2–7 mm in diameter.

2.4. Facile Preparation of PLA Composites and PLA/NF/Talc Hybrid Composites

PLA resin was dried at 60 °C in a vacuum oven for 12 h. The various compositions of hybrid fillers were easily loaded together with PLA into a hopper, with and without peroxide, as listed in Table 1. PLA, NF and/or talc were melt-blended using a twin-screw extruder (SHJ-26, L/D = 40, ENMACH Co., Ltd., Nonthaburi, Thailand). The temperature profile of the twin-screw extruder was

set from the feed zone to die as 130, 140, 150, 170, 180, 190, 190, 180, 170, and 170 °C under a screw speed of 150 rpm. The scheme of the extrusion compounding process of the reactive hybrid composites was shown in Figure 1. After that, hybrid composite extrudates were cut to produce pellets and then dried for 24 h at 60 °C in a hot air oven.

Table 1. List of material compositions for extrusion compounding.

Sample Codes	PLA (g)	Natural Fiber (g)	Talc (g)	CEGMA (phr)	MAH (phr)	Peroxide (phr)
neat PLA	100					
PLA/NF	70	30	0			
PLA/NF2/T1	70	20	10			
PLA/NF1/T1	70	15	15			
PLA/NF1/T2	70	10	20			
PLA/T	70	0	30			
PLA/NF/CEGMA	70	30	0	1.5		
PLA/NF2/T1/CEGMA	70	20	10	1.5		
PLA/NF1/T1/CEGMA	70	15	15	1.5		
PLA/NF1/T2/CEGMA	70	10	20	1.5		
PLA/T/CEGMA	70	0	30	1.5		
PLA/NF/CEGMA/MAH	70	30	0	1.5	1.5	0.1
PLA/NF2/T1/CEGMA/MAH	70	20	10	1.5	1.5	0.1
PLA/NF1/T1/CEGMA/MAH	70	15	15	1.5	1.5	0.1
PLA/NF1/T2/CEGMA/MAH	70	10	20	1.5	1.5	0.1
PLA/T/CEGMA/MAH	70	20	10	1.5	1.5	0.1

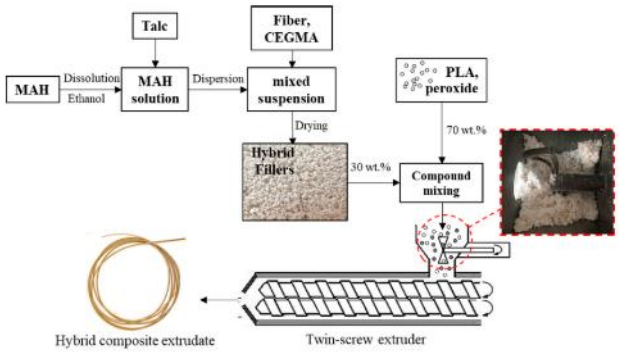

Figure 1. Schematic representation of the simplified preparation of hybrid fillers and extrusion compounding process of the reactive hybrid composites.

2.5. Tensile Specimens Preparation

After drying, the hybrid composites and neat PLA pellets were placed in an injection molding machine (SM-22, Battenfeld, Kottingbrunn, Austria) in order to produce tensile test specimens. The processing conditions for the injection molding are summarized as follows: Nozzle temperature and cooling time were 190 °C and 42 s, respectively.

2.6. Testing and Characterization

2.6.1. Mechanical Properties

Mechanical properties were carried out by using a universal testing machine (Instron 5969, Norwood, MA, USA) according to ASTM D638 [30], specimen type I, and a 5-KN load cell. The testing was conducted under ambient conditions using a cross-head speed of 5 mm/min. All reported values were obtained as averages of five specimens.

2.6.2. Morphological Observation

The tensile fracture surface morphology of the PLA composite and hybrid composite specimens were observed using a Field Emission Scanning Electron Microscope (FE-SEM) (TESCAN MIRA3 LMH Schottky, Brno, Czech Republic) at an accelerating voltage of 5 kV. Prior to observations, the samples were sputter coated with a thin layer of gold to avoid charging.

2.6.3. Dynamic-Mechanical Thermal Analysis (DMTA)

To produce DMTA specimens, the PLA composite and hybrid composite were pre-heated for 4 min and then compressed at 190 °C and 1000 psi pressure for 1 min. After that, the samples were laser-cut to dimensions of 10 × 1.16 × 40 mm^3. Dynamic-mechanical thermal properties of PLA composites and the hybrid composite were examined using an ANTON PAAR, modular compact rheometer (MCR302, Graz, Austria) equipped with rectangular fixture (SRF) holders. A temperature sweep was heated from 30 to 110 °C at a heating rate of 3 °C/min under the DMTA torsion mode at a frequency of 1 Hz.

2.6.4. Differential Scanning Calorimetry (DSC)

Differential scanning calorimetry (DSC) of samples were carried out on a DSC1 STAR instrument (METTLER TOLEDO, Greifensee, Switzerland) under a nitrogen atmosphere. The samples were first heated from 30 to 200 °C at a rate of 10 °C/min and held on for 1 min. The samples were then cooled down to 30 °C at the rate of 10 °C/min and reheated to 200 °C at the same conditions. The degree of crystallinity (X_c) was calculated according to the following equation [31]:

$$Xc\ (\%) = \frac{\Delta H_m - \Delta H_{cc}}{(\omega_{PLA})\Delta H_m^o} \times 100, \quad (1)$$

where ΔH_m was the melting enthalpy and ΔH_{cc} was the cold crystallization enthalpy measured from the thermogram peak, ω_{PLA} was the weight fraction of PLA, and ΔH_m^o was the ideal melting enthalpy for completely crystalline PLA of 93.6 J/g [32].

3. Results

3.1. Mechanical Properties

Modulus, tensile strength and elongation at break of neat PLA and PLA/NF/T hybrid composites at different ratios, with and without various reactive compatibilizers, are shown in Figure 2. All PLA hybrid composites showed a much higher modulus and lower elongation at break than that of neat PLA, indicating the enhanced stiffness due to the presence of fillers [33,34]. In addition, the tensile strength of all PLA hybrid composites increased when compared to that of neat PLA, caused by the reinforcing effect of the fillers [35]. As the talc content increased for non-reactive hybrid composites, the modulus tended to increase slightly by 2%, 10% and 14% for NF2/T1, NF1/T1 and NF1/T2 ratios, respectively, compared to PLA-composite-added fiber. These results indicated a more enhanced stiffness of PLA hybrid composites due to the presence of talc. PLA-composite-added talc showed an increase in the modulus, as reported by many researchers [36]. The tensile strength and elongation at

break of the hybrid composites were decreased after increasing the talc content, resulting from the poor interfacial adhesion between the fillers and matrix; hence, the stress concentration under loading conditions [29].

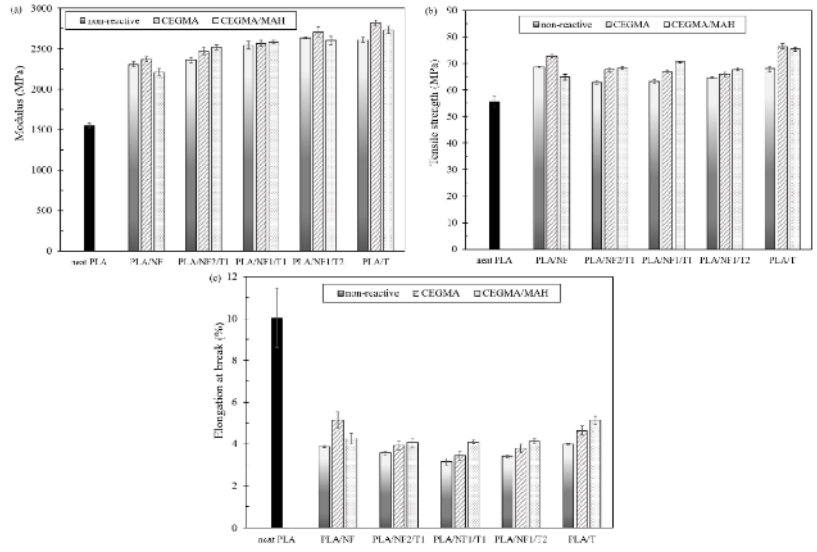

Figure 2. (**a**) Modulus; (**b**) tensile strength and (**c**) elongation at break of PLA hybrid composites at different fillers ratios, with and without various reactive compatibilizers.

The incorporation of reactive compatibilizers (CEGMA or CEGMA/MAH) into PLA/NF/T hybrid composites did not change the modulus significantly compared to non-compatibilized composite and hybrid composite, except at a higher fiber content. On the other hand, the presence of CEGMA/MAH in PLA hybrid composites showed a higher tensile strength than adding CEGMA, compared to their non-compatibilized hybrid composites. In the case of the PLA/T composite, it showed the highest tensile strength, regardless of whether CEGMA or CEGMA/MAH was added. This implied a better interfacial adhesion between the PLA matrix and fiber or talc with the addition of reactive compatibilizer, which caused a better stress transfer from the PLA matrix to the fillers. Furthermore, the incorporation of both reactive compatibilizers demonstrated an improvement in the elongation at break of the hybrid composites. The presence of CEGMA/MAH showed the highest elongation at break of about 14%, 30%, and 21% for PLA/NF2/T1, PLA/NF1/T1 and PLA/NF1/T2, respectively, when compared to the non-compatibilized hybrid composites. This indicated the synergistic effect of the compatibilizer between CEGMA and MAH.

3.2. Morphological Observation

The tensile fracture surfaces of PLA/NF/T hybrid composites at different filler ratios, with and without various reactive compatibilizers, were observed using FE-SEM, as shown in Figure 3. The different filler ratios did not affect the interfacial adhesion of hybrid composites. PLA hybrid composites without reactive compatibilizer, as illustrated in Figure 3a–c, exhibited voids between the PLA matrix and fiber or talc, and some pull-outs of talc because of the poor interfacial adhesion between the fillers and PLA matrix. In contrast, the incorporation of CEGMA and CEGMA/MAH

in PLA hybrid composites, as shown in Figure 3a′–c′ and 3a″–c″, respectively, showed that fiber was broken and torn out on the fracture surface without voids between the fiber and matrix being observed. In addition, they PLA matrix tightly adhered to both fiber and talc surfaces. This indicated that the interfacial adhesion of the PLA matrix, with both fiber and talc in hybrid composites, was considerably improved by adding multifunctional epoxide compatibilizer with and without MAH.

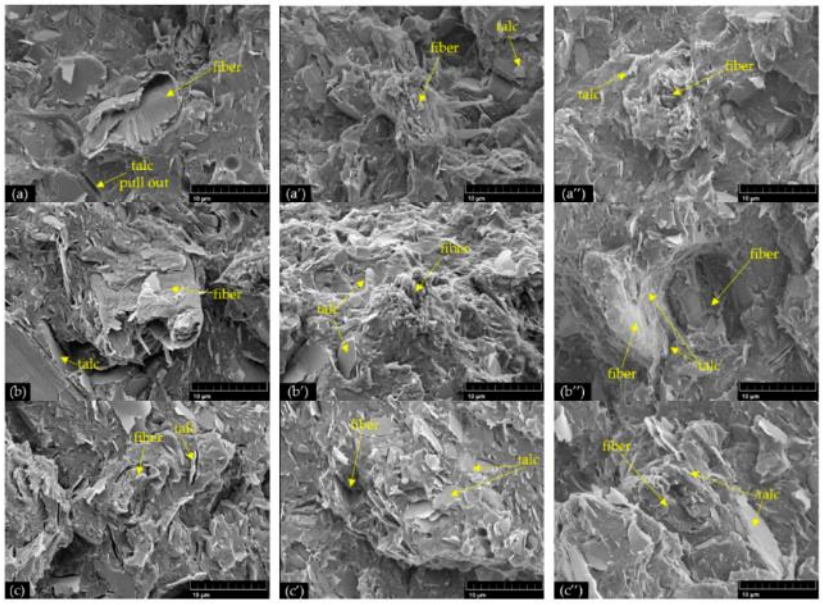

Figure 3. Tensile fracture surfaces of PLA hybrid composites with and without reactive compatibilizers: (**a**) PLA/NF2/T1; (**a′**) PLA/NF2/T1/CEGMA; (**a″**) PLA/NF2/T1/CEGMA/MAH; (**b**) PLA/NF1/T1; (**b′**) PLA/NF1/T1/CEGMA; (**b″**) PLA/NF1/T1/CEGMA/MAH; (**c**) PLA/NF1/T2; (**c′**) PLA/NF1/T2/CEGMA; (**c″**) PLA/NF1/T2/CEGMA/MAH.

3.3. Dynamic-Mechanical Thermal Analysis (DMTA)

The dependence of the storage modulus versus the temperature of the PLA hybrid composites at different fillers ratios, with and without reactive compatibilizers, is depicted in Figure 4. The storage moduli of all hybrid composites and single filler composites were much higher than that of neat PLA in the glassy region (30–50 °C), which is obviously seen in PLA/T composite. It was noticed that PLA hybrid composites and neat PLA started softening above glass transition temperatures of around 60 °C. It is clear from Figure 4a that the storage moduli of PLA/NF1/T1 and PLA/NF1/T2 hybrid composites dropped slightly in the rubbery region and then leveled off (70–80 °C), indicating an improvement in the heat distortion temperature (HDT) [37] of the hybrid composites compared to neat PLA and single filler composites. In the rubbery region, the storage moduli of hybrid composites at NF2/T1, NF1/T1 and NF1/T2 ratios were increased by 10, 64 and 64 times compared to that of neat PLA, and increased by 2, 10 and 10 times compared to that of the single filler composite. The remarkably-higher storage modulus in the rubbery region of the PLA/NF1/T1 and PLA/NF1/T2 hybrid composites was due to the effect of hybridization, which could not happen in the single filler composites. For the addition of CEGMA or CEGM/MAH, it can be seen in Figure 4b that the storage modulus of the hybrid

composite was decreased. For the addition of CEGMA or CEGM/MAH, it was found from Figure 4b that the storage modulus of the hybrid composite was decreased. It was determined that the storage modulus of neat PLA and PLA/NF started to increase again after 90 °C, which was relevant to its recrystallization [38]. The storage moduli of other PLA hybrid composites, with and without both reactive compatibilizers, started to increase again at around 80 °C, indicating a faster crystallization than that of neat PLA and PLA/NF [37]. Figure 5 shows a plot of tan δ (ratio of the loss modulus to the storage modulus) versus temperature of PLA hybrid composites, with and without reactive compatibilizers. Figure 5a illustrates that the tan δ peak height of the PLA/NF/T hybrid composite was lower than that of only the PLA/NF composite, and was much lower than that of neat PLA. PLA-composite-added talc showed the lowest tan δ peak height. This could describe that the mobility of the PLA chain was restricted by the addition of natural fiber [4], and, especially, by adding talc because it was a platy filler [39]. Figure 5b shows that the tan δ peak height of the PLA/NF1/T1 hybrid composite with CEGMA/MAH was higher than that incorporated with CEGMA, and much higher than those of the non-compatibilized hybrid composites.

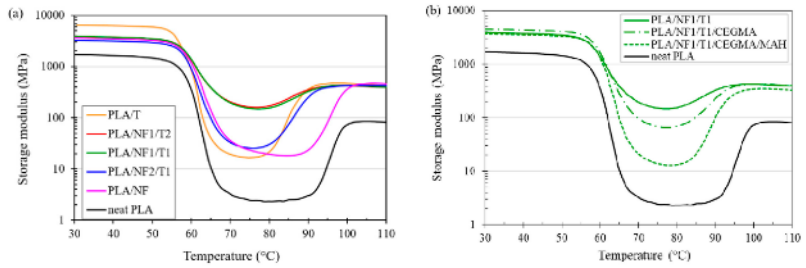

Figure 4. Plot of storage modulus against temperature of PLA hybrid composites at: (**a**) different fillers ratios; (**b**) with and without various reactive compatibilizers.

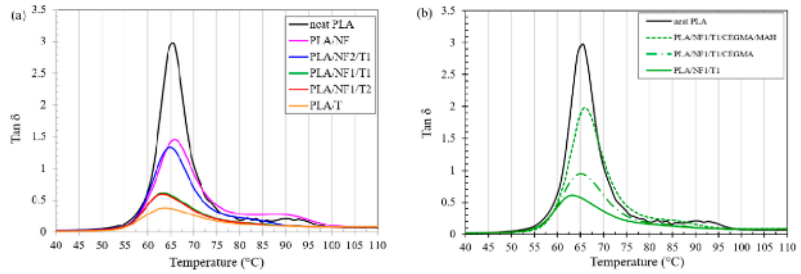

Figure 5. Plot of tan δ against temperature of PLA hybrid composites at: (**a**) different fillers ratios; (**b**) with and without various reactive compatibilizers.

3.4. Differential Scanning Calorimetry (DSC)

DSC thermograms of neat PLA and PLA hybrid composites at different filler ratios, without reactive compatibilizers, are shown in Figure 6. As the talc ratio increased in the PLA hybrid composites, a large crystallization peak and higher crystallization temperature (compared to that of neat PLA in the cooling scan) were observed. In addition, it was noticed that the peak of the cold crystallization temperature for PLANF1/T1 and PLA/NF1/T2 almost disappeared in the heating scan because the crystallization was completed during a cooling step. In contrast, the cold

crystallization peak of neat PLA and PLA/NF appeared at about 110 and 105 °C, respectively, in the heating scan (Figure 7b), due to the low crystallization ability [32]. As is well known, talc is able to induce the crystallization of PLA [12,31,37,40]; hence, more talc concentrations added caused more crystallinity of PLA in hybrid composites as seen in Figure 8. In the case of short-fiber introduction, a slight improvement in crystallinity of the PLA/NF composite compared to that of neat PLA was ddmonstrated. This effect could be attributed to the fact that a small and short fiber acted as a nucleating site for the crystallization of PLA around the surface of the fiber [41]. The effect of the incorporation of various reactive compatibilizers on crystallization of the compatibilized PLA hybrid composites is shown in Figure 7. It was found that the crystallization and crystallinity of the PLA hybrid composites tended to decrease compared to the non-compatibilized hybrid composites, which are clearly illustrated in Figures 7 and 8. However, the cold crystallization on the set temperature of the compatibilized PLA hybrid composites was lower than that of neat PLA, suggesting that its overall cold crystallization rate was faster [42].

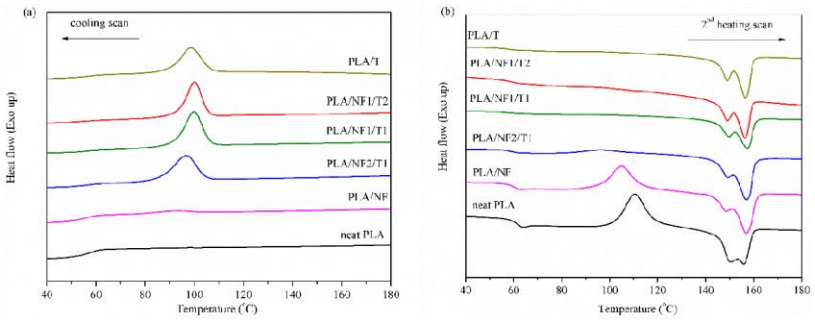

Figure 6. DSC thermograms of PLA hybrid composites at different filler ratios: (**a**) cooling scan and (**b**) second heating scan.

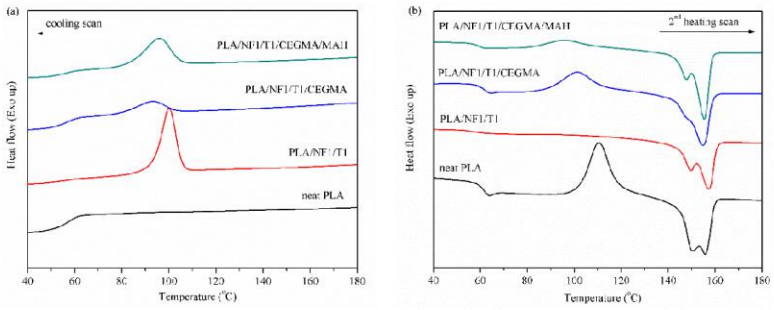

Figure 7. DSC thermograms of PLA hybrid composites with and without reactive compatibilizers at NF1/T1 ratio: (**a**) cooling scan and; (**b**) second heating scan.

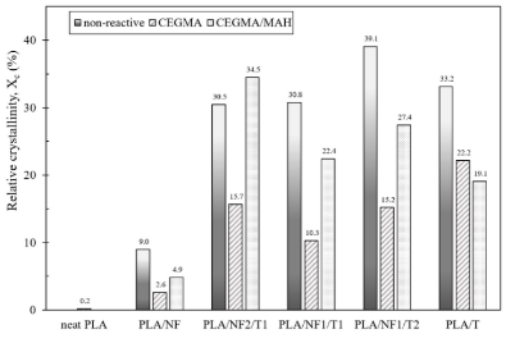

Figure 8. Degree of crystallinity (X_c) of PLA hybrid composites at different filler ratios, with and without various reactive compatibilizers.

4. Discussion

The large improvement in tensile strength could be described by the better interfacial adhesion between the fillers and PLA matrix when the multifunctional epoxide-based compatibilizer, with and without MAH, was added. This led to a decrease in the stress concentration and a better stress transfer from the PLA matrix to fiber or talc. From the morphology results, a significant improvement in the interfacial adhesion between PLA matrix and fibers or talc in hybrid composites was found after adding multifunctional epoxide terpolymer. This phenomenon could be attributed to the reaction between the presence of the epoxide groups in the multifunctional epoxide terpolymer and the hydroxyl groups in the fibers or talc structure and the end group of the PLA molecular chain during the melt-blending process, as proved by FT-IR analysis of the extracted fibers (reported elsewhere) [10,29]. Huda and colleagues reported that the -OH in talc structure could react with MA- and GMA-grafted-PLA, which led to good compatibilization of PLA/talc compounds with good processability [12]. Generally, MAH could be grafted onto PLA chains via free radical reactions using peroxide in the melt state. From these results and reports, it could be implied that the addition of CEGMA and/or MAH with peroxide could reactively bond with the hydroxyl group on fiber, talc and the chain-end of PLA via an in situ melting-process and, thus, improved the interfacial adhesion. In addition, crystallization of the PLA hybrid composite, incorporating reactive compatibilizers, tended to decrease compared to non-compatibilized hybrid in the cooling step. This might be due to the lower molecular chain mobility of PLA in the presence of CEGMA, which acted as a chain extender and led to an increase in PLA molecular weight. However, the presence of CEGMA with MAH and peroxide in the PLA/NF/T hybrid composite showed a higher crystallinity than adding CEGMA without MAH/peroxide. One possible explanation was that PLA-grafted-MAH using peroxide had a low molecular weight and could act as a lubricant on the PLA matrix, which enhanced PLA chain mobility and led to increasing the crystallization activity [36], more than adding only CEGMA. More studies on the interfacial reaction and microstructure of PLA/fiber/talc hybrid composites incorporating CEGMA and/or MAH should be conducted in the future in order to understand the chemical reactions of the reactive compatibilizers.

5. Conclusions

The short-fiber and talc reinforced PLA hybrid composites, with and without reactive compatibilizers, were successfully prepared using one-step direct feeding via a twin-screw extruder. For the influence of the filler ratios as the talc ratio increased, the modulus of the hybrid composites was increased while the tensile strength and elongation at break were decreased compared to PLA/NF

In the rubbery region, the storage modulus of hybrid composites was increased by 10 times for the NF1/T1 and NF1/T2 ratios compared to PLA/NF3/T0. Talc was able to induce the crystallization of PLA hybrid composites. The interfacial adhesion between fibers or talc and the PLA matrix was significantly improved when the in situ reactive compatibilizers (CEGMA or CEGMA/MAH) were incorporated. The largest improvements in tensile strength were 8% and 11% for the addition of CEGMA and CEGMA/MAH, respectively, when compared to the non-compatibilized hybrid composites. In addition, the elongation at break showed the highest increase, by 10% and 30% for the addition of CEGMA and CEGMA/MAH, respectively, compared to non-compatibilized hybrid composites. The reaction and microstructure of PLA/fiber/talc hybrid composites incorporated with CEGMA and/or MAH with peroxide will be conducted by our group in the near future in order to further understand the role of each reactive compound.

Author Contributions: P.N. and S.S. conceived and designed the experiments; P.N. performed the experiments; P.N. and S.S. analyzed the data; S.P.-A., M.S. and H.H. contributed reagents/materials/analysis tools; P.N. and S.S. wrote the paper.

Funding: This research was funded by National Research Council of Thailand (NRCT) and BIODIVERSITY-BASED ECONOMY DEVELOPMENT OFFICE (BEDO) fiscal year 2018 for the financial support."

Acknowledgments: We also appreciate SCG Packaging PLC., Thailand for Bleach Eucalyptus Kraft Paper Pulps supply and Kosin Hachawee for his assistance.

Conflicts of Interest: The authors declare no conflict of interest.

References

1. Fu, S.-Y.; Xu, G. On the elastic modulus of hybrid particle/short-fiber/polymer composites. *Compos. Part B Eng.* **2002**, *33*, 291–299. [CrossRef]
2. Hartikainen, J.; Hine, P. Polypropylene hybrid composites reinforced with long glass fibres and particulate filler. *Compos. Sci. Technol.* **2005**, *65*, 257–267. [CrossRef]
3. Thwe, M.M.; Liao, K. Durability of bamboo-glass fiber reinforced polymer matrix hybrid composites. *Compos. Sci. Technol.* **2003**, *63*, 375–387. [CrossRef]
4. Huda, M.S.; Drzal, L.T. The effect of silane treated- and untreated-talc on the mechanical and physico-mechanical properties of poly(lactic acid)/newspaper fibers/talc hybrid composites. *Compos. Part B Eng.* **2007**, *38*, 367–379. [CrossRef]
5. Singh, S.; Mohanty, A.K. Hybrid bio-composite from talc, wood fiber and bioplastic: Fabrication and characterization. *Compos. Part A Appl. Sci. Manuf.* **2010**, *41*, 304–312. [CrossRef]
6. Lee, S.H.; Wang, S. Isothermal crystallization behavior of hybrid biocomposite consisting of regenerated cellulose fiber, clay, and poly(lactic acid). *J. Appl. Polym. Sci.* **2008**, *108*, 870–875. [CrossRef]
7. Piekarska, K.; Sowinski, P. Structure and properties of hybrid PLA nanocomposites with inorganic nanofillers and cellulose fibers. *Compos. Part A Appl. Sci. Manuf.* **2016**, *82*, 34–41. [CrossRef]
8. Senturk, O.; Senturk, A.E. Evaluation of hybrid effect on the thermomechanical and mechanical properties of calcite/SGF/PP hybrid composites. *Compos. Part B Eng.* **2018**, *140*, 68–77. [CrossRef]
9. De Oliveira Sousa Neto, V.; Saraiva, G.D. 11—Hybrid polymers composite: Effect of hybridization on the some propers of the materials. In *Hybrid Polymer Composite Materials: Processing*; Woodhead Publishing: Cambridge, UK, 2017; pp. 291–312.
10. Nanthananon, P.; Seadan, M. Reactive Compatibilization of Short-Fiber Reinforced Polylactic acid Biocomposites. *J. Renew. Mater.* **2018**, in press.
11. Barletta, M.; Moretti, P. Engineering of Poly Lactic Acids (PLAs) for melt processing: Material structure and thermal properties. *J. Appl. Polym. Sci.* **2017**, *134*. [CrossRef]
12. Barletta, M.; Pizzi, E. Thermal behavior of extruded and injection-molded poly(lactic acid)–Talc engineered biocomposites: Effects of material design, thermal history, and shear stresses during melt processing. *J. Appl. Polym. Sci.* **2017**, *134*, 45179. [CrossRef]
13. Zheng, Y.; Gu, F. Improving Mechanical Properties of Recycled Polypropylene-based Composites Using TAGuchi and ANOVA Techniques. *Procedia CIRP* **2017**, *61*, 287–292. [CrossRef]

14. Faruk, O.; Bledzki, A.K. Biocomposites reinforced with natural fibers: 2000–2010. *Prog. Polym. Sci.* 2012, *37*, 1552–1596. [CrossRef]
15. Yang, N.; Zhang, Z. C. Effect of surface modified kaolin on properties of polypropylene grafted maleic anhydride. *Results Phys.* 2017, *7*, 969–974. [CrossRef]
16. Pradipta, A.; Mardiyati. Effect of maleic anhydride treatment on the mechanical properties of sansevieria fiber/vinylester composites. *AIP Conf. Proc.* 2017, *1823*, 020097. [CrossRef]
17. Chow, W.S.; Tham, W.L. Effects of maleated-PLA compatibilizer on the properties of poly(Lactic acid)/halloysite clay composites. *J. Thermoplast. Compos. Mater.* 2012, *26*, 1249–1263. [CrossRef]
18. Lu, L.; Song, G. Novel biodegradable polylactide/poly(butylene succinate) composites via cross-linking with methylene diphenyl diisocyanate. *Polym. Plast. Technol. Eng.* 2013, *52*, 1183–1187. [CrossRef]
19. Meng, M.; Huiming, Z. Super-toughened poly(L-lactic acid) fabricated via reactive blending and interfacial compatibilization. *Polym. Int.* 2016, *65*, 1187–1194. [CrossRef]
20. Ruyin, W.; Shifeng, W. Toughening modification of PLLA/PBS blends via in situ compatibilization. *Polym. Eng. Sci.* 2009, *49*, 26–33. [CrossRef]
21. Ma, P.; Hristova-Bogaerds, D.G.; Lemstra, P.J.; Zhang, Y.; Wang, S. Toughening of PHBV/PBS and PHB/PBS blends via in situ compatibilization using dicumyl peroxide as a free-radical grafting initiator. *Macromol. Mater. Eng.* 2012, *297*, 402–410. [CrossRef]
22. Ojijo, V.; Sinha Ray, S. Toughening of biodegradable polylactide/poly(butylene succinate-*co*-adipate) blends via in situ reactive compatibilization. *Polymer* 2013, *5*, 4256–4276. [CrossRef] [PubMed]
23. Sun, Q.; Mekonnen, T. Novel biodegradable cast film from carbon dioxide based copolymer and polylactic acid. *J. Polym. Environ.* 2016, *24*, 23–36. [CrossRef]
24. Aranda, L.C.; Magalon, M. Influence of chain extender on mechanical, thermal and morphological properties of blown films of PLA/PBAT blends. *Polym. Test.* 2015, *43*, 27–37. [CrossRef]
25. Liu, J.; Jiang, H. Grafting of glycidyl methacrylate onto poly(lactide) and properties of pla/starch blends compatibilized by the grafted copolymer. *J. Polym. Environ.* 2012, *20*, 10. [CrossRef]
26. Garcia-La, L.; Calabrese, M. PLA maleation: An easy and effective method to modify the properties of PLA/PCL immiscible blends. *Colloid Polym. Sci.* 2014, *292*, 2391–2398. [CrossRef]
27. Huneault, M.A.; Li, H. Morphology and properties of compatibilized polylactide/thermoplastic starch blends. *Polymer* 2007, *48*, 270–280. [CrossRef]
28. Teamsinsungvon, A.; Ruksakulwong, V. Preparation and characterization of poly(lactic acid)/poly(butylene adipate-*co*-terephthalate) blends and their composite. *Polym. Plast. Technol. Eng.* 2013, *52*, 1262–1267. [CrossRef]
29. Hao, M.; Wu, H. In situ reactive interfacial compatibilization of polylactide/sisal fiber biocomposites via melt-blending with an epoxy-functionalized terpolymer elastomer. *RSC Adv.* 2017, *7*, 52399–52412. [CrossRef]
30. ASTM D638-14. *Standard Test Method for Tensile Properties of Plastics*; ASTM International: West Conshohocken, PA, USA, 2014.
31. Khunkeeso, J.; Petchwattana, N. Thermal and mechanical properties of bioplastic poly(lactic acid) compounded with silicone rubber and talc. *AIP Conf. Proc.* 2016, *1725*, 080005. [CrossRef]
32. Nanthananon, P.; Seadan, M. Enhanced crystallization of poly(lactic acid) through reactive aliphatic bisamide. *IOP Conf. Ser. Mater.* 2015, *87*, 012057. [CrossRef]
33. Dash, J.-J.-L.; Gao, S.-L. Jute/polypropylene composites I. Effect of matrix modification. *Compos. Sci. Technol.* 2006, *66*, 952–963. [CrossRef]
34. Coutinho, F.M.B.; Costa, T.H.S. Performance of polypropylene–Wood fiber composites. *Polym. Test.* 1999, *18*, 581–587. [CrossRef]
35. Méndez, J.A.; Vilaseca, F. Evaluation of the reinforcing effect of glass and wood pulp in the preparation of polypropylene-based composites coupled with maleic anhydride grafted polypropylene. *J. Appl. Polym. Sci.* 2007, *105*, 3588–3596. [CrossRef]
36. Thomas, S.; Visakh, P.M. *Advances in Natural Polymers: Composites and Nanocomposites*; Springer: Berlin, Germany, 2012; pp. 375–376.
37. Shalwan, A. Development of Novel Bio-Derived Polymer Composites Reinforced with Natural Fibres and Mineral Fillers. Ph.D. Thesis, Loughborough University, Leicestershire, UK, 2013.

38. Gao, X.; Zhang, J. Poly (lactic acid)/polyoxymethylene blends: Morphology, crystallization, rheology, and thermal mechanical properties. *Polymer* **2015**, *69*, 103–109. [CrossRef]
39. Jain, S.; Misra, M. Thermal, mechanical and rheological behavior of poly(lactic acid)/talc composites. *J. Polym. Environ.* **2012**, *20*, 1027–1037. [CrossRef]
40. Vachon, A.; Pépin, K. Thermal, Mechanical and morphological properties of binary and ternary pla blends containing a poly(ether ester) elastomer. *J. Biobased Mater. Bioenergy* **2015**, *9*, 205–217. [CrossRef]
41. Joseph, P.V.; Joseph, K. The thermal and crystallisation studies of short sisal fibre reinforced polypropylene composites. *Compos. Part A Appl. Sci. Manuf.* **2003**, *34*, 253–266. [CrossRef]
42. Qian, L.; Ruijing, Z. Cold crystallization behavior of glassy poly (lactic acid) prepared by rapid compression. *Polym. Eng. Sci.* **2015**, *55*, 359–366. [CrossRef]

Reactive Compatibilization of Short-Fiber Reinforced Poly(lactic acid) Biocomposites

Phornwalan Nanthananon[1], Manus Seadan[2], Sommai Pivsa-Art[3], Hiroyuki Hamada[4] and Supakij Suttiruengwong[1,*]
[1]*Department of Materials Science and Engineering, Faculty of Engineering and Industrial Technology, Silpakorn University, Nakhon Pathom 73000, Thailand*
[2]*Department of Physics, Faculty of Science, Silpakorn University, Nakhon Pathom 73000, Thailand*
[3]*Department of Material and Metallurgical Engineering, Faculty of Engineering, Rajamangala University of Technology Thanyaburi, Pathumthani 12110, Thailand*
[4]*Kyoto Institute of Technology, Matsugasaki, Sakyo ku, Kyoto City 606 8585, Japan*

ABSTRACT: Poor interfacial adhesion between biobased thermoplastics and natural fibers is recognized as a major drawback for biocomposites. To be applicable for the large-scale production, a simple method to handle is of importance. This work presented poly(lactic acid) (PLA) reinforced with short-fiber and three reactive agents including anhydride and epoxide groups were selected as compatibilizers. Biocomposites were prepared by one-step melt-mixing methods. The influence of reactive agents on mechanical, dynamic mechanical properties and morphology of PLA biocomposites were investigated. Tensile strength and storage modulus of PLA biocomposites incorporated with epoxide-based reactive agent was increased 13.9% and 37.4% compared to non-compatibilized PLA biocomposite, which was higher than adding anhydride-based reactive agent. SEM micrographs and Mohn test exhibited an improvement of interfacial fiber-matrix adhesion in the PLA biocomposites incorporated with epoxide-based reactive agent. FTIR revealed the chemical reaction between the fiber and PLA with the presence of epoxide-based reactive agents.

KEYWORDS: Biocomposite, poly(lactic acid), Reactive agent, in situ compatibilization, interfacial adhesion

1 INTRODUCTION

Biocomposites based on biodegradable polymers and natural fibers have caught much attention in the last few decades due to less environmental impact with being fully biodegradable and more sustainable in terms of renewable resources. Among the biodegradable polymers, aliphatic poly(lactic acid) (PLA) is one of the most popular ones. PLA is eco-friendly, has a good processability in most equipment [1], high mechanical strength and high modulus, therefore PLA has the potential to replace the applications in some conventional plastics such as PET and PS. PLA has been reported as a matrix for several lignocelluloses reinforcing fibers such as kenaf [1-3], flax [4-6], abaca [7], jute [8, 9], coir [10], miscanthus [11], ramie [9, 12], bamboo [13, 14], coconut [13], vetiver [13] and wood pulp [15]. Natural fibers have many advantages such as light weight, renewability, biodegradability, and non-hazard are readily available at the relatively low cost compared to synthetic fibers [6, 15].

Using Bleached Kraft Pulp (BKP), especially Eucalyptus for PLA composites, has not yet been reported. Bleached Kraft Pulp is interesting in term of cost-effective cellulose fiber resource, which widely used in papermaking [16].

The advantages of Bleached Kraft Pulp are its whiteness, high purity of cellulose and aspect ratio with a uniform diameter at about 20 μm and length within 1 mm compared to wood pulp [17].

However, the poor interfacial adhesion between natural fiber and polymer matrix was commonly found in biocomposites systems [18], resulting in the unsatisfactory mechanical properties, which further limited their practical use. To overcome the weak fiber-polymer matrix adhesion, there are several existing approaches, including the surface modification of either polymer (e.g. grafting reaction) or fibers (e.g. silane coupling) or both polymers and fibers (e.g. the addition of some compatibilizer compounds). However, such methods are suitable mostly for polymer blends, time-consuming, and difficult to scale up for industrial production. The treatment prior to melt blending is not practical and costly. Therefore, based on these aspects, the concept of the reactive processing is introduced and applied for the biocomposite processing. The reactive processing is a cost-effective manufacturing technique with the possibility of increasing the level of interfacial adhesion [19]. The reaction occurs in situ during the melt processing.

Although a few types of the multifunctional reactive agents have been employed for either blends or

*Corresponding author: suttiruengwong_s@su.ac.th

DOI: 10.32604/JRM.2018.00129

composites of polyesters for different purposes including the use of multifunctional epoxides as thermal degradation control for PLA/nanoclay [20], anhydride as a chain extension for PET [21], diisocyanate as a chain extender for PET/PC recycling [22], and carbodiimide as a compatibilizer for PLA/cellulose biocomposites [15], for PLA and BKP biocomposites, the systematic approach for investigating the interfacial adhesion between two phases using various multifunctional reactive groups is still lacking.

In our previous works, Joncryl® or peroxide was used as the *in situ* compatibilizers for natural fiber to produce PLA and PBS biocomposites by one-step melt-mixing method [23]. Alternatively, A. Awal and colleagues studied thermorheological and mechanical properties of cellulose reinforced PLA biocomposites and reported that the addition of multifunctional bioadimide as a reactive agent could improve the adhesion between fibers and matrix [15]. Therefore, this work introduced the different types of reactive agents including multifunctional epoxides, reactive terpolymer (maleic anhydrides or epoxides) as in situ compatibilizers in the processing of PLA biocomposites. Maleic anhydride or epoxy based multifunctional group was highly reactive with hydroxyl groups (OH) in cellulose structure and formed carbon-carbon bond to the polymer chain [20, 24]. The bleached eucalyptus pulps (short fiber) with high cellulose compositions were used as a reinforcement incorporated with reactive agents for the PLA biocomposites. The influence of reactive agents on the morphology, mechanical and dynamic mechanical properties of PLA biocomposites were investigated and discussed. Furthermore, Molau test together with FT-IR technique was performed to examine the compatibility of biocomposite and verify the possible reactions of PLA, fibers and reactive agents.

2 EXPERIMENTAL

2.1 Materials

Poly(lactic acid) (PLA), 3052D injection grade was purchased from NatureWorks® LLC (USA). Bleach Eucalyptus Kraft Pulps (BEKP) were kindly provided by SCG Packaging PLC., Thailand. The average length and diameter of BEKP were 0.538 mm and 13.90 μm, respectively, which were analyzed by Fiber Quality Analyzer (FQA) assisted by SCG packaging PLC. The chemical compositions of the BEKP fibers were 83-86% α-cellulose, 12-15% hemicellulose, 1.5% lignin and less 0.5% extractives, which were analyzed according to Technical Association of the Pulp and Paper Industry (TAPPI) standard T 223 cm-01, T 236 om-99, T 203 cm-99 and T 222 om-02. An epoxy-based chain extender Joncryl® ADR-4368F (designated as CEGMA) was obtained from BASF Chemical Co., Ltd Thailand. A reactive terpolymer (ethylene, acrylic ester, and glycidyl methacrylate) Lotader® AX8900 (designated as EAGMA), and a random terpolymer (ethylene, acrylic ester and maleic anhydride) Lotader® 4210 (designated as EAMAH) were kindly supplied by 2 A.M. Connection Co. Ltd., Thailand. The chemical structures of three reactive agents were presented in Figure 1.

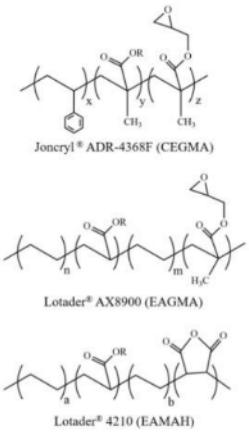

Figure 1 Chemical structures of three reactive agents used in this work.

2.2 Preparation of PLA Biocomposites

Eucalyptus paper pulps were first dried and ground to obtain short fibers using a high-speed grinder, with the rotation speed of 28,000 rpm. Prior to melt mixing, PLA was dried at 60°C in a vacuum oven for 6 h whereas the fibers were dried overnight at 80°C. PLA with 10 wt% of eucalyptus fibers loading (referred as PLA/FB10) without reactive agents was first prepared in an internal mixer (Chareon tut CO. LTD., model MX 105-D40L50) with the rotational speed of 60 rpm and the temperature of 190°C. Three Multifunctional group compounds such as multi-epoxide groups (designated as CEGMA) and two reactive terpolymers containing epoxide (designated as EAGMA) and maleic anhydride groups (designated as EAMAH) were selected as reactive compatibilizers in PLA biocomposites. The concentrations of 0.5 phr and 1.0 phr of each reactive agent were added along with 10 wt% fiber to produce PLA biocomposites. PLA

DOI: 10.32604/JRM.2018.00129

biocomposites specimens were prepared and referred as PLA/FB/CEGMAx, PLA/FB/EAGMAx and PLA/FB/EAMAHx, where *x* stands for the contents of reactive agents in phr for chain extender containing epoxide groups, terpolymers containing epoxide groups and terpolymers containing maleic anhydride groups, respectively.

2.3 Testing and Characterizations

2.3.1 Tensile Testing

The obtained PLA biocomposites and neat PLA were molded into tensile specimens at 190°C and 1,000 psi pressure for 1 minute after pre-heating for 4 min using the compression molding machine (Chareon tut CO. LTD.). Tensile properties were determined using a universal testing machine (Instron 5969) in accordance with ASTM D638, specimen type V, 5 KN load cell. The testing was carried out under ambient conditions using a cross-head speed of 1 mm/min. All the reported values were obtained by averaging over five specimens.

2.3.2 Dynamic mechanical analysis (DMA)

DMA specimens were prepared by compression molding at 190°C and 1,000 psi pressure for 1 minute after pre-heating for 4 minutes and then laser-cut to rectangular dimensions of 10×1.16×40 mm^3. Dynamic mechanical properties of PLA biocomposites were examined by using an ANTON PAAR, Modular Compact Rheometer (MCR302) equipped with rectangular fixtures (SRF) holder under the DMTA torsion mode at a frequency of 1 Hz. A temperature sweep was carried out from 30°C to 110°C at a heating rate of 3 °C/min.

2.3.3 Field Emission Scanning Electron Microscopy (FE-SEM)

The tensile fractured surface morphology of PLA biocomposite specimens was characterized by Field Emission Scanning Electron Microscope (FE-SEM) (TESCAN MIRA3 LMH Schottky) at an accelerating voltage of 5 kV. Prior to observations, the samples were sputter coated with a thin layer of gold to avoid charging.

2.3.4 Molau Test

Molau test was performed by dissolving 0.5 g of PLA biocomposite samples in 10 mL chloroform and thoroughly shaking. The solutions were left to stand for 48 h at room temperature before the visual observation recorded by a digital camera.

2.3.5 Fourier Transformation Infrared Spectroscopy (FTIR)

The fibers in each sample of Molau test was precipitated and PLA solution was removed. Each precipitated fiber sample was transferred to 50 mL chloroform and stirred to ensure the complete removal of PLA. The insoluble fiber was collected via filtration by vacuum suction. Afterward, the extracted fibers were dried in an oven at 60°C for an hour for complete solvent removal. Finally, the filtered fiber samples in comparison with pristine fibers were analyzed by using FT-IR spectrometer (VERTEX70) at a resolution of 4 cm^{-1} with background and sample 32 scans in the spectral range of 4000-400 cm^{-1}.

3 RESULTS AND DISCUSSION

3.1 Mechanical Properties

The averaged stress-strain diagrams of neat PLA and PLA biocomposites with and without reactive agents were shown in Figure 2. It was seen that all PLA biocomposites showed a stiffer and more brittle behavior than neat PLA. The summary of mechanical properties of PLA biocomposites with and without 0.5 phr or 1.0 phr of reactive agents were shown in Table 1. It was found that the tensile strength of PLA with 10 wt% fibers loading without reactive agent (PLA/FB10) was slightly increased about 7.4% compared to neat PLA. A. Awal and colleagues reported that the tensile strength of PLA/wood fiber biocomposites was increased because of the reinforcement of fibers and the addition of bioadimide even improved the tensile strength of wood fiber reinforced PLA biocomposites due to the better interfacial adhesion within PLA and wood fiber [15]. The tensile strength of PLA biocomposites with EAGMA and EAMAH was slightly higher than non-compatibilized PLA biocomposite (PLA/FB10) whereas the tensile strength of PLA biocomposites with CEGMA showed the greater improvement than non-compatibilized PLA biocomposite. The increase of the tensile strength was more pronounced for PLA/FB/CEGMA1.0, which was corresponded to 22.4% and 13.9% higher than that of neat PLA and non-compatibilized PLA biocomposite, respectively, indicating a better interfacial adhesion within PLA and fiber. In case of Young's modulus, all PLA biocomposites possessed the higher Young's modulus when incorporating 10 wt% fiber with and without reactive agents compared to neat PLA, suggesting the better transfer of stress to the added fibers [25] (except the addition of EAMAH). Young's modulus of the PLA biocomposites was greatly improved due to the presence of the fiber that caused the stiffening effect obtained from the decrease in the mobility of the polymer matrix chains [26-28]. Although it was known that the improvement of the quality of the polymer interface did not significantly affect Young's moduli or stiffness of the materials [29], the addition of 0.5 phr EAMAH in PLA biocomposite showed the lowest Young's modulus

value, which was decreased by 7.3% compared to non-compatibilized PLA biocomposite. In case of elongation at break, it was noticed that the elongation at break of non-compatibilized PLA biocomposites was slightly lower than neat PLA. However, the incorporation with 0.5 phr of all reactive agents showed a slight increase in the elongation at break compared to non-compatibilized PLA biocomposite. The presence of 0.5 phr of CEGMA demonstrated a large improvement in the elongation at break, which was 16.1% higher than non-compatibilized PLA biocomposite. This might be due to the fact that all reactive agents contained acrylic ester acted as a soft segment of their molecule. In addition, the incorporation of CEGMA could change the molecular weight distribution of PLA matrix due to the chain extension effect [30], which might lead to the improvement of the elongation at break.

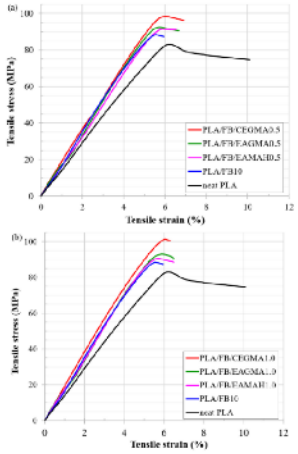

Figure 2 Tensile stress-strain diagrams of neat PLA and PLA biocomposites with and without reactive agents 0.5 phr (a) and 1.0 phr (b).

Table 1 Summary of mechanical properties of neat PLA and PLA biocomposites with and without reactive agents.

Sample codes	Tensile strength (MPa)	Young's modulus (MPa)	Elongation at break (%)
neat PLA	82.86 (4.79)	1603 (30)	10.09 (1.73)
PLA/FB10	89.03 (2.66)	1948 (23)	5.95 (0.29)
PLA/FB/CEGMA0.5	99.05 (3.62)	1941 (26)	6.91 (0.64)
PLA/FB/CEGMA1.0	101.44 (3.76)	1961 (20)	6.31 (0.38)
PLA/FB/EAGMA0.5	92.67 (2.40)	1937 (23)	6.65 (0.62)
PLA/FB/EAGMA1.0	92.09 (2.57)	1927 (31)	6.47 (0.71)
PLA/FB/EAMAH0.5	93.80 (6.46)	1805 (47)	6.54 (0.63)
PLA/FB/EAMAH1.0	91.16 (5.46)	1875 (30)	6.49 (0.41)

The standard deviation of samples were shown in parentheses.

3.2 Dynamic Mechanical Properties

The temperature dependence of storage moduli of neat PLA and PLA biocomposites with and without reactive agents were presented in Figure 3. In the glassy region (from 30°C to 50°C), all PLA biocomposite samples displayed the higher values of storage modulus (G') than that of neat PLA. The storage modulus of PLA with 10 wt% fiber loading was increased by 60% compared to that of neat PLA (1,564 MPa) due to the reinforcement effect. It was observed in Figure 3(a) that PLA biocomposites incorporated with 0.5 phr of all reactive agents had a higher storage modulus than non-compatibilized PLA biocomposite. The addition of CEGMA into PLA and fibers exhibited higher storage modulus than EAGMA and EAMAH, respectively. However, in the case of adding 1.0 phr of the anhydride-based reactive agent, the storage modulus was comparable to non-compatibilized PLA biocomposite. Upon increasing the temperature, it was seen that the storage modulus of neat PLA and all PLA biocomposites dropped at around 65°C, which corresponded to their glass transition temperature. As the temperature continued to increase, the storage moduli decreased as PLA matrix became soft at higher temperatures. In the rubbery region (from 75°C to 90°C), all PLA biocomposites exhibited significantly higher storage modulus than that of neat PLA, especially for the addition of the epoxide-based reactive agent. From Figure 3(b), the storage moduli of neat PLA and PLA incorporated with 1.0 phr EAGMA started to increase at about 98°C while the other PLA biocomposites started to increase at slightly lower temperature. These storage moduli were recovered due to the cold crystallization of PLA tested specimen in DMA temperature sweep [31].

DOI: 10.32604/JRM.2018.00129

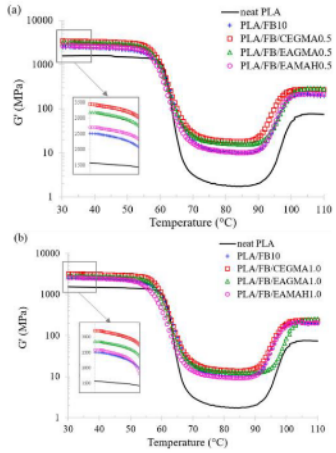

Figure 3 Storage modulus of neat PLA and PLA biocomposites with and without reactive agents 0.5 phr (a) and 1.0 phr (b).

Figure 4 depicted the curves of damping or tan δ, which was defined as the ratio of the loss to the storage modulus. The loss and storage modulus were referred as an ability for dissipating energy (viscous phase) and storing mechanical energy (elastic phase), respectively [32]. In the transition region, composites had essentially lower tan δ than neat PLA because the addition of fibers increased the mobility of the amorphous phase in the polymer matrix [32, 33]. For composites, tan δ was affected by the distribution of fibers, a concentration of shear stress, viscoelastic energy dissipation as well as the fiber and matrix interfacial adhesion [34, 35]. Therefore, tan δ peak height might be used in order to investigate the interfacial adhesion between fiber and polymer matrix [36-40]. As reported elsewhere [37, 39-41], the higher tan δ values indicated a weak interfacial adhesion whereas the lower tan δ values indicated a good interfacial adhesion due to a reduction in mobility of the polymer chain. From Figures 4(a) and 4(b), the tan δ curves of all PLA biocomposites with reactive agents shifted toward lower values than non-compatibilized PLA biocomposite, implying the better interface between the components compared to non-compatibilized PLA biocomposite. However, the incorporating of 0.5 phr anhydride-based reactive agent showed the similar tan δ value to non-compatibilized PLA biocomposite.

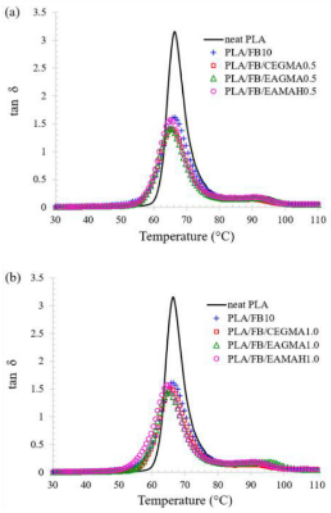

Figure 4 Tan δ of neat PLA and PLA biocomposites with and without reactive agents 0.5 phr (a) and 1.0 phr (b).

One of the parameters used to evaluate a degree of interfacial adhesion between fiber and polymer matrix due to the reduction of molecular mobility of polymer around the fiber surface compared to the matrix is called an adhesion factor (A). The adhesion factor (A) was determined using Equation (1) [41], where V_f was the volume fraction of the fiber (0.1), tan δ_c was the relative damping of the PLA biocomposites and tan δ_p was the relative damping of the pure PLA. The relative damping of the materials was determined by the maximum tan δ peak [39]. The results were presented in Table 2.

$$A = \left(\frac{1}{1 - V_f}\frac{\tan\delta_c}{\tan\delta_p}\right) - 1 \quad (1)$$

As seen in Table 2, PLA/FB/CEGMA0.5 and PLA/FB/EAGMA0.5 showed the lowest adhesion factor, which implied the strong interfacial adhesion between the fiber and PLA matrix. Furthermore, the effectiveness of stress transfer between the PLA and filler could be demonstrated by effectiveness coefficient parameter (C) [41]. The effectiveness coefficient was defined as the ratio of storage

modulus of the composite in the glassy region and the rubbery region in relation to the pure resin [41]. The effectiveness coefficient (C) was computed using Equation (2) [41], where G'_g and G'_r were the storage modulus in the glassy region and rubbery region, respectively.

$$C = \frac{G'_g/G'_r\,(composite)}{G'_g/G'_r\,(resin)} \quad (2)$$

Table 2 Tan δ peak values, Adhesion factor (A) and Effectiveness coefficient (C) parameters of neat PLA and PLA biocomposites.

Sample codes	Max tan δ peak value	Adhesion factor (A)	Effectiveness coefficient (C)
neat PLA	3.15	0	1.00
PLA/FB10	1.61	-0.43	0.27
PLA/FB/CEGMA0.5	1.40	-0.50	0.21
PLA/FB/CEGMA1.0	1.52	-0.46	0.25
PLA/FB/EAGMA0.5	1.43	-0.50	0.22
PLA/FB/EAGMA1.0	1.46	-0.49	0.25
PLA/FB/EAMAH0.5	1.57	-0.45	0.29
PLA/FB/EAMAH1.0	1.57	-0.45	0.30

From Table 2, PLA/FB/CEGMA0.5 exhibited the lowest C, which indicated the most effectiveness of stress transfer from PLA matrix to the fiber, similar to PLA/FB/EAGMA0.5 while PLA/FB/EAMAH1.0 showed the highest C compared to all PLA biocomposites. For the comparison, the incorporation the epoxide-based reactive agent exhibited more improved interfacial adhesion or compatibility between PLA and the fiber than the anhydride-based reactive agent. This could result from reactive epoxide group, which was more selective to the fiber and PLA system.

The changes introduced by reinforced filler into the structural properties of the polymeric matrix could be studied from Cole-Cole analysis [42]. The shape of Cole-Cole curve (plotted loss modulus G'' *vs.* storage modulus G') reflected the homogeneity of the system [43, 44]. The homogeneous materials showed the perfect semicircle curve while the composite systems showed the imperfect semicircle curve [42]. The elliptical or imperfect semicircle curve denoted the good adhesion between the filler and the polymer matrix [42]. In Figure 5, the Cole-Cole characteristics of all PLA biocomposites revealed the semicircles. It was also reported that the compatibility of polymer blends was represented by the slope of the curve in the low G' region [43]. At the beginning of the curve, the nearer the slope approached 2 referred a better compatibility of the blend [43]. The calculated slope of all PLA biocomposites was lower than 2, but PLA/FB/CEGMA showed the nearest slope to 2 as seen in Figure 5. Therefore, it was implied that the addition of CEGMA in PLA biocomposite could lead to the improvement of compatibility between the fiber and PLA. The better compatibility of these PLA biocomposites samples could be confirmed by SEM, Molau test, and FT-IR.

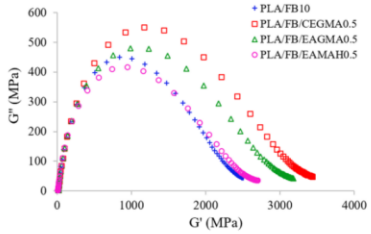

Figure 5 Cole-cole plot for PLA biocomposites with and without reactive agents 0.5 phr.

3.3 Morphology of PLA Biocomposites

Field emission scanning electron microscopy (FE-SEM) micrographs of the tensile fractured surface of PLA biocomposites with and without reactive agents were depicted in Figure 6. The micrograph of non-compatibilized PLA biocomposite in Figure 6(a) exhibited the remaining pores due to the pull-out of fibers and the space between the fiber and PLA matrix, suggesting a lack of interfacial adhesion. Figure 6 (b, b', c, and c') showed the micrographs of PLA biocomposites incorporated with epoxide-based reactive agents. The fibers breakage and disappearance of space between PLA and fibers were observed rather than pullout, indicating better interfacial adhesion between the fibers and PLA matrix. Whereas the micrographs of PLA biocomposites incorporated with the anhydride-based reactive agent showed the smooth of the fiber without the remaining pores as seen in Figures 6 (d, d'). Figure 6a, which indicates the pullout of the fiber from the PLA matrix. From FE-SEM results, it could be concluded that PLA biocomposites with epoxide-based reactive agents helped to promote the better interfacial adhesion, essentially resulting in more efficient transfer of stress from the PLA matrix to the reinforcement than that with the anhydride-based reactive agent. R. Gunti and colleagues reported that the fiber reinforced PLA composites had exhibited fiber breakage rather than pullout due to the better stress transfer between fiber and matrix [45]. The results were in good agreement with the improved mechanical properties of the PLA

DOI: 10.32604/JRM.2018.00129

composites with the epoxide-based reactive agent (CEGMA) discussed earlier.

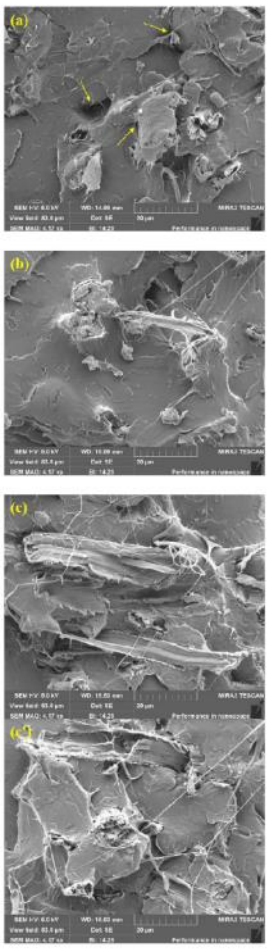

Figure 6 FE-SEM micrographs of tensile fractured surface of PLA biocomposites; PLA/FB10 (a), PLA/FB/CEGMA 0.5 phr (b) and 1.0 phr (b'), PLA/FB/EAGMA 0.5 phr (c) and 1.0 phr (c'), PLA/FB/EAMAH 0.5 phr (d) and 1.0 phr (d').

3.4 Molau Test of PLA Biocomposites

In order to investigate any changes in physical properties due to interfacial bonding or compatibility in PLA biocomposites with and without reactive agents, Molau test of these PLA biocomposites compared to neat PLA were presented in Figure 7. It was observed that neat PLA could be dissolved completely in chloroform, thus a transparent solution was obtained. In the case of non-compatibilized PLA biocomposite (PLA/FB10), the phase separation was clearly noticed. The lower layer contained the insoluble fiber and the upper layer was the PLA solution, indicating the lack of interaction between the fiber and PLA. When 1.0 phr of EAGMA or EAMAH was used as reactive agents for PLA biocomposite, more turbidity of the solution was observed even though the phase separation was still observed. The addition of CEGMA in PLA biocomposite exhibited the most turbid solution. This indicated that the addition of CEGMA could lead to some chemical reactions between fibers and PLA. A. Mujica-Garcia and colleagues also used the Molau test to study the interfacial interaction between PLA matrix and CNC. They observed that CNC of both neat CNC and mixture of CNC/PLA solutions precipitated, but the suspension of functionalized CNC in the CNC-g-PLLA solution was maintained stable, as a consequence of the well-done functionalization [46].

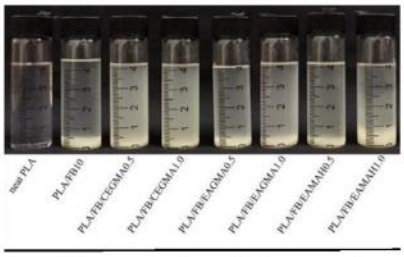

Figure 7 Photographs obtained by Molau test of neat PLA and PLA biocomposites with and without reactive agents (0.5 phr and 1.0 phr).

3.5 Characterization of Compatibilized PLA Biocomposites

The interaction between the fiber and PLA within the biocomposites was analyzed by FTIR. Figure 8 illustrated FT-IR spectra of virgin fiber and the

precipitated fibers of PLA biocomposites with and without reactive agents. The intensity of the broad peak at 3480 cm^{-1}, which assigned to the -OH stretching of cellulose fibers in all samples, was unchanged (data not shown). Considering the characteristic at peak 1758 cm^{-1}, it was assigned to the remaining carbonyl groups (C=O) of PLA chains in precipitated fibers. It was clearly seen that the peak was disappeared at 1758 cm^{-1} for virgin fiber, fibers without reactive agents (PLA/FB10) and fibers with 0.5 phr EAMAH (PLA/FB/EAMAH0.5). On the other hand, the strong peak at 1758 cm^{-1} for precipitated fiber sample of CEGMA was indicative of a strong interaction between the fiber and PLA matrix. A. Mujica-Garcia and colleagues reported that FTIR spectrum of CNC-g-PLLA was the presence of the peak at 1753 cm^{-1}, corresponding to the stretching frequency of the carbonyl group in PLA and/or lactic acid oligomers, which confirmed the success of the grafting procedure [46]. It suggested that CEGMA was significantly improved the interfacial adhesion between the fiber and PLA matrix. Since CEGMA had multiple reactive epoxide groups, CEGMA might be chemically reacted with hydroxyl groups in fiber and also the PLA chain ends (-OH and -C=O groups) during melt processing, resulting in the significant increase in the compatibility between the fiber and PLA matrix. However, this was the first evidence, the chemical reaction between the fiber and PLA needed to be clarified. Furthermore, the weak peak at 1758 cm^{-1} for precipitated fiber sample of EAGMA or 1.0 phr EAMAH was observed. Similarly, EAGMA could improve the interfacial adhesion between the fiber and PLA matrix but not as much as CEGMA. In contrast, the addition of anhydride-based reactive agent as much as 1.0 phr would result in the improved interaction between the fiber and PLA matrix.

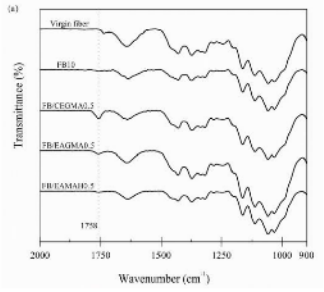

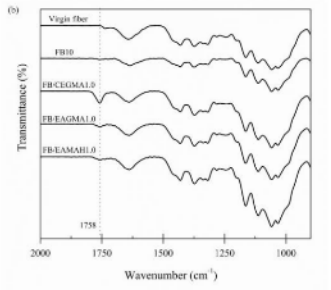

Figure 8 FT-IR spectra of virgin fiber and fibers with and without reactive agents 0.5 phr (a) and 1.0 phr (b) after dissolving from PLA biocomposites.

4 CONCLUSION

The *in situ* reactive compatibilization of short-fiber reinforced PLA biocomposites were successfully prepared by melt-mixing. Multifunctional group reagents such as CEGMA, EAGMA, and EAMAH were selected as reactive compatibilizers for PLA biocomposites. The influence of reactive agents on mechanical, dynamic mechanical properties and morphology of PLA biocomposites were investigated. The following conclusions could be drawn from this study:

1) PLA biocomposites loaded with 1.0 phr of CEGMA provided the most improvement of tensile strength about 22.4% and 13.9% compared to neat PLA and non-compatibilized PLA biocomposite, respectively. However, the effect of different reactive agents was not so dominant in terms of Young's modulus. The presence of all reactive agents also improved the elongation at break of PLA due to the existing acrylic ester in their molecules.

2) The storage modulus of PLA biocomposites showed the most increased when loading 0.5 phr of CEGMA followed by EAGMA and EAMAH, respectively.

3) The adhesion factor and effectiveness of the PLA biocomposites revealed that the interfacial adhesion of PLA/fiber was improved with the addition of the epoxide-based reactive agent (CEGMA and EAGMA).

4) The FE-SEM micrographs of PLA biocomposites incorporated with epoxide-based reactive agents (CEGMA and EAGMA) displayed fibers breakage and continuous matrix, indicating a better interfacial adhesion between the fibers and PLA matrix.

5) Molau test confirmed that epoxide-based reactive agent, CEGMA, enhanced the interaction between the fiber and PLA matrix.

6) FTIR spectra revealed that carbonyl groups appeared in precipitated fibers samples of epoxide-based reactive agents (CBGMA). However, the chemical reaction between the fiber and PLA would be further clarified.
7) The present results indicated that CBGMA was the most effective compatibilizer for PLA biocomposite.

ACKNOWLEDGMENTS

The authors would like to gratefully thank the Department of Materials Science and Engineering, Faculty of Engineering and Industrial Technology for financial support, and Department of Physics, Faculty of Science, Silpakorn University for the facility, Silpakorn University, Thailand.

We also appreciate SCG Packaging PLC., Thailand for bleach eucalyptus paper pulps supply and Mr. Kesin Hachaiwee for his assistance. We also acknowledged Mr. Witoon Wattanaut for his help on the FE-SEM observation.

REFERENCES

1. M. S. Huda, L. T. Drzal, A. K. Mohanty and M. Misra, Effect of fiber surface-treatments on the properties of laminated biocomposites from poly(lactic acid) (PLA) and kenaf fibers. *Compos. Sci. Technol.* **68**, 424–432 (2008).
2. T. Nishino, K. Hirao, M. Kotera, K. Nakamae and H. Inagaki, Kenaf reinforced biodegradable composite. *Compos. Sci. Technol.* **63**, 1281–1286 (2003).
3. S. M. Lee, D. Cho, W. H. Park, S. G. Lee, S. O. Han and L. T. Drzal, Novel silk/poly(butylene succinate) biocomposites: The effect of short fibre content on their mechanical and thermal properties. *Compos. Sci. Technol.* **65**, 647–657 (2005).
4. A. Le Duigou, P. Davies and C. Baley, Interfacial bonding of Flax fibre/Poly(l-lactide) biocomposites. *Compos. Sci. Technol.* **70**, 231–239 (2010).
5. F. Nassiopoulos and J. Njuguna, Thermo-mechanical performance of poly(lactic acid)/flax fibre reinforced biocomposites. *Mater. Design* **66**, 473–485 (2015).
6. K. Oksman, M. Skrifvars and J. F. Selin, Natural fibres as reinforcement in polylactic acid (PLA) composites. *Compos. Sci. Technol.* **63**, 1317–1324 (2003).
7. A. K. Bledzki, A. Jaszkiewicz and D. Scherzer, Mechanical properties of PLA composites with man-made cellulose and abaca fibres. *Compos. Part A Appl. Sci. Manuf.* **40**, 404–412 (2009).
8. D. Plackett, T. Løgstrup Andersen, W. Batsberg Pedersen and L. Nielsen, Biodegradable composites based on l-polylactide and jute fibres. *Compos. Sci. Technol.* **63**, 1287–1296 (2003).
9. T. Yu, Y. Li and J. Ren, Preparation and properties of short natural fiber reinforced poly(lactic acid) composites. *J. Wuhan. Mater. Sci.* **19**, 65–68 (2004).
10. Y. Dong, A. Ghataura, H. Takagi, H. J. Haroosh, A. N. Nakagaito and K. T. Lau, Polylactic acid (PLA) biocomposites reinforced with coir fibres: Evaluation of mechanical performance and multifunctional properties. *Compos. Part A Appl. Sci. Manuf.* **63**, 76–84 (2014).
11. A. Bourmaud and S. Pimbert, Investigations on mechanical properties of poly(propylene) and poly(lactic acid) reinforced by miscanthus fibers. *Compos. Part A Appl. Sci. Manuf.* **39**, 1444–1454 (2008).
12. T. Yu, J. Ren, S. Li, H. Yuan and Y. Li, Effect of fiber surface-treatments on the properties of poly(lactic acid)/ramie composites. *Compos. Part A Appl. Sci. Manuf.* **41**, 499–505 (2010).
13. W. Sujaritjun, P. Uawongsuwan, W. Pivsa-Art and H. Hamada, Mechanical property of surface modified natural fiber reinforced PLA biocomposites. *Energy Procedia* **34**, 664–672 (2013).
14. K. Okubo, T. Fujii and R.T. Thostenson, Multi-scale hybrid biocomposite: Processing and mechanical characterization of bamboo fiber reinforced PLA with microfibrillated cellulose. *Compos. Part A Appl. Sci. Manuf.* **40**, 469–475 (2009).
15. A. Awal, M. Rana and M. Sain, Thermorheological and mechanical properties of cellulose reinforced PLA bio composites. *Mech. Mater.* **80**, 87–95 (2015).
16. Y. Du, T. Wu, N. Yan, M.T. Kortschot and R. Farnood, Pulp fiber reinforced thermoset polymer composites: Effects of the pulp fibers and polymer. *Composites Part B: Engineering* **48**, 10–17 (2013).
17. F. X. Espinach, S. Boufi, M. Delgado-Aguilar, F. Julián, P. Mutjé and J.A. Méndez, Composites from poly(lactic acid) and bleached chemical fibres: Tactical properties. *Composites Part B: Engineering* **134**, 169–176 (2018).
18. M. Murariu and P. Dubois, PLA composites: From production to properties. *Adv. Drug Deliver. Rev.* **107**, 17–46 (2016).
19. K. Formela, A. Hejna, J. Haponiuk and A. Torcpale, *R In Situ Processing of Biocomposites via Reactive*

Extrusion. Biocomposites for High-Performance Applications, 135-216 (2017).
20. Q. Meng, M. C. Heuzey and P. J. Carreau, Control of thermal degradation of polylactide/clay nanocomposites during melt processing by chain extension reaction. *Polym. Degrad. Stab.* **97**, 2010-2020 (2012).
21. B. H. Bilodeau and C. Saron, Chain extension of poly (ethylene terephthalate) by reactive extrusion with secondary stabilizer. *Mat. Res.* **15**, 467-472 (2012).
22. X. Tang, W. Gao, G. Yin, B. Li and C. Wu, Reactive extrusion of recycled poly(ethylene terephthalate) with polycarbonate by addition of chain extender. *J. Appl. Polym. Sci.* **104**, 2602-2607 (2007).
23. P. Nantiananon, M. Seadan, S. Pivsa-Art, H. Hamyaki and S. Suttirungyong, Biodegradable polyesters reinforced with eucalyptus fiber: effect of reactive agents. *AIP Conference Proceedings 1914* (2016).
24. M. M. Kabir, H. Wang, K. T. Lau and F. Cardona, Chemical treatments on plant-based natural fibre reinforced polymer composites: An overview. *Compos. Part B Eng.* **43**, 2883-2892 (2012).
25. T. H. Nam, S. Ogihara and S. Kobayashi, Interfacial, mechanical and thermal properties of coir fiber reinforced poly(lactic acid) biodegradable composites. *Advanced Composite Materials* **21**, 103-122 (2012).
26. J. A. Méndez, F. Vilaseca, M. A. Pèlach, I. P. López, L. Barberà, X. Turon, J. Girones and P. Mutjé, Evaluation of the reinforcing effect of ground wood pulp in the preparation of polypropylene-based composites coupled with maleic anhydride grafted polypropylene. *J. Appl. Polym. Sci.* **105**, 3538-3546 (2007).
27. T. T. L. Doan, S. L. Gao and E. Mader, Jute/polypropylene composites. I. Effect of matrix modification. *Compos. Sci. Technol.* **66**, 952-963 (2006).
28. F. M. B. Coutinho and T.H.S. Costa, Performance of polypropylene-wood fiber composites. *Polym. Test.* **18**, 581-587 (1999).
29. L. A. Granda, F. X. Espinach, J. A. Méndez, J. Tresserras, M. Delgado-Aguilar and P. Mutjé, Semichemical fibres of Leucaena collinsii reinforced polypropylene composites: Young's modulus analysis and fibre diameter effect on the stiffness. *Compos. Part B Eng.* **92**, 332-337 (2016).
30. R. Khankrua, S. Pivsa-Art, H. Hamyaki and S. Suttirungyong, Effect of chain extenders on thermal and mechanical properties of poly(lactic acid) at high processing temperatures: Potential application in PLA/Polyamide 6 blend. *Polym. Degrad. Stab.* **108**, 232-240 (2014).
31. X. Gao, J. Zhang and L. Huang, Poly(lactic acid)/polyoxymethylene blends: Morphology, crystallization, rheology, and thermal mechanical properties. *Polym.* **69**, 103-109 (2015).
32. Y. Z. Hao Ren, Huamin Zhai and Jinsong Chen, Production and evaluation of biodegradable composites based on polyhydroxybutyrate and polylactic acid reinforced with short and long pulp fibers. *Cellul. Chem. Technol.* **49**, 641-652 (2015).
33. P. V. Joseph, G. Mathew, K. Joseph, G. Groeninckx and S. Thomas, Dynamic mechanical properties of short sisal fibre reinforced polypropylene composites. *Compos. Part A Appl. Sci. Manuf.* **34**, 275-290 (2003).
34. D. Shanmugam and M. Thiruchitrambalam, Static and dynamic mechanical properties of alkali treated unidirectional continuous Palmyra Palm Leaf Stalk Fiber/jute fiber reinforced hybrid polyester composites. *Mater. Design* **50**, 533-542 (2013).
35. P. A. Sreekumar, R. Saiah, J. M. Saiter, K. Leblanc, K. Joseph, G. Unnikrishnan and S. Thomas, Dynamic mechanical properties of sisal fiber reinforced polyester composites fabricated by resin transfer molding. *Polym. Compos.* **30**, 768-775 (2009).
36. A. Bianu, S. Paiber, Z. Feng and H. Wang, The study of fibre/matrix bond strength in short hemp polypropylene composites from dynamic mechanical analysis. *Compos. Part B Eng.* **62**, 19-28 (2014).
37. K. V. Krishna and K. Kanny, The effect of treatment on jute fiber using green approach and their reinforced epoxy composites. *Compos. Part B Eng.* **104**, 111-117 (2016).
38. H. L. Cavaglia, A. S. Balmer, R. Fiorio, A. J. Zattera and S. C. Amico, Mechanical and dynamic mechanical analysis of hybrid composites molded by resin transfer molding. *J. Appl. Polym. Sci.* **118**, 887-896 (2010).
39. C. A. Correa, C. A. Razzino and L. B. Hage, Role of maleated coupling agents on the interface adhesion of polypropylene-wood composites. *J. Thermoplast. Compos.* **20**, 323-339 (2007).
40. C. A. Correa, C. A. Razzino and L. Hage Jr, Role of Maleated Coupling Agents on the Interface Adhesion of Polypropylene-Wood Composites. *Journal of Thermoplastic Composite Materials* **20** (2007).
41. J. O. Akindoyo, M. D. H. Beg, S. Ghazali, H. P. Heim and M. Feldmann, Effects of surface modification on dispersion, mechanical, thermal and dynamic

mechanical properties of injection molded PLA-hydroxyapatite composites. *Compos. Part A Appl. Sci. Manuf.* **103**, 96-105 (2017).
42. A. K. Pandey, R. Kumar, V.S. Kachhavah and K. K. Kar, Mechanical and thermal behaviours of graphite flake-reinforced acrylonitrile-butadiene-styrene composites and their correlation with entanglement density, adhesion, reinforcement and Cfactor. *RSC Adv.* **6**, 50559-50571 (2016).
43. C. Zhang, Y. Huang, C. Liu, L. Jiang and Y. Dan, Enhanced ductility of polylactide/natural rubber blends with pre-butylated natural rubber. *J. Polym. Res.* **20**, 121 (2013).
44. L. Mancic, P. I. Pomrén, S. Lebichevsky, A. M. Costa, B. A. Marinkovic and F.C. Rizzo, Application of silane grafted titanate nanotubes in reinforcing of polyamide 11 composites. *Compos. Part B: Eng.* **93**, 153-162 (2016).
45. R. Sarai, A. V. Ratna Prasad and A. V. S. S. K. S. Gupta, Mechanical and degradation properties of natural fiber reinforced PLA composites: Jute, sisal, and elephant grass. *Polymer Composites* **39**, 1125-1136 (2016).
46. A. Mujica-Garcia, S. Houshmand, M. Skrifvars, J. M. Kenny, K. Oksman and L. Peponi, Poly(Lactic acid) melt-spun fibers reinforced with Electrosprayed cellulose nanocrystals. *RSC Advances* **6**, 9221-9231 (2016).

Biodegradable polyesters reinforced with eucalyptus fiber: effect of reactive agents

P. Nanthananon[a], M. Seadan[b], S. Pivsa-Art[c], H. Hiroyuki[d] and S. Suttiruengwong[a*]

[a]*Department of Materials Science and Engineering, Faculty of Engineering and Industrial Technology, Silpakorn University, Sanamchandra Palace Campus, Nakhon Pathom 73000, Thailand*
[b]*Department of Physics, Faculty of Science, Silpakorn University, Nakhon Pathom 73000, Thailand*
[c]*Department of Material and Metallurgical Engineering, Faculty of Engineering, Rajamangala University of Technology Thanyaburi, Klong 6, Thanyaburi, Pathumthani 12110, Thailand*
[d]*Kyoto Institute of Technology, Matsugasaki, Sakyo-ku, Kyoto City 606-8585, Japan*

p.nanthananon@hotmail.com
[*]*suttiruengwong_s@su.ac.th*

Abstract. The aim of this work was to investigate the effect of reactive agents on the rheological behaviors, morphology and mechanical properties of two biodegradable polyesters; poly(lactic acid) (PLA) and poly(butylene succinate) (PBS) reinforced with eucalyptus fiber. Two types of reactive agents, chain extender (Joncryl®) and peroxide (Perkadox® 14), were selected. Biocomposites consisting of a constant fiber loading of 10 wt% with and without reactive agents were prepared by one-step melt-mixing methods via an internal mixer with the rotational speed of 60 rpm and the temperature of 150 and 190 °C for PBS and PLA, respectively. The biocomposite samples were then compression-molded for tensile testing. Rheological and morphological properties of the biocomposites were also investigated by means of dynamical mechanical analysis (DMA) and scanning electron micrograph (SEM). The results revealed the presence of Joncryl® in PLA biocomposites caused the increase of mixing torque, complex viscosity, storage modulus and mechanical properties when compared to the addition of peroxide. The increase of complex viscosity of PLA biocomposites added Joncryl® was due to the increase in the population of the higher molecular weights as confirmed by GPC analysis. In the case of PBS biocomposites, it showed a dramatic increase in the complex viscosity and storage modulus with decreasing crossover frequencies when adding peroxide rather than adding Joncryl®. The SEM micrographs demonstrated that the compatibility between the polymer matrix and fiber was improved when adding a small amount of Joncryl® and peroxide for both polymers, except for 0.5 phr peroxide loading, leading to an improvement of their modulus and tensile strength.

Keywords: Biocomposite, Biodegradable polymer, Natural fiber, Reactive agent
PACS: 81.05.Lg, 81.05.Qk, 82.35.Gh, 82.35.Pq, 83.80.Ab, 83.85.Cg

INTRODUCTION

Biocomposites based on biopolymers and natural fibers have caught much attention in the last few decades due to the combination of a good mechanical performance as well as less environmental impact with being fully biodegradable and more sustainable in terms of renewable resources. Many commercially available biodegradable polyesters have readily been produced on an industrial scale with a wide range of grades and applications. These include polylactic acid (PLA), polybutylene succinate (PBS), poly(caprolactone) (PCL) and poly(butylene adipate-co-terephthalate) (PBAT). Depending on the desired purposes, the properties of these classes of polymers could be effectively modified through polymer blending or composites. As far as the biocomposites are concerned, the major challenge is the improvement of an interfacial adhesion between natural fiber and biopolymer matrix. The better interfacial adhesion would result in an improvement in mechanical and rheological properties of composites [1]. In order to enhance the natural fiber-matrix adhesion; chemical treatments, *in-situ* reactive blending, and coupling agents have been considered as solutions with the aim of changing the surface tension and polarity through the modification of fiber surface, and thus facilitating coupling with the matrix [2]. The treatments can be achieved usually based on the use of reactive groups such as maleic anhydride (MA), silanes, isocyanate, and peroxide [2]. However, some treatments are robust and time-consuming. The interface properties of fiber and matrix could be improved by peroxide treatment as it initiated free radicals reacted with the hydrogen group of the cellulose fiber and matrix [2]. Alternatively, the presence of a chain extender, reactive multi-epoxy groups like Joncryl®, was used as a chain extension/branching agent in PLA/PBAT blends, and it showed an improvement of their thermal stability as reported by Al-Itry et al. [3]. The epoxide groups of Joncryl® could theoretically react with both hydroxyl and

Proceedings of PPS-32
AIP Conf. Proc. 1914, 070012-1–070012-5; https://doi.org/10.1063/1.5016739
Published by AIP Publishing. 978-0-7354-1606-2/$30.00

carboxyl end groups of the polyesters [3]. Meng et al. [4] reported that the addition of 1 wt% Joncryl® in PLA nanocomposites with 2 wt% organo-modified clay improved the PLA thermal stability by a chain extension reaction with PLA chain end groups as well and the possible reaction of Joncryl® epoxy groups with the hydroxyl groups in the organo-modifier clay. To the best of our knowledge, there have been no reports of using Joncryl® and peroxide as the *in-situ* compatibilizer in natural fiber to produce biocomposite. Thus, this work was aimed to propose the simple way for the reactive blending of the eucalyptus fiber and biodegradable polyesters (PBS or PLA) using two types of reactive agents; Joncryl® and Perkadox by one-step melt-mixing methods. The influence of reactive agents on rheology, morphology and mechanical properties of biocomposites were investigated.

EXPERIMENTAL

Materials and Biocomposites Preparation

Poly(butylene succinate) (PBS) (1001MD blown film grade) was purchased from Showa High Polymer Co., Ltd., Japan. Poly(lactic acid) (PLA) (3052D injection grade) was purchased from NatureWorks® LLC. (USA). The eucalyptus pulps (500-600 μm in length and 4-10 μm in diameter) were kindly provided by SCG Packaging PLC., Thailand. Peroxide (Perkadox® 14-40B-pd) (containing 40% with $CaCO_3$ and SiO_2) was purchased from AkzoNobel. Joncryl® (ADR-4368F), an epoxy-based chain extender, was obtained from BASF The Chemical Co., Thailand. Paper pulps were dried at 80 °C and ground to obtain eucalyptus fibers using a high-speed grinder. Prior to melt mixing, PLA and PBS were dried at 60 °C in a hot air oven for 6 hr and eucalyptus fibers were dried again at 80 °C overnight. The biocomposites without reactive agents were first prepared by adding 10 wt% of eucalyptus fibers into PLA or PBS (referred as PLA/FB10 or PBS/FB10 respectively) using an internal mixer (Chareon tut CO. LTD., model MX 105-D40L50) with the rotational speed of 60 rpm and the temperature of 190 °C and 150 °C for PLA and PBS, respectively. The concentrations of 0.1, 0.5, 1.0 phr of Joncryl® and 0.05, 0.1, 0.5 phr of peroxide were used for the PLA/FB10 and PBS/FB10 biocomposites. Samples for the rheological, morphological and mechanical analysis were prepared by compression molding at 150°C for PBS and 190 °C for PLA respectively.

Measurement and Testing

Rheological behavior measurements of PLA and PBS biocomposites were performed using an ANTON PAAR (MCR302) equipped with 25 mm parallel plate flow geometry. The over a frequency range of 0.1–100 rad/s (from high to low frequency) and 0.1% strain amplitude were carried out at 190 °C and using a gap size of 1 mm. The molecular weights of the polymer after compounding was determined using gel permeation chromatography technique (GPC) (Waters 2414) and the GPC columns were eluted using THF with a flow rate of 1.0 mL/min at 40°C and calibrated with polystyrene standards. Morphological observations were taken using a scanning electron microscope (SEM, TM3030 Hitachi, Japan) at an accelerating voltage of 15 kV. The samples were fractured in liquid nitrogen and then coated with a thin layer of palladium prior to observations. For mechanical testing, dog-bone-shaped specimens of 70 mm in total length, type V based on standard ASTM D638 were tested using an Instron tensile machine, model 5969 with a load cell of 5 kN, to measure Young's modulus, tensile strength, and elongation at break. All tests were carried out under ambient conditions using a cross-head speed of 1 mm/min.

RESULTS AND DISCUSSION

Rheological and Molecular Weight Analysis

The plot of mixing torque values against time of PBS and PLA biocomposites with and without Joncryl® and peroxide were shown in Fig. 1. It was observed that the final torque values of both PBS and PLA reinforced with fiber 10 wt% showed the 15% increase when compared with their neat ones as seen from Fig. 1(a) and (c), respectively. In addition, with the addition 0.1, 0.5 and 1.0 phr Joncryl®, it showed an increase of final torque 17%, 27% and 22%, respectively for PBS composites and 24%, 37% and 64% for PLA composites when compared with their neat. PBS biocomposites with 0.05, 0.1 and 0.5 phr peroxide (Fig. 1(b)) showed the increase in the torque values after loading all ingredients into an internal mixer, indicating some degree of chemical reaction. The torque curve slightly decreased to the final torque values of 23%, 159% and 223% with increasing the peroxide contents, but was still higher than the neat PBS. In the case of PLA biocomposites with 0.05, 0.1 and 0.5 phr peroxide, from

Fig. 1(d), the final torque values increases to 12%, 9.5%, and 57% respectively, when compared with neat PLA. It was generally known that an increase of torque value was related to an increase of molten polymer viscosity, which was caused by an increase in molecular weight. On the other hand, it was also reported that torque value increased with the presence of various bonding agents in composites (fiber-polymer adhesion enhancing) [1]. The complex viscosity, storage modulus and the plot of storage, loss modulus (G', G'') crossover frequencies of biocomposites having different reactive agents were shown in Fig. 2 (PBS) and Fig. 3 (PLA). The complex viscosity of neat PBS and PLA gradually decreased with increasing angular frequency, which is the typical shear thinning behavior. The incorporation of fiber and reactive agents gave rise to the higher viscosity for the whole frequency range and enhanced the shear thinning behavior comparing to neat polymers, therefore, shifted the Newtonian plateau to the lower angular frequency. It was well established that the addition of fiber into the polymer matrix increased the molten viscosity caused resistance against the flow. At an angular frequency of 0.1 rad/s in Fig. 2(a), the complex viscosity of PBS biocomposites with and without Joncryl® and 0.05 phr peroxide were about 4-fold but with the higher amount of peroxide exhibited 16-fold greater than neat PBS. The addition of the higher amount of peroxide in PBS biocomposite might cause more polymer-polymer interactions and increased resistance to flow, which was consistent with mixing torque values discussed earlier. In Fig. 2(b), the storage modulus values of PBS

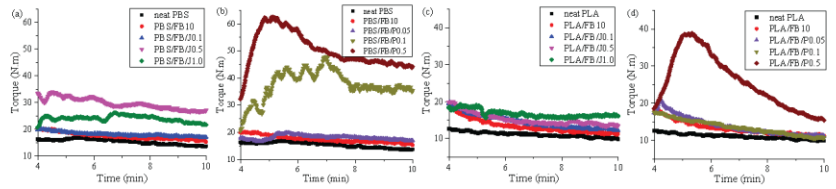

FIGURE 1. Mixing torque versus time after loading all ingredients together and continuous mixing until ten minutes of PBS and PLA composites with various content of Joncryl® (a), (c) and peroxide (b), (d), respectively.

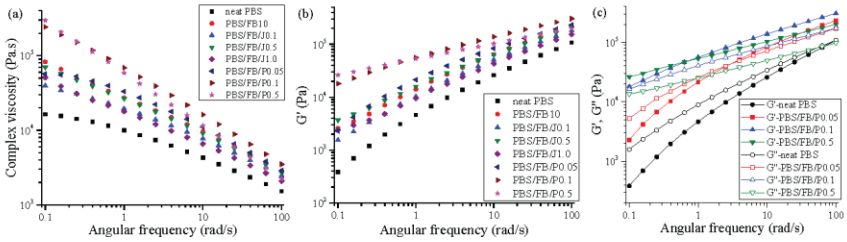

FIGURE 2. Complex viscosity (a), storage modulus (G') (b) and G',G'' cross-over frequencies of PBS biocomposites having various content of peroxide (c) as a function of frequency.

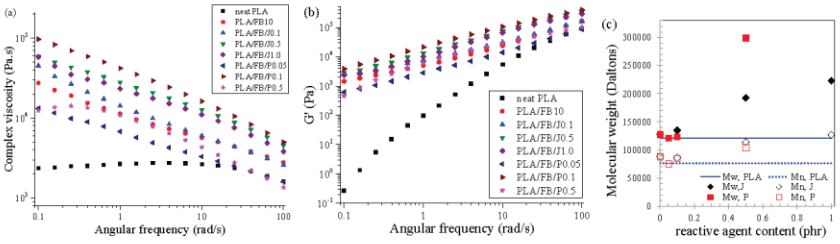

FIGURE 3. Complex viscosity (a) and storage modulus (G') (b) as a frequency dependence of PLA biocomposites having different reactive agents and their contents, and molecular weights of extracted PLA after compounding (c).

biocomposites showed a similar tendency to the complex viscosity. In Fig. 2(b), 3(b), both neat PBS and PLA showed the characteristic terminal liquid-like behaviors in the low-frequency region ($G' \alpha \omega^2$). However, the G' of the PBS and PLA biocomposites displayed a deviation from the liquid-like to solid-like behavior because of the slow relaxation process as noted in the decrease in the slope of G' at low frequencies. For the peroxide-PBS biocomposites system in Fig. 2(c), the G', G" crossover frequency (ω_c) shifted towards lower frequency with the increased peroxide contents, suggesting the slower relaxation processes (higher relaxation time, $\tau_R = 1/\omega_c$) and enhance of melt elasticity. Therefore, it was apparently seen that the terminal region of PBS added 0.5 phr peroxide dramatically shifted to low frequencies and the visually widened plateau modulus referred as entanglements between polymer chains and M_W increased [5]. This implied that adding high peroxide content could result in crosslinking or branching of PBS. The G', G" crossover frequency of PBS biocomposites with and without Joncryl® was insignificantly changed, similarly to PLA biocomposites with reactive agents (data not shown). From Fig. 3 (a-b), the complex viscosity and G' values increased with the Joncryl® contents increase and higher than adding peroxide (0.05 and 0.5 phr), compared to PLA biocomposites. This might be due to Joncryl® could epoxy groups reach chain extension reaction with PLA chain end groups as well and the possible reaction with the hydroxyl groups in the fiber [4]. This was confirmed by GPC results in Fig. 3(c), the molecular weight increased with the Joncryl® contents increased. Although adding 0.1 phr peroxide to the PLA biocomposites showed the highest complex viscosity and G' values, the only high content of peroxide added showed the high molecular weight of PLA. This might be caused by a good fiber-PLA adhesion and/or long-chain branches of PLA occurred when 0.1 phr peroxide was added. As reported by Henton et al. [1], the small amounts of peroxide resulted in long-chain branches of PLA via free radical.

Morphological Observations

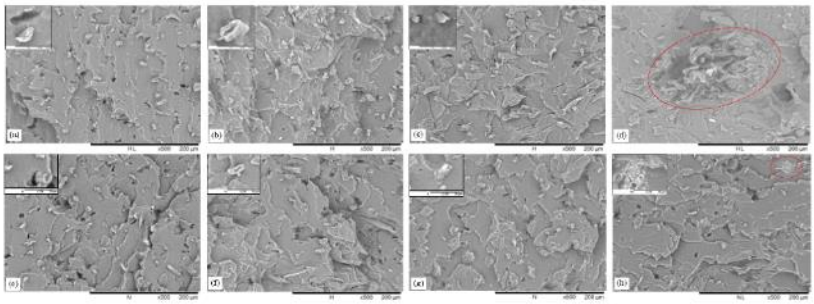

FIGURE 4. SEM micrographs of PBS biocomposites with 10 wt% fiber (a), having Joncryl® 0.5 phr (b), peroxide 0.1 phr (c) and 0.5 phr (d), and PLA biocomposites with 10 wt% fiber with (e), Joncryl® 0.5 phr (f), peroxide 0.1 phr (g) and 0.5 phr (h).

Fig. 4 depicted the SEM micrographs of the PBS and PLA biocomposites with and without reactive agents. When Joncryl® and peroxide were added, less voids and cavities were observed except for 0.5 phr peroxide in PBS biocomposites showing some aggregation of fibers. The decrease in fibers dispersion might be due to a high amount of peroxide affected to PBS matrix reaction, which led to a great increase in torque and complex viscosity values. Whereas, adding 0.5 phr peroxide to PLA biocomposites displayed an aggregation of peroxide. This indicated that small amount of Joncryl® and peroxide might improve the interfacial adhesion between fiber and matrix.

Mechanical Properties

Mechanical properties of PBS and PLA biocomposites with and without reactive agents were shown in Fig. 5. Fig. 5(a) presented an increase of modulus of both PBS and PLA biocomposites, about 1.5-fold and 1.2-fold, respectively, higher than for their neat. It could be seen that more increased modulus when Joncryl® and peroxide were added, except for 0.5 phr peroxide loading. In Fig. 5(b), the tensile strength values of PBS biocomposites only showed an increase of 2% and 4% compared to neat PBS when adding 0.1 phr peroxide and 0.5 phr Joncryl® respectively. From Fig. 5(c), it displayed 6% increase in tensile strength for PLA with 10 wt% fibers compared to

neat PLA. The significant increase in tensile strength of 16-19% was obtained upon adding Joncryl® while the presence of the small amount of peroxide caused the increase in tensile strength of 13% compared to neat PLA. A general increase in the modulus and strength was observed in the Joncryl®/PLA system due to the increased molecular weights [6] and also the good fiber-polymer adhesion. The elongation at break of PBS biocomposites decreased, in particular with the addition of 0.5 phr peroxide whiles the elongation at break of PLA biocomposites was maintained. The decrease in mechanical properties when adding 0.5 phr peroxide of both biocomposites might be due to a high-stress concentration from the fiber aggregation (in PBS) and peroxide (in PLA) as observed by SEM micrographs.

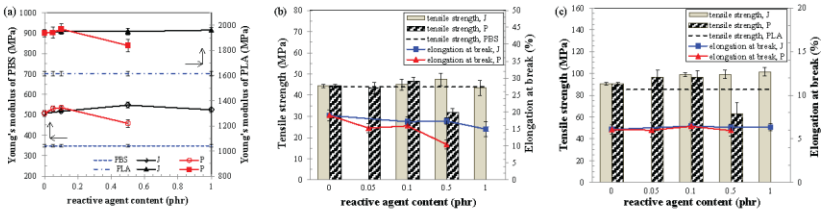

FIGURE 5. Effects of fiber with and without reactive agents on Young's modulus of PBS and PLA biocomposites (a), tensile strength and elongation at break of PBS biocomposites (b) and PLA biocomposites (c).

CONCLUSION

The presence of Joncryl® in PLA biocomposites caused the increase of molecular weights, mixing torque, complex viscosity, storage modulus and mechanical properties when compared to the addition of peroxide. The increase of complex viscosity of PLA biocomposites added Joncryl® was due to the increase in the population of the higher molecular weights as confirmed by GPC analysis. In the case of PBS biocomposites, it showed a dramatic increase in the mixing torque, complex viscosity and storage modulus with decreasing in crossover frequencies with the increase of peroxide content rather than adding Joncryl®. Peroxide was extremely reactive with PBS than with PLA at the same concentrations. The SEM micrographs demonstrated that the compatibility between the polymer matrix and fiber was improved when adding a small amount of Joncryl® and peroxide for both polymers, leading to an improvement of their modulus and tensile strength. However, it revealed some aggregated fibers when adding the high contents of peroxide up to 0.5 phr, which resulted in a decrease in modulus and tensile strength.

ACKNOWLEDGMENTS

The authors would like to gratefully thank the department of Materials Science and Engineering, Faculty of Engineering and Industrial Technology, Silpakorn University, Thailand for financial supports. We are aslo indebted to SCG Packaging PLC., Thailand for paper pulps supply. National Research Council of Thailand was gratefully acknowledged for financial supports under Bioplastics framework.

REFERENCES

1. A.K. Mohanty, M. Misra, and L.T. Drzal, *Natural Fibers, Biopolymers, and Biocomposites*. 2005: CRC Press.
2. M.M. Kabir, et al., *Chemical treatments on plant-based natural fibre reinforced polymer composites: An overview*. Composites Part B: Engineering, 2012. **43**(7): pp. 2883-2892.
3. R. Al-Itry, K. Lamnawar, and A. Maazouz, *Improvement of thermal stability, rheological and mechanical properties of PLA, PBAT and their blends by reactive extrusion with functionalized epoxy*. Polymer Degradation and Stability, 2012. **97**(10): pp. 1898-1914.
4. Q. Meng, M.-C. Heuzey, and P.J. Carreau, *Control of thermal degradation of polylactide/clay nanocomposites during melt processing by chain extension reaction*. Polymer Degradation and Stability, 2012. **97**(10): pp. 2010-2020.
5. C. Liu, et al., *Evaluation of different methods for the determination of the plateau modulus and the entanglement molecular weight*. Polymer, 2006. **47**(13): pp. 4461-4479.
6. N. Najafi, M.C. Heuzey, and P.J. Carreau, *Polylactide (PLA)-clay nanocomposites prepared by melt compounding in the presence of a chain extender*. Composites Science and Technology, 2012. **72**(5): pp. 608-615.

REFERENCES

1. Shih, Y.-F.; Huang, C.-C. Biodegradable green composites reinforced by the fiber recycling from disposable chopsticks. *Materials Science and Engineering: A* **2010**, *527*, pp. 1516-1521, https://doi.org/10.1016/j.msea.2009.10.024.
2. Joseph, P.V.; Mathew, G. Dynamic mechanical properties of short sisal fibre reinforced polypropylene composites. *Compos. Part A Appl. Sci. Manuf.* **2003**, *34*, pp. 275-290, https://doi.org/10.1016/S1359-835X(02)00020-9.
3. Singh, S.; Mohanty, A.K. Hybrid bio-composite from talc, wood fiber and bioplastic: Fabrication and characterization. *Composites Part A* **2010**, *41*, pp. 304-312, https://doi.org/10.1016/j.compositesa.2009.10.022.
4. Cho, D.; Seo, J.M. Improvement of the Interfacial, Flexural, and Thermal Properties of Jute/Poly(lactic acid) Biocomposites by Fiber Surface Treatments. *Journal of Biobased Materials and Bioenergy* **2007**, *1*, pp. 331-340, 10.1166/jbmb.2007.007.
5. Oksman, K.; Skrifvars, M. Natural fibres as reinforcement in polylactic acid (PLA) composites. *Compos. Sci. Technol.* **2003**, *63*, pp. 1317-1324, https://doi.org/10.1016/S0266-3538(03)00103-9.
6. Gardella, L.; Calabrese, M. PLA maleation: An easy and effective method to modify the properties of PLA/PCL immiscible blends. *Colloid Polym. Sci.* **2014**, *292*, pp. 2391-2398, 10.1007/s00396-014-3328-3.
7. Dong, Y.; Ghataura, A. Polylactic acid (PLA) biocomposites reinforced with coir fibres: Evaluation of mechanical performance and multifunctional properties. *Compos. Part A Appl. Sci. Manuf.* **2014**, *63*, pp. 76-84, https://doi.org/10.1016/j.compositesa.2014.04.003.
8. Piekarska, K.; Sowinski, P. Structure and properties of hybrid PLA nanocomposites with inorganic nanofillers and cellulose fibers. *Composites Part A* **2016**, *82*, pp. 34-41, https://doi.org/10.1016/j.compositesa.2015.11.019.
9. Huda, M.S.; Drzal, L.T. Effect of fiber surface-treatments on the properties of laminated biocomposites from poly(lactic acid) (PLA) and kenaf fibers. *Compos.*

Sci. Technol. **2008**, *68*, pp. 424-432, https://doi.org/10.1016/j.compscitech.2007.06.022.

10. Huda, M.S.; Drzal, L.T. Effect of fiber surface-treatments on the properties of laminated biocomposites from poly(lactic acid) (PLA) and kenaf fibers. *Composites Science and Technology* **2008**, *68*, pp. 424-432, http://dx.doi.org/10.1016/j.compscitech.2007.06.022.
11. Lee, S.M.; Cho, D. Novel silk/poly(butylene succinate) biocomposites: the effect of short fibre content on their mechanical and thermal properties. *Composites Science and Technology* **2005**, *65*, pp. 647-657, http://dx.doi.org/10.1016/j.compscitech.2004.09.023.
12. Ochi, S. Mechanical properties of kenaf fibers and kenaf/PLA composites. *Mechanics of Materials* **2008**, *40*, pp. 446-452, http://dx.doi.org/10.1016/j.mechmat.2007.10.006.
13. Nishino, T.; Hirao, K. Kenaf reinforced biodegradable composite. *Composites Science and Technology* **2003**, *63*, pp. 1281-1286, http://dx.doi.org/10.1016/S0266-3538(03)00099-X.
14. Le Duigou, A.; Davies, P. Interfacial bonding of Flax fibre/Poly(l-lactide) bio-composites. *Composites Science and Technology* **2010**, *70*, pp. 231-239, http://dx.doi.org/10.1016/j.compscitech.2009.10.009.
15. Nassiopoulos, E.; Njuguna, J. Thermo-mechanical performance of poly(lactic acid)/flax fibre-reinforced biocomposites. *Materials & Design* **2015**, *66, Part B*, pp. 473-485, http://dx.doi.org/10.1016/j.matdes.2014.07.051.
16. Oksman, K.; Skrifvars, M. Natural fibres as reinforcement in polylactic acid (PLA) composites. *Composites Science and Technology* **2003**, *63*, pp. 1317-1324, http://dx.doi.org/10.1016/S0266-3538(03)00103-9.
17. Bledzki, A.K.; Jaszkiewicz, A. Mechanical properties of PLA composites with man-made cellulose and abaca fibres. *Composites Part A: Applied Science and Manufacturing* **2009**, *40*, pp. 404-412, http://dx.doi.org/10.1016/j.compositesa.2009.01.002.
18. Goriparthi, B.K.; Suman, K.N.S. Effect of fiber surface treatments on mechanical and abrasive wear performance of polylactide/jute composites. *Composites Part*

A: Applied Science and Manufacturing **2012**, *43*, pp. 1800-1808, https://doi.org/10.1016/j.compositesa.2012.05.007.

19. Rajesh, G.; Prasad, A.V.R. Tensile Properties of Successive Alkali Treated Short Jute Fiber Reinforced PLA Composites. *Procedia Materials Science* **2014**, *5*, pp. 2188-2196, https://doi.org/10.1016/j.mspro.2014.07.425.
20. Dong, Y.; Ghataura, A. Polylactic acid (PLA) biocomposites reinforced with coir fibres: Evaluation of mechanical performance and multifunctional properties. *Composites Part A: Applied Science and Manufacturing* **2014**, *63*, pp. 76-84, http://dx.doi.org/10.1016/j.compositesa.2014.04.003.
21. Bourmaud, A.; Pimbert, S. Investigations on mechanical properties of poly(propylene) and poly(lactic acid) reinforced by miscanthus fibers. *Composites Part A: Applied Science and Manufacturing* **2008**, *39*, pp. 1444-1454, http://dx.doi.org/10.1016/j.compositesa.2008.05.023.
22. Yu, T.; Ren, J. Effect of fiber surface-treatments on the properties of poly(lactic acid)/ramie composites. *Composites Part A: Applied Science and Manufacturing* **2010**, *41*, pp. 499-505, http://dx.doi.org/10.1016/j.compositesa.2009.12.006.
23. Yu, T.; Li, Y. Preparation and properties of short natural fiber reinforced poly(lactic acid) composites. *Transactions of Nonferrous Metals Society of China* **2009**, *19, Supplement 3*, pp. s651-s655, http://dx.doi.org/10.1016/S1003-6326(10)60126-4.
24. Sujaritjun, W.; Uawongsuwan, P. Mechanical Property of Surface Modified Natural Fiber Reinforced PLA Biocomposites. *Energy Procedia* **2013**, *34*, pp. 664-672, https://doi.org/10.1016/j.egypro.2013.06.798.
25. Okubo, K.; Fujii, T. Multi-scale hybrid biocomposite: Processing and mechanical characterization of bamboo fiber reinforced PLA with microfibrillated cellulose. *Composites Part A: Applied Science and Manufacturing* **2009**, *40*, pp. 469-475, http://dx.doi.org/10.1016/j.compositesa.2009.01.012.
26. Fu, S.-Y.; Xu, G. On the elastic modulus of hybrid particle/short-fiber/polymer composites. *composites Part B* **2002**, *33*, pp. 291-299, https://doi.org/10.1016/S1359-8368(02)00013-6.
27. Mustapa, I.; Shanks, R. Poly(lactic acid)-Hemp-Nanosilica Hybrid Composites:

Thermomechanical, Thermal Behavior and Morphological Properties. *IJASET* **2013**, *3*, pp. 192-199,

28. Hartikainen, J.; Hine, P. Polypropylene hybrid composites reinforced with long glass fibres and particulate filler. *Compos. Sci. Technol.* **2005**, *65*, pp. 257-267, 10.1016/j.compscitech.2004.07.010.
29. Thwe, M.M.; Liao, K. Durability of bamboo-glass fiber reinforced polymer matrix hybrid composites. *Compos. Sci. Technol.* **2003**, *63*, pp. 375-387, https://doi.org/10.1016/S0266-3538(02)00225-7.
30. Huda, M.S.; Drzal, L.T. The effect of silane treated- and untreated-talc on the mechanical and physico-mechanical properties of poly(lactic acid)/newspaper fibers/talc hybrid composites. *Composites Part B: Engineering* **2007**, *38*, pp. 367-379, https://doi.org/10.1016/j.compositesb.2006.06.010.
31. Senturk, O.; Senturk, A.E. Evaluation of hybrid effect on the thermomechanical and mechanical properties of calcite/SGF/PP hybrid composites. *Composites Part B* **2018**, *140*, pp. 68-77, https://doi.org/10.1016/j.compositesb.2017.12.021.
32. Lee, S.H.; Wang, S. Isothermal crystallization behavior of hybrid biocomposite consisting of regenerated cellulose fiber, clay, and poly(lactic acid). *J. Appl. Polym. Sci.* **2008**, *108*, pp. 870-875, doi:10.1002/app.26853.
33. Manickam, R.; Johns Retnam, S. A review on Biodegradability of Hybrid Bamboo/Glass fiber polymer composites. **2015**, *10*, pp. 10565,
34. Thakur, V.K.; Thakur, M.K. *Hybrid Polymer Composite Materials: Structure and Chemistry*; Elsevier Science, 2017; pp. 291-312, 9780081007921.
35. de Oliveira Sousa Neto, V.; Saraiva, G.D. 11 - Hybrid polymers composite: Effect of hybridization on the some propers of the materials. in *Hybrid Polymer Composite Materials*. Woodhead Publishing, 2017; pp. 291-312, 978-0-08-100791-4.
36. Barletta, M.; Pizzi, E. Thermal behavior of extruded and injection-molded poly(lactic acid)–talc engineered biocomposites: Effects of material design, thermal history, and shear stresses during melt processing. *J. Appl. Polym. Sci.* **2017**, *134*, pp. 45179, doi:10.1002/app.45179.

37. Barletta, M.; Moretti, P. Engineering of Poly Lactic Acids (PLAs) for melt processing: Material structure and thermal properties. *J. Appl. Polym. Sci.* **2017**, *134*, doi:10.1002/app.44504.

38. Zheng, Y.; Gu, F. Improving Mechanical Properties of Recycled Polypropylene-based Composites Using TAGuchi and ANOVA Techniques. *Proc CIRP* **2017**, *61*, pp. 287-292, https://doi.org/10.1016/j.procir.2016.11.137.

39. Hisakura, Y.; Kitahara, K. Mechanical Properties of Composite Compounded with ABS (GF) and CF by DFFIM. *Key Engineering Materials* **2017**, *728*, pp. 240-245, 10.4028/www.scientific.net/KEM.728.240.

40. Yan, X.; Cao, S. *Structure and Interfacial Shear Strength of Polypropylene-Glass Fiber/Carbon Fiber Hybrid Composites Fabricated by Direct Fiber Feeding Injection Molding*, 2018; pp.,

41. Mathurosemontri, S.; Uawongsuwan, P. *The Effect of Processing Parameter on Mechanical Properties of Short Glass Fiber Reinforced Polyoxymethylene Composite by Direct Fiber Feeding Injection Molding Process*, 2016; pp.,

42. Chaitanya, S.; Singh, I. *Processing of PLA/Sisal Fiber Biocomposites Using Direct and Extrusion-Injection Molding*, 2016; pp.,

43. Faruk, O.; Bledzki, A.K. Biocomposites reinforced with natural fibers: 2000–2010. *Prog. Polym. Sci.* **2012**, *37*, pp. 1552-1596, https://doi.org/10.1016/j.progpolymsci.2012.04.003.

44. Yang, N.; Zhang, Z.-C. Effect of surface modified kaolin on properties of polypropylene grafted maleic anhydride. *RESULTS PHYS.* **2017**, *7*, pp. 969-974, https://doi.org/10.1016/j.rinp.2017.02.030.

45. Pradipta, R.; Mardiyati. Effect of maleic anhydride treatment on the mechanical properties of sansevieria fiber/vinyl ester composites. *AIP Conf. Proc.* **2017**, *1823*, pp. 020097, 10.1063/1.4978170.

46. Chow, W.S.; Tham, W.L. Effects of maleated-PLA compatibilizer on the properties of poly(lactic acid)/halloysite clay composites. *J. Thermoplast. Compos. Mater.* **2012**, *26*, pp. 1349-1363, 10.1177/0892705712439569.

47. González-López, M.E.; Robledo-Ortíz, J.R. Polylactic acid functionalization with maleic anhydride and its use as coupling agent in natural fiber biocomposites: a

review. *Composite Interfaces* **2018**, *25*, pp. 515-538, 10.1080/09276440.2018.1439622.

48. Birnin-yauri, A.U.; Ibrahim, N. *Effect of Maleic Anhydride-Modified Poly(lactic acid) on the Properties of Its Hybrid Fiber Biocomposites*, 2017; pp.,
49. Xanthos, M. *Reactive Extrusion : Principles and Practice*, 1992; pp.,
50. Fayt, R.; Jérôme, R. Interface Modification in Polymer Blends. in *Multiphase Polymers: Blends and Ionomers*. American Chemical Society, 1989; pp. 38-66, 0-8412-1629-0.
51. Bimestre, B.H.; Saron, C. Chain extension of poly (ethylene terephthalate) by reactive extrusion with secondary stabilizer. *Mat. Res.* **2012**, *15*, pp. 467-472, http://www.scielo.br/scielo.php?script=sci_arttext&pid=S1516-14392012000300019&nrm=iso
52. Hao, M.; Wu, H. In situ reactive interfacial compatibilization of polylactide/sisal fiber biocomposites via melt-blending with an epoxy-functionalized terpolymer elastomer. *RSC Adv.* **2017**, *7*, pp. 32399-32412, 10.1039/C7RA03513F.
53. Jamshidian, M.; Tehrany, E.A. Poly-Lactic Acid: Production, Applications, Nanocomposites, and Release Studies. *Comprehensive Reviews in Food Science and Food Safety* **2010**, *9*, pp. 552-571, 10.1111/j.1541-4337.2010.00126.x.
54. Hendrick, E.; Frey, M. *Increasing Surface Hydrophilicity in Poly(Lactic Acid) Electrospun Fibers by Addition of Pla-b-Peg Co-Polymers*, 2014; pp.,
55. Castro-Aguirre, E.; Iñiguez-Franco, F. Poly(lactic acid)—Mass production, processing, industrial applications, and end of life. *Advanced Drug Delivery Reviews* **2016**, *107*, pp. 333-366, https://doi.org/10.1016/j.addr.2016.03.010.
56. Gupta, B.; Revagade, N. Poly(lactic acid) fiber: An overview. *Progress in Polymer Science* **2007**, *32*, pp. 455-482, https://doi.org/10.1016/j.progpolymsci.2007.01.005.
57. Sreekumar, P.A.; Saiah, R. Dynamic mechanical properties of sisal fiber reinforced polyester composites fabricated by resin transfer molding. *Polym. Compos.* **2009**, *30*, pp. 768-775, 10.1002/pc.20611.
58. Kabir, M.M.; Wang, H. Chemical treatments on plant-based natural fibre reinforced polymer composites: An overview. *Compos. Part B Eng.* **2012**, *43*, pp.

2883-2892,
http://www.sciencedirect.com/science/article/pii/S1359836812002922

59. Bledzki, A.K.; Gassan, J. Composites reinforced with cellulose based fibres. *Progress in Polymer Science* **1999**, *24*, pp. 221-274, http://dx.doi.org/10.1016/S0079-6700(98)00018-5.

60. Reddy, N.; Yang, Y. Biofibers from agricultural byproducts for industrial applications. *Trends in Biotechnology* **2005**, *23*, pp. 22-27, http://dx.doi.org/10.1016/j.tibtech.2004.11.002.

61. Jawaid, M.; Abdul Khalil, H.P.S. Cellulosic/synthetic fibre reinforced polymer hybrid composites: A review. *Carbohydrate Polymers* **2011**, *86*, pp. 1-18, http://dx.doi.org/10.1016/j.carbpol.2011.04.043.

62. Lindström, N.; Fardim, P. *Chemistry and surface chemistry of vessels in eucalyptus kraft pulps*, 2012; pp.,

63. Tonoli, G.H.D.; Teixeira, E. *Cellulose micro/nanofibres from Eucalyptus kraft pulp: Preparation and properties*, 2012; pp.,

64. Espinach, F.X.; Boufi, S. Composites from poly(lactic acid) and bleached chemical fibres: Thermal properties. *Composites Part B: Engineering* **2018**, *134*, pp. 169-176, https://doi.org/10.1016/j.compositesb.2017.09.055.

65. Hao Ren, Y.Z., Huamin Zhai, Jinxiang Chen. Production and evaluation of biodegradable composites based on polyhydroxybutyrate and polylactic acid reinforced with short and long pulp fibers. *Cellul. Chem. Technol.* **2015**, *49*, pp. 641-652,

66. Du, Y.; Wu, T. Pulp fiber-reinforced thermoset polymer composites: Effects of the pulp fibers and polymer. *Composites Part B: Engineering* **2013**, *48*, pp. 10-17, https://doi.org/10.1016/j.compositesb.2012.12.003.

67. Méndez, J.A.; Vilaseca, F. Evaluation of the reinforcing effect of ground wood pulp in the preparation of polypropylene-based composites coupled with maleic anhydride grafted polypropylene. *J. Appl. Polym. Sci.* **2007**, *105*, pp. 3588-3596, 10.1002/app.26426.

68. Espinach, F.X.; Granda, L.A. Mechanical and micromechanical tensile strength of eucalyptus bleached fibers reinforced polyoxymethylene composites.

Composites Part B: Engineering **2017**, *116*, pp. 333-339, https://doi.org/10.1016/j.compositesb.2016.10.073.

69. César de Carvalho Pinto, P.; Ribeiro da Silva, V. *Synthesis of flexible polyurethane foams by the partial substitution of polyol by steatite*, 2018; pp.,
70. Chang, B.P.; Mohanty, A.K. Tuning the compatibility to achieve toughened biobased poly(lactic acid)/poly(butylene terephthalate) blends. *RSC Advances* **2018**, *8*, pp. 27709-27724, 10.1039/C8RA05161E.
71. Hao, M.; Wu, H. Interface Bond Improvement of Sisal Fibre Reinforced Polylactide Composites with Added Epoxy Oligomer. *Materials* **2018**, *11*, pp. 398, 10.3390/ma11030398.
72. Fowlks, A.C.; Narayan, R. The effect of maleated polylactic acid (PLA) as an interfacial modifier in PLA-talc composites. *Journal of Applied Polymer Science* **2010**, *118*, pp. 2810-2820, doi:10.1002/app.32380.
73. Pan, Y.-J.; Lin, Z.-I. Polylactic acid/carbon fiber composites: Effects of polylactic acid-g-maleic anhydride on mechanical properties, thermal behavior, surface compatibility, and electrical characteristics. *Journal of Composite Materials* **2018**, *52*, pp. 405-416, 10.1177/0021998317708020.
74. Yan, X.; Uawongsuwan, P. *Tensile Properties of Glass Fiber/Carbon Fiber Reinforced Polypropylene Hybrid Composites Fabricated by Direct Fiber Feeding Injection Molding Process*, 2016; pp.,
75. Arruda, L.C.; Magaton, M. Influence of chain extender on mechanical, thermal and morphological properties of blown films of PLA/PBAT blends. *Polymer Testing* **2015**, *43*, pp. 27-37, https://doi.org/10.1016/j.polymertesting.2015.02.005.
76. Buggy, M. Natural fibers, biopolymers, and biocomposites. Edited by Amar K Mohanty, Manjusri Misra and Lawrence T Drzal. *Polymer International* **2006**, *55*, pp. 460, doi:10.1002/pi.2084.
77. Punyamurthy, R.; Dhanalakshmi, D. *Abaca Fiber Reinforced Hybrid Composites*, 2014; pp.,
78. Khankrua, R.; Pivsa-Art, S. Effect of chain extenders on thermal and mechanical properties of poly(lactic acid) at high processing temperatures: Potential

application in PLA/Polyamide 6 blend. *Polym. Degrad. Stab.* **2014**, *108*, pp. 232-240, https://doi.org/10.1016/j.polymdegradstab.2014.04.019.

79. Gunti, R.; Ratna Prasad, A.V. Mechanical and degradation properties of natural fiber reinforced PLA composites: Jute, sisal, and elephant grass. *Polymer Composites* **2016**, pp. n/a-n/a, 10.1002/pc.24041.
80. Guo, X.; Zhang, J. Poly(lactic acid)/polyoxymethylene blends: Morphology, crystallization, rheology, and thermal mechanical properties. *Polym.* **2015**, *69*, pp. 103-109, https://doi.org/10.1016/j.polymer.2015.05.050.
81. Shanmugam, D.; Thiruchitrambalam, M. Static and dynamic mechanical properties of alkali treated unidirectional continuous Palmyra Palm Leaf Stalk Fiber/jute fiber reinforced hybrid polyester composites. *Mater. Design* **2013**, *50*, pp. 533-542, http://www.sciencedirect.com/science/article/pii/S0261306913002483
82. Etaati, A.; Pather, S. The study of fibre/matrix bond strength in short hemp polypropylene composites from dynamic mechanical analysis. *Compos. Part B Eng.* **2014**, *62*, pp. 19-28, https://doi.org/10.1016/j.compositesb.2014.02.011.
83. Krishna, K.V.; Kanny, K. The effect of treatment on kenaf fiber using green approach and their reinforced epoxy composites. *Compos. Part B Eng.* **2016**, *104*, pp. 111-117, https://doi.org/10.1016/j.compositesb.2016.08.010.
84. Ornaghi, H.L.; Bolner, A.S. Mechanical and dynamic mechanical analysis of hybrid composites molded by resin transfer molding. *J. Appl. Polym. Sci.* **2010**, *118*, pp. 887-896, 10.1002/app.32388.
85. Correa, C.A.; Razzino, C.A. Role of Maleated Coupling Agents on the Interface Adhesion of Polypropylene—Wood Composites. *J. Thermoplast. Compos.* **2007**, *20*, pp. 323-339, 10.1177/0892705707078896.
86. Akindoyo, J.O.; Beg, M.D.H. Effects of surface modification on dispersion, mechanical, thermal and dynamic mechanical properties of injection molded PLA-hydroxyapatite composites. *Compos. Part A Appl. Sci. Manuf.* **2017**, *103*, pp. 96-105, https://doi.org/10.1016/j.compositesa.2017.09.013.
87. Pandey, K.K. A study of chemical structure of soft and hardwood and wood polymers by FTIR spectroscopy. *Journal of Applied Polymer Science* **1999**, *71*,

pp. 1969-1975, doi:10.1002/(SICI)1097-4628(19990321)71:12<1969::AID-APP6>3.0.CO;2-D.

88. Simão, J.; Carmona, V. *Effect of Fiber Treatment Condition and Coupling Agent on the Mechanical and Thermal Properties in Highly Filled Composites of Sugarcane Bagasse Fiber/PP*, 2016; pp.,

89. Bouafif, H.; Koubaa, A. Analysis of Among-Species Variability in Wood Fiber Surface Using DRIFTS and XPS: Effects on Esterification Efficiency. *Journal of Wood Chemistry and Technology* **2008**, *28*, pp. 296-315, 10.1080/02773810802485139.

90. Chen, Z.; Hu, T.Q. Multivariate Analysis of Hemicelluloses in Bleached Kraft Pulp Using Infrared Spectroscopy. *Applied Spectroscopy* **2016**, *70*, pp. 1981-1993, 10.1177/0003702816675363.

91. Hao, M.; Wu, H. In situ reactive interfacial compatibilization of polylactide/sisal fiber biocomposites via melt-blending with an epoxy-functionalized terpolymer elastomer. *RSC Advances* **2017**, *7*, pp. 32399-32412, 10.1039/C7RA03513F.

92. Doan, T.-T.-L.; Gao, S.-L. Jute/polypropylene composites I. Effect of matrix modification. *Compos. Sci. Technol.* **2006**, *66*, pp. 952-963, https://doi.org/10.1016/j.compscitech.2005.08.009.

93. Coutinho, F.M.B.; Costa, T.H.S. Performance of polypropylene–wood fiber composites. *Polym. Test.* **1999**, *18*, pp. 581-587, https://doi.org/10.1016/S0142-9418(98)00056-7.

94. Ganster, J.; Fink, H.-P. Novel cellulose fibre reinforced thermoplastic materials. *Cellulose* **2006**, *13*, pp. 271-280, 10.1007/s10570-005-9045-9.

95. Jaszkiewicz, A.; Bledzki, A.K. How does a chain-extended polylactide behave?: a comprehensive analysis of the material, structural and mechanical properties. *Polymer Bulletin* **2014**, *71*, pp. 1675-1690, 10.1007/s00289-014-1148-8.

96. Sahu, S.; Broutman, L.J. Mechanical properties of particulate composites. *Polymer Engineering & Science* **1972**, *12*, pp. 91-100, doi:10.1002/pen.760120204.

97. Yu, T.; Jiang, N. Study on short ramie fiber/poly(lactic acid) composites compatibilized by maleic anhydride. *Composites Part A: Applied Science and*

Manufacturing **2014**, *64*, pp. 139-146, https://doi.org/10.1016/j.compositesa.2014.05.008.

98. Abdul Shakoor. Development of novel bio-derived polymer composites reinforced with natural fibres and mineral fillers. A Doctoral Thesis, Loughborough University, Leicestershire, UK, 2013.
99. Japon, S.; Boogh, L. Reactive processing of poly(ethylene terephthalate) modified with multifunctional epoxy-based additives. *Polymer* **2000**, *41*, pp. 5809-5818, https://doi.org/10.1016/S0032-3861(99)00768-5.
100. Lamnawar, K.; Maazouz, A. Rheological study of multilayer functionalized polymers: characterization of interdiffusion and reaction at polymer/polymer interface. *Rheologica Acta* **2006**, *45*, pp. 411-424, 10.1007/s00397-005-0062-2.
101. Lamnawar, K.; Baudouin, A. Interdiffusion/reaction at the polymer/polymer interface in multilayer systems probed by linear viscoelasticity coupled to FTIR and NMR measurements. *European Polymer Journal* **2010**, *46*, pp. 1604-1622, https://doi.org/10.1016/j.eurpolymj.2010.03.019.
102. H. Eberlein, T. *Instant Notes in Organic Chemistry, 2nd Edition (Graham L. Patrick)*, 2005; pp.,
103. Vieira, A.; Santana, S. *High performance maleated lignocellulose epicarp fibers for copper ion removal*, 2014; pp.,
104. Yingfeng, Z.; Jiyou, G. *Synthesis and characterization of Maleic Anhydride Esterified Corn Starch by the Dry Method*, 2013; pp.,
105. Granda, L.A.; Espinach, F.X. Semichemical fibres of Leucaena collinsii reinforced polypropylene composites: Young's modulus analysis and fibre diameter effect on the stiffness. *Compos. Part B Eng.* **2016**, *92*, pp. 332-337, https://doi.org/10.1016/j.compositesb.2016.02.023.
106. Muenprasat, D.; Suttireungwong, S. Functionalization of poly (lactic acid) with maleic anhydride for biomedical application. *Journal of Metals, Materials and Minerals* **2010**, *20*, pp. 189-192,
107. Abramovitch, R.A. THE INFRARED SPECTRA OF MALONATE ESTERS. *Canadian Journal of Chemistry* **1958**, *36*, pp. 151-158, 10.1139/v58-019.
108. Interpretation of Infrared Spectra, A Practical Approach. in *Encyclopedia of*

Analytical Chemistry.

109. Fink, J.K. *Reactive Polymers Fundamentals and Applications: A Concise Guide to Industrial Polymers*; Elsevier Science, 2013; pp., 9781455731589.
110. Ismail, N.I.; Ishak, Z.A.M. Effect of fiber loading on mechanical and water absorption capacity of Polylactic acid/Polyhydroxybutyrate-co-hydroxyhexanoate/Kenaf composite. *IOP Conference Series: Materials Science and Engineering* **2018**, *368*, pp. 012014, 10.1088/1757-899x/368/1/012014.
111. Husseinsyah, S.; Koay, S.C. *Surface modification of coconut shell powder filled polylactic acid biocomposites*, 2013; pp.,
112. Hedenberg, P.; Gatenholm, P. Conversion of plastic/cellulose waste into composites. I. Model of the interphase. *Journal of Applied Polymer Science* **1995**, *56*, pp. 641-651, 10.1002/app.1995.070560601.

มหาวิทยาลัยศิลปากร

VITA

NAME	Phornwalan Nanthananon
DATE OF BIRTH	27 November 2532
PLACE OF BIRTH	Phetchabun Province
INSTITUTIONS ATTENDED	Ph.D. candidate in Polymer Science and Engineering program (International program), Department of Materials Science and Engineering, Faculty of Engineering and Industrial Technology, Silpakorn University. Master of Engineering in polymer science and engineering, Department of Materials Science and Engineering, Faculty of Engineering and Industrial Technology, Silpakorn University. Bachelor of Engineering in petrochemical and polymeric materials, Department of Materials Science and Engineering, Faculty of Engineering and Industrial Technology, Silpakorn University. Senior project: Preparation and properties of chitosan/starch blend film. Science-Math program in Secondary education, Kanchanapisekwitthayalai Chaiyaphum school, Chaiyaphum
HOME ADDRESS	185 Moo 1, Laem Thong sub-district, Phakdi Chumphon District, Chaiyaphum Province, 36260
PUBLICATION	- Nanthananon, P., Seadan, M., Pivsa-Art, S. and Suttiruengwong, S. (2015): Enhanced Crystallization of Poly

(Lactic Acid) through Reactive Aliphatic Bisamide, IOP Conf. Ser.: Mater. Sci. Eng. 87(1) p. 012067

- Nanthananon, P., Seadan, M., Pivsa-Art, S., Hamada, H. and Suttiruengwong, S. (2017): Biodegradable Polyesters Reinforced with Eucalyptus Fiber: Effect of Reactive Agents, AIP Conference Proceedings, p. 070012
- Nanthananon, P., Seadan, M., Sripethdee, C., Pivsa-Art, S., Hamada, H. and Suttiruengwong, S. (2018): Reactive Compatibilization of Short-Fiber Reinforced Poly(lactic acid) Biocomposites, Journal of Renewable Materials, 6, p.573-583.
- Nanthananon, P., Seadan, M., Sripethdee, C., Pivsa-Art, S., Hamada, H. and Suttiruengwong, S. (2018): Facial Preparation and Characterization of Short-Fiber and Talc Reinforced Poly(lactic acid) Hybrid composite with In Situ Reactive Compatibilizers, Materials, 11(7), p. 1183-1195